Stimuli-Responsive Metal-Ligand Assemblies

*Anna J. McConnell,[†] Christopher S. Wood, [†] Prakash P. Neelakandan[†] and Jonathan R. Nitschke**

Department of Chemistry, University of Cambridge, Lensfield Road, Cambridge CB2 1EW, United Kingdom

Contents

1 Introduction

Within living systems, molecular-scale responses to stimuli flow together into the intricate and robust signal transduction networks that process information for an organism. Studies of stimuli-responsive behavior at the molecular scale can help elucidate the foundations of biological function, as well as enabling the design of new materials capable of changing one or more of their properties in response to an external stimulus, such as pH, light, or the presence of a chemical species. Investigations of stimuli-responsive behavior have thus attracted the attention of chemists from many subdisciplines.[1] As many aspects of chemical synthesis are mastered to prepare complex materials, control of stimuli-responsive behavior represents a complementary step toward increasing the functionality and utility of these materials. The applications of stimuli-responsive materials range from sensors to information displays and molecular machines; however, this review will focus less on applications and more upon the concepts behind the design and control of stimuli-responsive behavior.

1.1 Scope of the Review

This review is limited to the discussion of stimuli-responsive metal-ligand assemblies. We exclude metal-organic frameworks, which have been the subject of several excellent recent reviews,[2,3] and concentrate on assemblies where the metal has a well-defined coordination geometry, focusing upon transition metals rather than alkali metals, for example.

Reasonable points of view may diverge as to what constitutes a stimulus, as opposed to the addition of a constituent to a system that becomes incorporated ultimately into the system as part of a response. In this review we define stimuli broadly, including chemical stimuli that

become part of a structure giving rise to a response. Our focus is ultimately upon the complexity and subjective interest of the response, such as a structural rearrangement or disassembly. In some sections, stimuli-responsive will be more specifically defined in terms of the assembly under review. In general, simple guest binding to a host and any optical or electrochemical responses resulting from addition of a chemical stimulus are excluded from discussion under the above definition. Furthermore, we have chosen to exclude heat as a stimulus (except in the context of more complex responses, as in Section 6.1.1), due to the inherent thermal responsive behavior of all molecules. Thus, metal-ligand assemblies responding to mechanical, chemical, electrical and light stimuli will be the focus of the review.

We divide the review into sections based on the type of assembly, subdividing by stimulus. We have begun with simpler systems based on transition metal complexes and macrocycles before discussing molecular machines and switches where stimuli-responsive behavior is exploited to develop molecular analogs of tweezers, muscles, rotors and locks. Molecular machines and switches based on interlocked catenane and rotaxane structures are treated in a separate section to non-interlocked examples and they are further classified according to the type of motion, for example shuttling or pirouetting, to simplify the discussion. Stimuli-responsive metal-organic cages will then be introduced before concluding with metallo-polymers and metallo-gels.

Given the broad scope of the review, it is impossible to include a detailed discussion of every stimuli-responsive metal-ligand assembly. Instead, the intention of this review is to highlight seminal work and examples of complex responses that appeared not easily predictable based on the stimuli-responsive definition (*vide supra*). The inherent subjectivity of this definition led to cases where it was necessary to make a subjective decision. We ask for understanding in these cases, and apologize for any inadvertent omissions of relevant examples. For further information on particular metal-ligand assemblies, the reader's attention is drawn to the reviews cited in each section.

2 Transition Metal Solid State Materials

The photophysical properties of transition metal complexes in the solid state have been exploited in the development of stimuli-responsive materials for a variety of applications, including information displays, memories, sensors, probes and photomodulation.[4] This section describes materials that change optical properties (color or luminescence) in response to mechanical and chemical stimuli. While many examples are based on Au^{I} complexes, the stimuli-responsive behavior of these materials was the subject of a recent review.[5] Therefore, this section will highlight several key examples based on gold before focusing on other transition metals.

2.1 Mechanically Responsive Solid State Materials

Luminescence mechanochromism (also known as luminescence tribochromism[6]) is the luminescence change due to mechanical grinding of a solid sample. This change can be reversed by recrystallization or heating. Although this field was the topic of a recent review,[7] there are relatively few examples of transition metal based mechano-responsive luminescent materials.[6] This is because the design of mechanochromic luminescent complexes is difficult for two reasons. First, luminescence of a complex can be weakened in the solid state due to the aggregation-caused quenching (ACQ) effect.[7] Metal complexes that undergo aggregation-induced emission will be briefly discussed as a potential solution to this problem in Section 2.3. Second, no single mechanism explains all mechanochromic behavior, and the exact cause of the mechanochromism is often obscure.[6] The observation of mechanochromism has been attributed to intermolecular interactions, such as metal-metal contacts and π–π stacking interactions, as these are known to affect the emission properties of transition metal complexes.

Many reported mechano-responsive systems are based on gold complexes, where aurophilic interactions are believed to be responsible for the change in luminescent properties.[6,8] Ito, Sawamura and co-workers reported the luminescence of complex $[(F_5C_6Au)_2$-(μ-1,4-

diisocyanobenzene)] (Figure 1) to change from blue (**1a**) to yellow (**1b**) upon grinding, with the original blue luminescence being restored upon exposure to solvent.[8a] Cycling between blue and yellow luminescence was reversible with no evidence of intensity degradation even after 20 cycles. The blue luminescence was attributed to phosphorescence from the intraligand-localised π–π* excited state, with the crystal structure of the blue luminescent material revealing that the gold centers were 5.19 Å apart, which is too far apart for aurophilic interactions.[9] In contrast, grinding gave an amorphous material, in which the gold centers are proposed to be close enough for aurophilic interactions, resulting in the lower energy yellow emission. Similarly, Eisenberg and Lee's gold thiouracilate complexes undergo a structural change and release of volatile acid upon grinding, resulting in a change from weak white to blue luminescence;[8b] mechanical stress breaks the weakly emissive helical structure's intermolecular aurophilic interactions into dimers having stronger intermolecular gold-gold interactions.

While the cause of the mechanochromism is relatively well understood in the previous two examples, this cause may be more obscure in other cases. Fackler and co-workers reported that [(1,3,5-triaza-7-phosphaadamantane)$_2$Au][Au(CN)$_2$] is not luminescent as a single crystal but luminesces strongly as a powder.[8d] X-ray powder diffraction data ruled out the possibility of a phase transformation upon grinding. Instead, the authors propose that the luminescence results from surface defect sites in the powder.

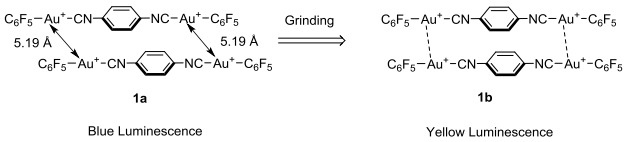

Figure 1. Ito, Sawamura and co-workers' mechano-responsive gold complex.

Metal-metal interactions other than those involving gold are also believed to play an important role in mechano-responsive systems. Zhang, Chen and co-workers reported that the luminescence of platinum(II) complexes **2** (Figure 2) is significantly red-shifted upon grinding

and this shift can be reversed by exposure to organic vapor or heating.[10] The red shift is attributed to emission from the ^{3}MLCT/^{3}LLCT (metal-to-ligand-charge transfer / ligand-to-ligand-charge transfer) state in the crystals converting to the ^{3}MMLCT (metal-metal-to-ligand-charge transfer) state in the amorphous powder due to the formation of dimers or aggregates through interactions between platinum centers. The Pt-Pt distance between molecules of the complex with the bulkier ^{t}Bu substituent (**2b**) was longer and as a result, the red shift was smaller for this complex than the unsubstituted complex (**2a**). Similarly, Shinozaki and co-workers report that the mechanochromic behavior of Pt(dpb)Cl (**3a**, Figure 2), where dpb is 1,3-di(2-pyridyl)benzene), is due to emission from a dimer or aggregate in the amorphous state.[11] For the related complex Pt(5dpb)Cl (5dpb = 1,3-di(5-methyl-2pyridyl)benzene), **3b**), however, grinding alone does not bring the platinum molecules close enough together to produce excimer emission. Instead, the orange emission observed after grinding arises from photodynamically generated excimer emission. Grinding maintains the molecular packing but increases the surface area. As a result, molecules on the surface are less constrained by the crystal lattice, freeing them to form excimers upon absorption of light.

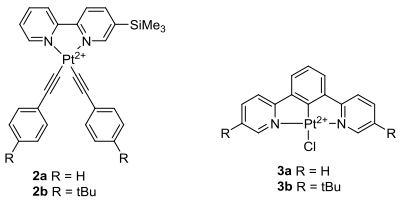

Figure 2. Mechano-responsive Pt^{II} complexes.

Luminescence mechanochromism is not limited to metal-metal interactions as there are examples where intermolecular π–π stacking interactions also play a role. Grinding Zn^{II}-salen (salen is 2,2'-ethylenebis(nitrilomethylidene)diphenol) helical complex **4** (Figure 3a) reduced intermolecular π–π stacking interactions, resulting in a change of luminescence color from blue-green to blue.[12] In contrast, the loss of intermolecular π–π stacking interactions between the phenylene rings of the *o*-bis(diphenylphosphino)benzene (dppbz) ligand in Tsubomura's

silver(I) complex **5** (Figure 3b) resulted in a color change from blue to green emission upon grinding.[13] Commonly, π–π stacking interactions result in a red shift of the emission wavelength, as observed with Pt(5dpb)Cl (**3b**)[11] and the Zn^{II}-salen helical complex **4**.[12] The unusual blue shift of the silver complex's emission in the presence of π–π stacking interactions was attributed to these intermolecular interactions preventing distortion of the ligands upon excitation.

There are also several examples of Ir^{III} complexes displaying a change in luminescence upon mechanical grinding.[14] An interesting example is $[(ppy)_2Ir(pam)]^+$ (**6**, Figure 3c, ppy = phenylpyridine, pam = 2-picolylamine) where hydrogen bonding interactions between the amine group of the pam ligand and the counter-ions affect the molecular packing in the crystalline state.[14a] When the anion is chloride (**6a**), two pseudopolymorphs crystallize (a solvated and non-solvated species) whereas unique forms are obtained with the non-coordinating hexafluorophosphate (**6b**) and perchlorate (**6c**) anions. The two pseudopolymorphs have different luminescent properties; the green emission of the solvated species does not change with grinding whereas the non-solvated species has dual green and orange luminescence, which is fully converted to green emission upon grinding. The dual emission of the crystalline material was attributed to the partial transformation from the non-solvated to solvated crystalline species, dependent on crystallization time. In contrast, the orange emission of the crystals with non-coordinating anions was converted to dual green and orange emission by grinding. Complete conversion from orange to green emission was not possible under the experimental conditions tested. X-ray crystallography suggested that distortion of the five-membered chelate ring formed by the Ir center and pam ligand was responsible for the observed photophysical property changes; the dual green and orange emission was attributed to emission from two different kinds of center, one on the surface and one in the crystalline bulk. Grinding increased the surface area, thereby increasing the contribution of the surface site to the observed emission.

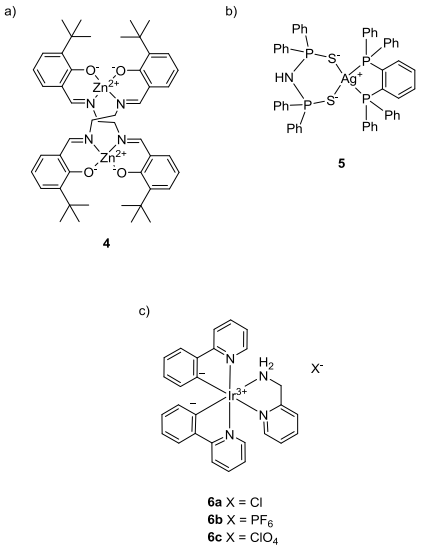

Figure 3. a) Zn^{II} salen helical complex b) Tsubomura's Ag^{I} complex and c) $[(ppy)_2Ir(pam)]^+$.

2.2 Chemically Responsive Solid State Materials

Vapochromic systems and vapoluminescent systems respond to volatile organic compounds (VOCs) with a detectable color or luminescence change and as such, they have potential application as chemosensors for these VOCs in the environment and workplace.[15]

There are a number of similarities between vapochromic/luminescent systems and the mechano-responsive systems described in Section 2.1; the design of vapochromic/luminescent systems is difficult as often the desired properties are discovered serendipitously. Furthermore, the properties are highly dependent on the polymorph or solvate, such that one polymorph/solvate may respond to VOCs whereas a related one may not. As a result, attempted optimization of the system can result in a loss of desired response.[16] As with mechanochromic systems, optical changes can also result from metal-metal, solvent-metal, π–π stacking and hydrogen bonding interactions.[16] As vapochromic and vapoluminescent systems have been recently reviewed comprehensively,[16-17] we highlight here only examples involving unusual mechanisms. This includes systems where the VOC binds in a well-defined way, resulting in a change in ligand field around the metal center.

Catalano's $Au^{I}Cu^{I}_{2}$ complex **7** acts as a vapochromic sensor, involving the exchange of ligands coordinated to the Cu^{I} centers in a solid-vapor reaction (Figure 4).[18] Complex **7a** exhibits blue luminescence when two acetonitrile molecules are coordinated to each copper center. Upon exposure to methanol vapor, these acetonitrile pairs are each replaced by a single methanol molecule. This results in a significant reorganization to complex **7b**, where each copper binds to the gold center. The luminescence color change from blue to green is attributed to these Au-Cu interactions, which are uncommon compared to Pt-Pt and Au-Au interactions. The Au-Cu interactions can be switched on and off: the coordinated methanol can be removed under vacuum resulting in yellow-orange luminescence, and then replaced with two molecules of acetonitrile upon exposure to acetonitrile vapor to regenerate the original complex.

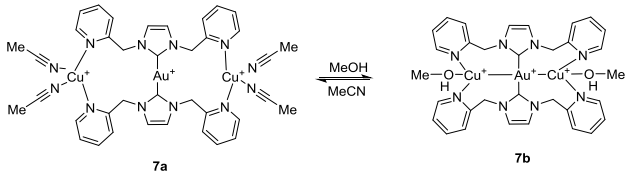

Figure 4. Catalano's Au^{I} vapochromic sensor with "on-off" Au-Cu interactions.[18]

Recently, Wang and co-workers reported that methanol drives the conversion of binuclear Cu^{I} complex **8** from one linkage isomer to another in the solid state (Figure 5), although the methanol does not coordinate directly to the metal center.[19] The head-to-tail isomer (**8a**) emits blue light in the solid state and can be transformed to the green-emitting head-to-head isomer (**8b**) by exposure to methanol vapor. Recrystallisation from MeCN/Et_2O regenerates the head-to-tail isomer. DFT calculations attribute the red-shift in the head-to-head isomer to π–π stacking interactions between the phenyl and pyridyl rings, lowering the energy of the LUMO.

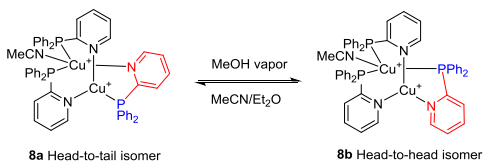

Figure 5. Wang's vapochromic binuclear copper(I) complex.[19]

Vapochromism can also have interesting applications in spin-crossover (SCO) systems. Tao, Zheng and co-workers recently reported the single-crystal-to-single-crystal transformation of the well-studied SCO complex $Fe(tpa)(NCS)_2$ (**9a**, tpa = tris(2-pyridylmethyl)amine) into $[Fe(tpa)(NCS)_2]\cdot[Fe(tpa)(NCS)_2\cdot CH_3OH]$ (**9b**) upon exposure to methanol vapor (Figure 6).[20] The transformation was accompanied by changes in the color from yellow to red, in the crystal structure, and most interestingly, in the magnetic properties. The crystal structure of $Fe(tpa)(NCS)_2$ reveals a 2D supramolecular array stabilized by π–π interactions in one direction and S···H-C bonds in both dimensions (Figure 6a). Adsorption of methanol results in a new structure with an asymmetric unit containing two crystallographically independent $Fe(tpa)(NCS)_2$ molecules, one of which binds a methanol molecule via a S···H-O hydrogen bond (Figure 6b). Unlike $Fe(tpa)(NCS)_2$ where an incomplete spin transition from low spin (LS) to high spin (HS) was observed, the spin transition from LS-LS to HS-HS for $[Fe(tpa)(NCS)_2]\cdot[Fe(tpa)(NCS)_2\cdot CH_3OH]$ was a two-step process via a HS-LS intermediate. This intermediate was resolved crystallographically, revealing that the iron centers in $[Fe(tpa)(NCS)_2]\cdot[Fe(tpa)(NCS)_2\cdot CH_3OH]$ were high and low spin respectively at room temperature.

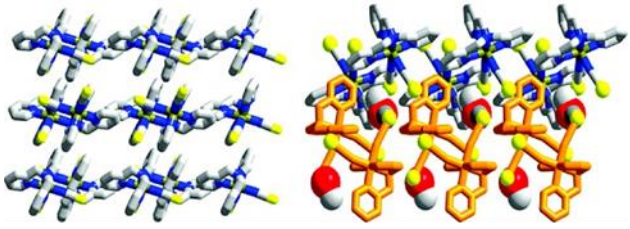

Figure 6. Crystal packing of a) $Fe(tpa)(NCS)_2$ **9a** and b) $[Fe(tpa)(NCS)_2]\cdot[Fe(tpa)(NCS)_2\cdot CH_3OH]$ **9b**. Reprinted with permission from ref[20]. Copyright 2010 American Chemical Society.

Vapochromic systems that can discriminate between VOCs are of interest for the development of selective chemosensors. The hydrogen-bonded proton transfer (HBPT) assembly **10,** consisting of a metal-hydrazone complex as a proton acceptor and bromanilic acid (H_2BA) as a proton donor, was recently reported as the first proton donor-acceptor based vapochromic material that does not involve metal-metal interactions (Figure 7).[21] Interestingly, this material can recognize the proton donating/accepting ability of the VOC; the adsorption band around 600 nm is red-shifted upon exposure to the vapors of DMF, pyridine, DMA and DMSO, whereas it is blue-shifted in the presence of the vapors of 1,4-dioxane, acetonitrile, methanol and ethanol. These shifts appear to be correlated to the Gutmann donor and acceptor numbers of the solvents. Proton-accepting compounds are more easily adsorbed because they can form a more stable hydrogen bond between the hydroxyl group of HBA^- than between HBA^- and H_2BA.

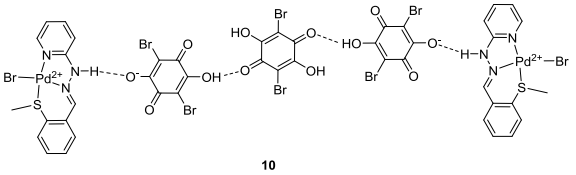

10

Figure 7. Vapochromic hydrogen-bonded proton transfer assembly.

The triarylboron Pt^{II} complex **11** reported by Wang (Figure 8) also exhibits color shifts to shorter or longer wavelengths based on the nature of the vapor; an emission color change from yellow to green is observed for CH_2Cl_2, $CHCl_3$, CH_3CN, acetone, THF or ethanol while the emission color changes to red for benzene or cyclohexane.[22] Furthermore, the luminescence is quenched upon exposure to hexane, toluene or methanol. Unlike assembly **10**, the emission shift of **11** is correlated with the polarity of the solvent, with polar solvents (excepting methanol) inducing blue shifts, whereas non-polar solvents cause red shifts or emission quenching. The vapoluminescent response is attributed to changes in excited-state energy levels, with the green emission due to a change from MLCT to ligand-centered (LC) transition. Non-polar solvents lower the energy of the MLCT state, resulting in red-shifted

emission and for hexane, toluene or methanol the MLCT state is lowered in energy so much so that vibronic quenching dominates (Figure 8).

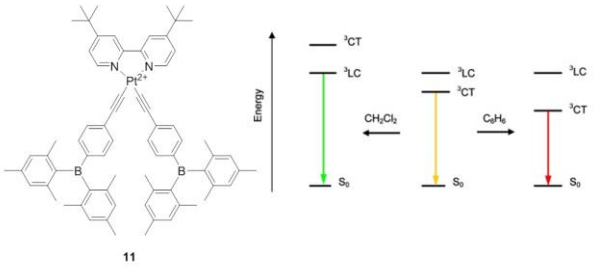

Figure 8. Impact of excited-state level modulation on the emission colors of **11**, using CH_2Cl_2 and benzene as representative examples. Reprinted with permission from ref [22]. Copyright 2011 American Chemical Society.

The previous two examples demonstrate that groups of vapors can elicit the same vapochromic response, but such cases preclude the development of selective sensors for a particular VOC. Castellano and co-workers, however, have demonstrated that microarray pattern recognition can be used as an alternative strategy.[23] Eighteen distinct cross-reactive Pt^{II} terpyridyl chloride complexes (**12a-f**), where the ligand substitution and counter-anion were varied, were incorporated into a microarray and exposed to different VOCs. The various Pt^{II} complexes respond differently to the VOCs, generating a pattern of colorimetric and luminescent changes (Figure 9).

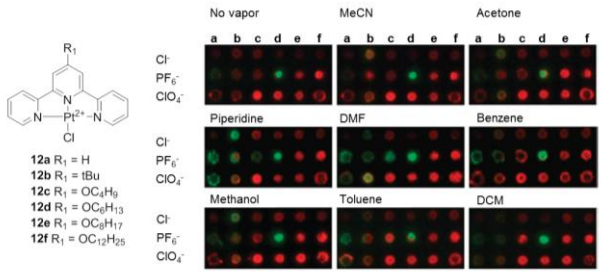

Figure 9. Vapoluminescent responses of Pt^{II} terpyridyl chloride-based microarrays to sense different VOCs. Adapted from ref [23] with permission of The Royal Society of Chemistry.

2.3 Multi-stimuli Responsive Solid State Materials

In the previous two sections, mechanochromic and vapochromic luminescent systems were described. This section focuses on multi-responsive systems. These systems are rare due to the difficulty in designing systems that respond to either grinding or VOCs, as highlighted in Sections 2.1-2.

Boilot and co-workers reported the copper iodide cluster $[Cu_4I_4(PPh_2(CH_2CH{=}CH_2))_4]$, which responds to both mechanical and thermal stimuli.[24] At room temperature, grinding converts the weak green emission into intense yellow emission, while at 77 K blue and purple emission are observed for the unground and ground samples, respectively. As the thermochromic properties of copper(I) iodide clusters have been well-studied,[25] these emission changes can be rationalized. These clusters typically have two emission bands, a low energy (LE) and a high energy (HE) one, with temperature dependent intensities; the LE band is attributed to a cluster-centered (CC) excited state due to a combination of halide-to-metal-charge transfer (XMCT) and copper-centered d to s and p transitions, while the HE band is attributed to a triplet halide-to-ligand charge transfer (XLCT) excited state. In the crystalline state, the CC and XLCT states do not appear to be coupled. At low temperature, emission from the XLCT state (HE band) dominates, resulting in blue emission. The intensity of this band decreases with increasing temperature (Figure 10). At room temperature, the weak green emission at room temperature is due to the LE band. Grinding restores the intensity and temperature dependent behavior of the LE band, resulting in intense yellow emission at room temperature. As the temperature decreases, this band decreases in intensity as the HE band intensity increases and at low temperature emission from the HE band dominates. These mechanochromic properties are believed to be due to Cu-Cu interactions.

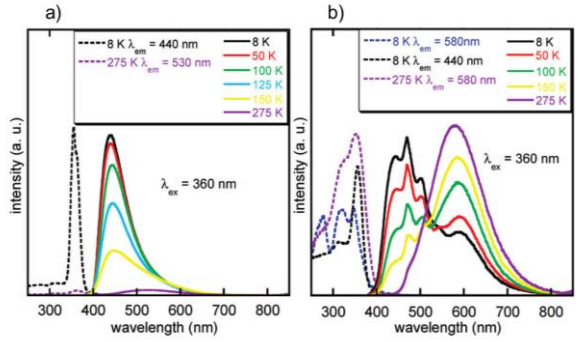

Figure 10. Solid-state luminescence spectra of a) uncrushed and b) crushed $[Cu_4I_4(PPh_2(CH_2CH{=}CH_2))_4]$ recorded between 275 and 8 K. Reprinted with permission from ref [24]. Copyright 2010 American Chemical Society.

Chen's Pt^{II} complex **13** exhibits remarkable luminescence responses to mechanical, chemical and thermal stimuli as highlighted in Figure 11.[26] The luminescence of the desolvated complex is bright yellow, with emission bands at 561 and 608 nm. Interestingly, the complex is unresponsive to VOCs such as 1,2-dichloroethane (DCE) and dichloromethane (DCM), but exhibits a selective vapochromic response for the O-heterocyclic VOCs tetrahydrofuran (THF), tetrahydropyrane (THP) and dioxane resulting in a red shift of the emission. The observed mechanochromism is dependent on the solvation state of the complex; emission of the desolvated complex and solvates with DCE or DCM is red-shifted upon grinding, whereas grinding induces a blue shift of the vapochromic solvates with THF, THP and dioxane. Finally, heating triggers a luminescence change from yellow to red emission for the desolvated complex and solvates with DCE or DCM. The cause of the multi-stimuli responsive behavior has been attributed to intermolecular Pt-Pt interactions based on DFT and X-ray crystallographic studies.

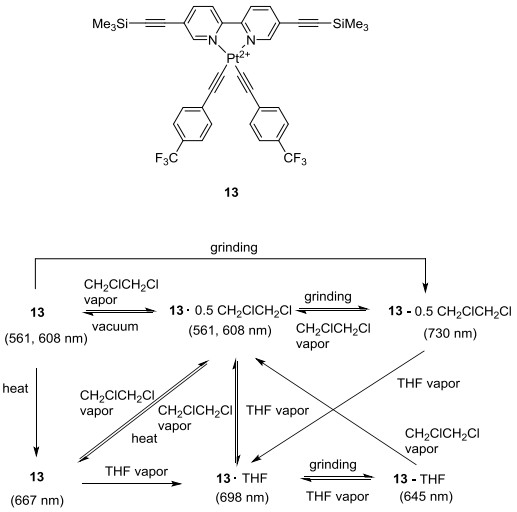

Figure 11. Interconversion processes for solid material based on Chen's vapo- and mechanochromic Pt^{II} complex.[26]

As discussed in Section 2.1, the luminescence of metal complexes in the solid state can be reduced by ACQ, making the observation of stimuli-responsive behavior more difficult. Conversely, aggregation induced emission[27] (AIE) materials emit more efficiently when aggregated than in dissolved form, and furthermore, mechanochromic luminescent properties are expected with the introduction of an AIE unit into a metal complex. Therefore, AIE metal complexes have the potential to sidestep problems associated with ACQ and expand the family of mechanochromic luminescent complexes.[7] The Zn^{II} complex **14** (Figure 12) is the first metal complex reported to exhibit both multi-stimuli responsiveness and AIE.[28] Grinding causes an emission color change from blue to yellow which can be reversed upon exposure to methanol vapor. Heating the ground sample did not reverse the color change but instead resulted in green emission. Regrinding samples exposed to heat or methanol vapor restored their yellow luminescence. The complex was also responsive to acid and base due to protonation of the pyridine moiety; upon exposure to trifluoroacetic acid vapors the luminescence was switched off. Emission could be switched on again by exposure to triethylamine vapors.

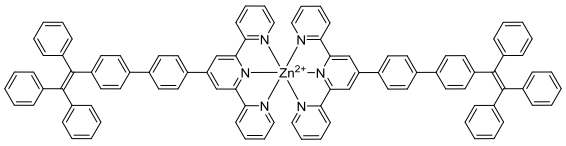

14

Figure 12. Multi-stimuli responsive Zn complex exhibiting aggregation-induced emission.[28]

3 Macrocycles

The discussion in this section will focus on metallacycles referred hereon as macrocycles rather than coordination complexes of macrocyclic ligands which are described within sections 5 and 6. The formation of macrocycles using the defined geometries of metal-ligand coordination to control structure is an extensive field.[29] However, there are relatively few examples of stimuli-responsive metal organic macrocycles. Common strategies to incorporate stimuli responsiveness include designing ligands that on application of a stimulus change their geometry, taking advantage of the stimuli-responsiveness of the metal ions themselves, and addition of competing ligands.

3.1 Light Responsive Macrocycles

Macrocycles can be rendered photo-responsive by incorporating photoactive functional groups that cause the ligand geometry to change. A key example of this is Lees *et al*.'s azobenzene incorporating homo- or hetero-metallic macrocycles,[30] which exhibit reversible interconversion between tetranuclear (**15** and **17**) and dinuclear (**16** and **18**) squares through the *cis*/*trans* isomerization of azobenzene on irradiation with light or heating (Figure 13).

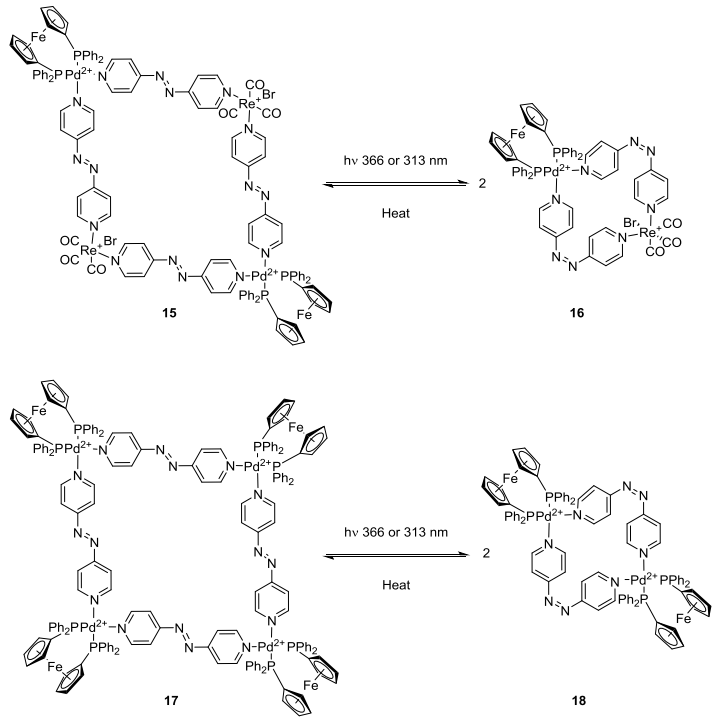

Figure 13. Light driven interconversion of both homo- and hetero-metallic macrocycles.[30]

Yam *et al.* have also introduced azobenzene based photoresponsive groups into tetranuclear macrocyclic Au^{I} alkynyl phosphine complex **19**, which upon irradiation with UV light distorts as one azobenzene unit isomerizes. This distortion was reversible but could be prevented by the addition of Ag^{I} cations, which locked the assembly in the all *trans* isomer (Figure 14).[31]

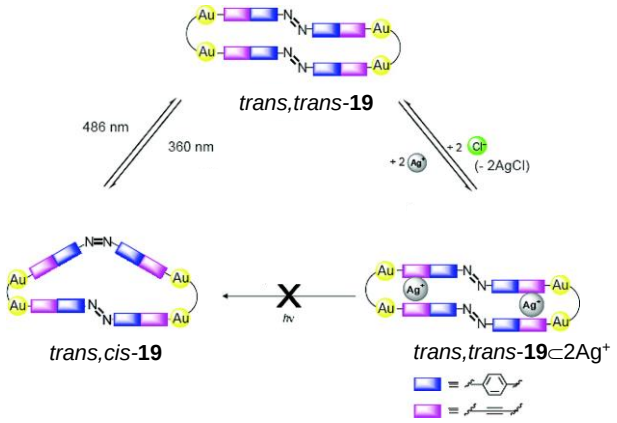

Figure 14. Light driven interconversion of *trans,trans*-**19** into *trans,cis*-**19** and locking via Ag^{I} coordination. Reprinted with permission from ref [31]. Copyright 2007 American Chemical Society.

Recently Yang and Zhu *et al.* have also created photoresponsive macrocycles **23 and 24** which incorporate a bisthienylethene photoswitch into an angled dipyridyl ligand **20**.[32] Self-assembly with either a linear diplatinum species **22** or a bent diplatinum species **21** produced either a [6 + 6] (**24**) or a [3 + 3] (**23**) hexagon, respectively (Figure 15). It was observed that upon irradiation with UV light, the bisthienylethene photoswitches cyclize and rigidify the macrocycle.

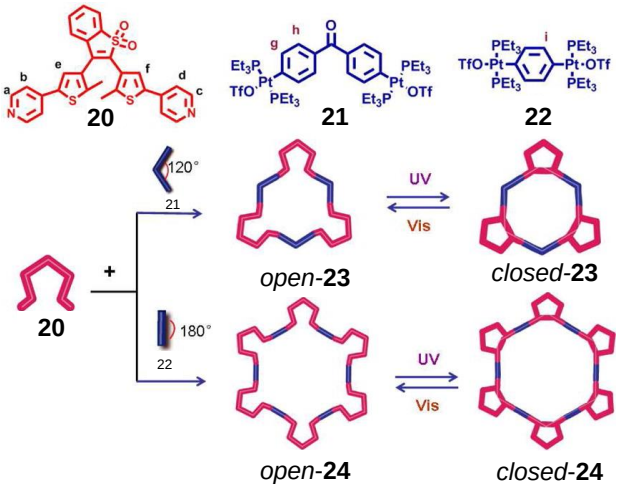

Figure 15. Poly-bisthienylethene containing macrocycles **23** and **24** and their cyclisation via UV irradiation. Reprinted with permission from ref [32]. Copyright 2012 American Chemical Society.

3.2 Chemically Responsive Macrocycles

Ligands can also be designed to contain functional groups that react to change the geometry of the ligand in a defined way. Stang *et al.* exploited the coordination of $Co_2(CO)_8$ **29** to alkynes in order to bend a bis(4-pyridyl)acetylene ligand **25**, and thus cause the structural transformation of both a [6+6] hexagon **28** into a [3+3] hexagon **30** and a mixture of [4+4] square **31** and [3+3] triangle **32** into a [2+2] rhomboid **33** (Figure 16).[33]

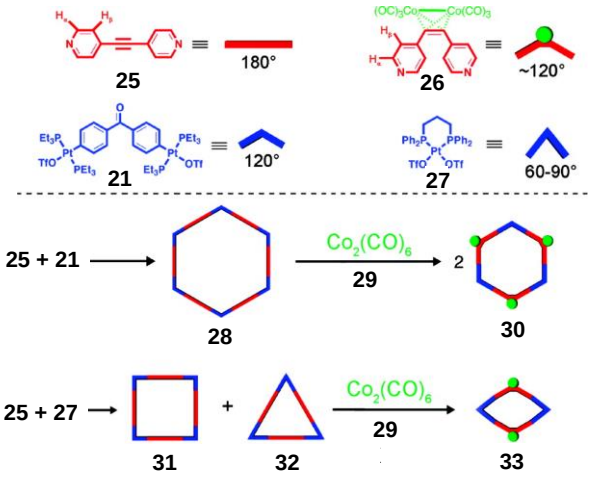

Figure 16. The structural interconversion of a metallo-macrocycle *via* chemical modification of the geometry of a ligand. Reprinted with permission from ref [33]. Copyright 2008 American Chemical Society.

Similarly, Hupp *et al.* introduced a salen-based metal ion coordinating site into a dipyridyl ligand. The resulting [2+2] macrocycle **34** formed upon addition of *cis*-$(PEt_3)_2Pt(OTf)_2$ transformed upon addition of Zn^{II} ions into the related [4+4] square **35** (Figure 17).[34]

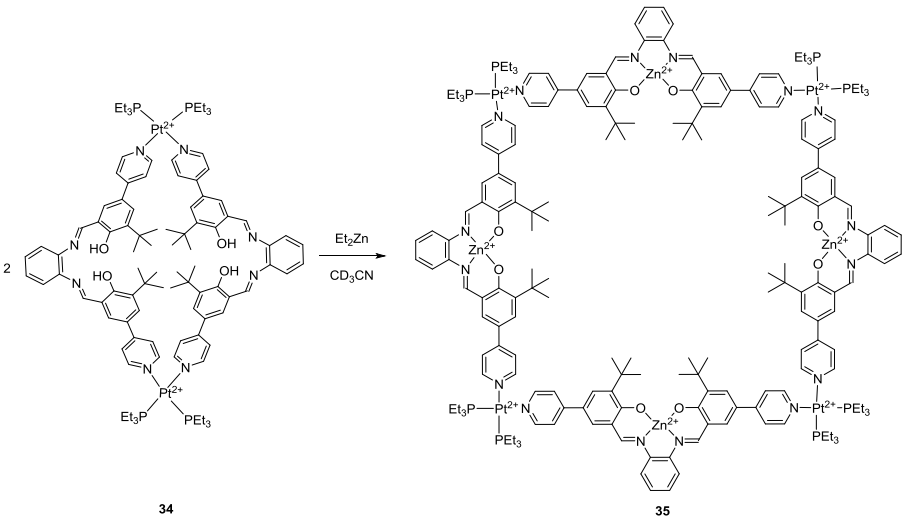

Figure 17. The expansion of a metallo-macrocycle upon coordination of Zn^{II} to a salen type ligand.[34]

The chemical responsiveness of the metal centers that make up the metallo-macrocycles has also been exploited. Mirkin *et al.* have developed the "weak link"[35] and halide induced

rearrangement[36] approaches to stimuli responsive assemblies and have created a range of macrocycles and other complexes that respond to the coordination of ligands such as CO, MeCN and chloride to transition metal complexes.

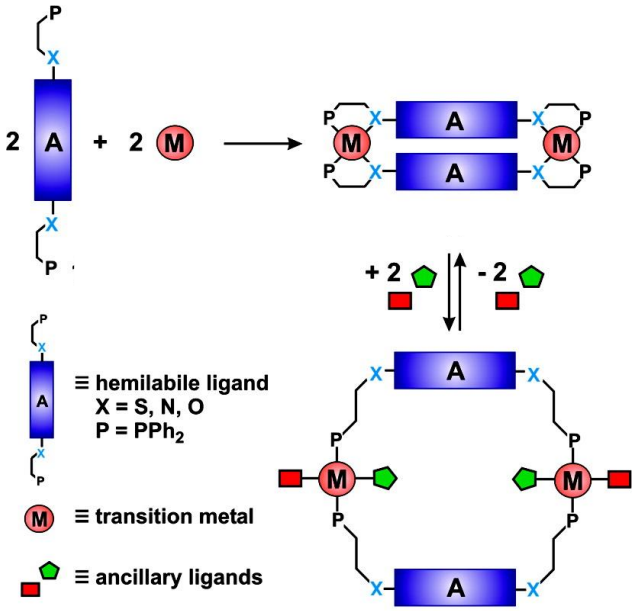

Figure 18. The weak link approach to chemically responsive metallomacrocycles. Reprinted with permission from ref [36]. Copyright 2008 American Chemical Society.

The weak link approach uses flexible hemilabile ligands that form both strong and weak coordination bonds with a metal center to construct multimetallic macrocycles (Figure 18). These macrocycles can be switched between different structures by selectively and reversibly breaking the weak coordination bonds through coordination of competing small molecules.[37] This approach has been exploited in the formation of allosteric catalysts and enzyme mimics.[38]

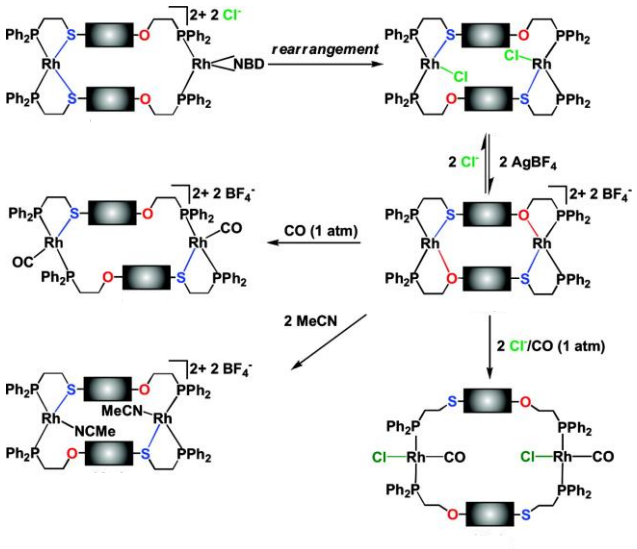

Figure 19. The halide induced rearrangement approach to chemically responsive metallo-macrocycles. Reprinted with permission from ref [36]. Copyright 2008 American Chemical Society.

The first halide induced ligand rearrangement was observed in macrocycles containing Rh^{I} *cis*-thioether/cis-phosphine and Rh^{I}-NBD/*cis*-phosphine (NBD is norbornadiene) metal centers. On addition of a halide, the complexes are converted to condensed hetero ligated macrocycles not accessible by any other technique (Figure 19).[39] These too can be interconverted between closed and open forms on addition of coordinating ligands and have been used to form macrocycles containing salen type ligands[40] and porphyrins.[41]

Mirkin *et al.* have also reported copper-based triangular macrocycle **38** that converts into a helical coordination polymer **39** upon changes in solvent.[42] The conversion is reversible and relies on the coordination of either a methanol or pyridine molecule to the copper ion that interconnects the carboxylate groups (Figure 20).

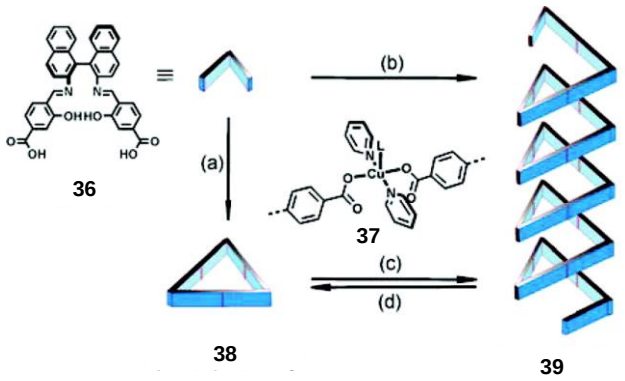

Figure 20. Solvent-induced formation of a helical coordination polymer from a Cu-based macrocycle. (a) $Cu(OAc)_2 \cdot 6H_2O$, MeOH/pyridine = 3/10; (b) $Cu(OAc)_2 \cdot 6H_2O$, MeOH/pyridine = 10/1; (c) MeOH; (d) pyridine. Reprinted with permission from ref [42]. Copyright 2007 American Chemical Society.

Ligand exchange was also found to cause structural rearrangement in a Ni^{II} based metallomacrocycle formed from artificial β dipeptides. The addition or removal of water induced the coordination of a nitrate molecule to the Ni^{II} center, thus causing structural interconversion in the solid state.[43]

Stang *et al.* have also developed a series of macrocycles and cages that form and interconvert based on the principal of self-assembly via charge separation.[44] A variety of hetero-ligated Pt^{II}-based metallomacrocycles have been formed and, can be converted into related supramolecular boxes and cages (Figure 21).

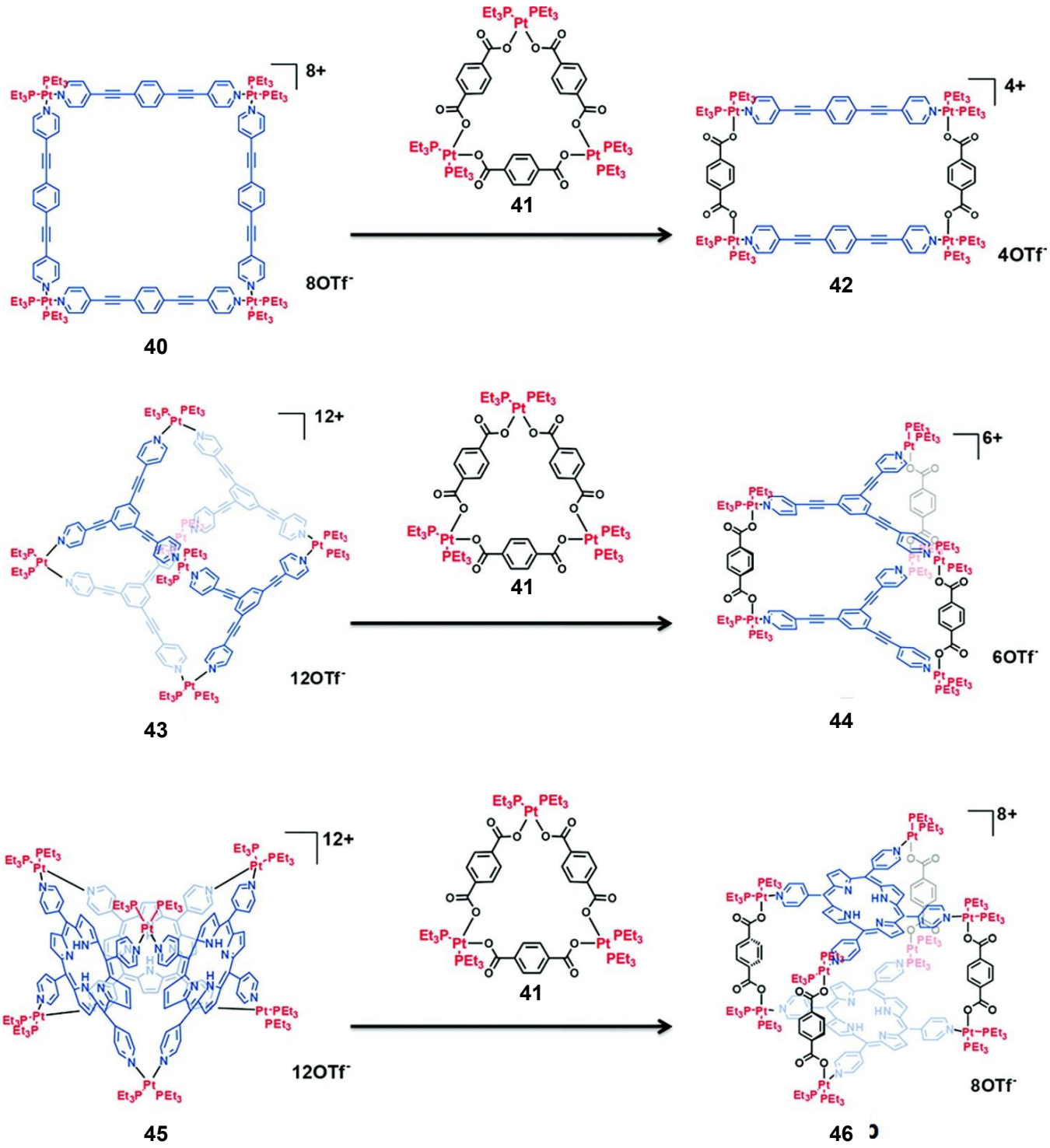

Figure 21. The conversion of Pt^{II}-based macrocycles based on the principle of self-assembly via charge separation. Reprinted with permission from ref [44]. Copyright 2010 American Chemical Society.

Similarly, Schmittel *et al.* have demonstrated the spontaneous fusion of Cu^{I}-based triangles and a Cu^{I}- and Zn-porphyrin-containing molecular square to form a mixed-ligand triangular

macrocycle.[45] In addition, they have developed metal-organic racks and ladders based on bis-phenathroline-containing ligands similar to those in the above example. Transmetalation of the Cu^{I} centers to Zn^{II} caused one metal organic ladder to become fluorescent, and further transmetalation with Hg^{II} returned it to a non-fluorescent state.[46] Recently, a similar Cu^{I} containing rack was shown to convert into the Cu^{I}-based ladder upon a change in stoichiometry.[47]

We have demonstrated the interconversion of macrocycles using the addition of carboxylate templates. A metallomacrocycle $[Cu_2L_3](BF_4)_2$ (**49**), formed via subcomponent self-assembly from 6-(diphenylphosphino)picolinaldehyde, $CuBF_4$ and a triethylene glycol linked dianiline, could be reversibly converted to the corresponding dimer (**47**) or trimer (**51**) upon addition or removal of either terephthalate (**48**) or 1,3,5-tris(4-carboxyphenyl)benzene (**50**, Figure 22).[48]

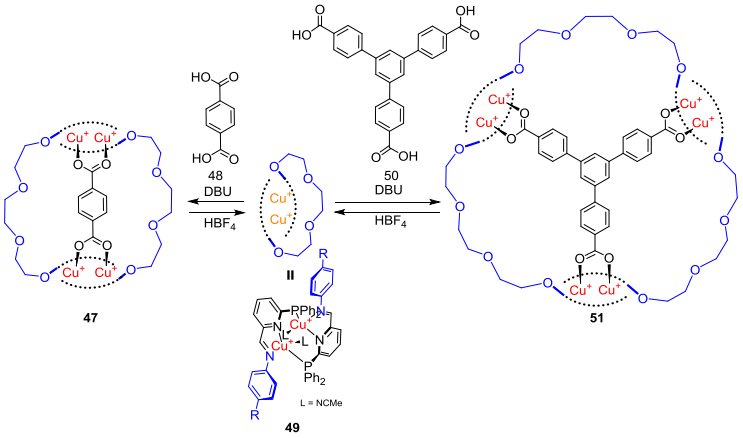

Figure 22. Template-induced structural rearrangement of a Cu^{I} based metallo macrocycle. Reprinted from ref [48] with permission of The Royal Society of Chemistry.

4 Helicates

Helicates have garnered much attention over the years[49] and many have included stimuli responsive properties. Recently, helicates synthesized with precise, easily modifiable structures similar to that of peptide α-helices, have shown potential as chemotherapy agents.[50]

4.1 Light Responsive Helicates

Nishihara *et al.* have reported the light responsive helical complex **52**[51] in which four azobenzene moieties are appended to the 6 and 6′ positions of two 2,2′-bipyridines coordinated to a copper(I) center (Figure 23). The crowded environment around the metal center allowed the *cis/trans* isomerization of the azobenzene units to influence the coordination of the ligands to, and thus modulate the redox properties of, the Cu^{I} center.

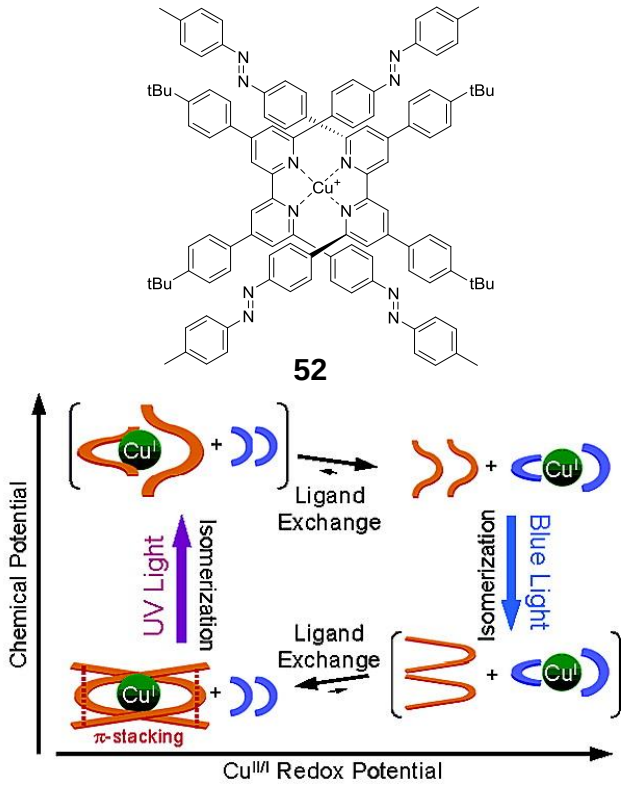

Figure 23. Light driven ligand exchange between two helical Cu^{I} complexes. Reprinted from ref [51]. Copyright 2005 American Chemical Society.

4.2 Electrochemically Responsive Helicates

Electrochemically responsive Cu^{I} based double stranded helicates have been the subject of a recent review;[52] this section will thus highlight only a few key examples. Many electrochemically responsive helicates rely on the alteration of the coordination preference of metal ions upon changes in oxidation state. Potts and Abruña *et al.* have designed helicate **55** that converts into mononuclear copper complex **54** upon oxidation (Figure 24).[53]

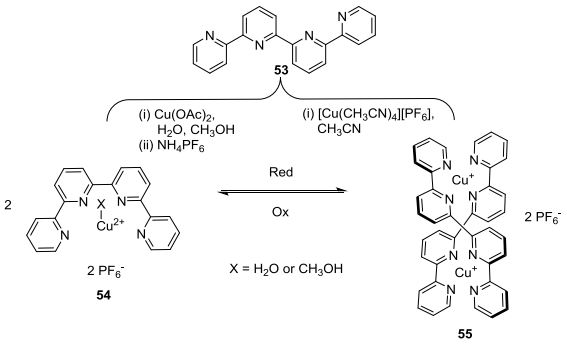

Figure 24. Helicate to mononuclear complex interconversion via changes in copper oxidation state.

Similarly Fabbrizzi *et al.* synthesized a subcomponent-based electrochemically responsive copper based helicate and further studied its interconversion using a second fluorescent ligand.[54]

Lehn et al. reported interconversion between a Cu^{II} based grid (**56**) and Cu^{I} helicate (**57**) through chemical oxidation or substitution. The response is reversible and the Cu^{II} can be reduced with ascorbic acid (Figure 25).[55]

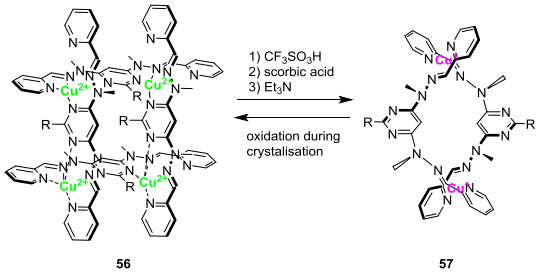

Figure 25. Interconversion between a Cu^{II} grid and Cu^{I} helicate via chemical oxidation.

4.3 Chemically Responsive Helicates

Lehn *et al.*'s earlier extensive studies of helicates have yielded many stimuli responsive examples. Many involve helical metal ion chelators and their transformation to linear strands, grids or expanded helicates on addition or removal of metal ions.[56] Due to the coiled nature of the helicates and the large number of monomer units that may be incorporated into them, a large change in molecular size can be effected (Figure 26).

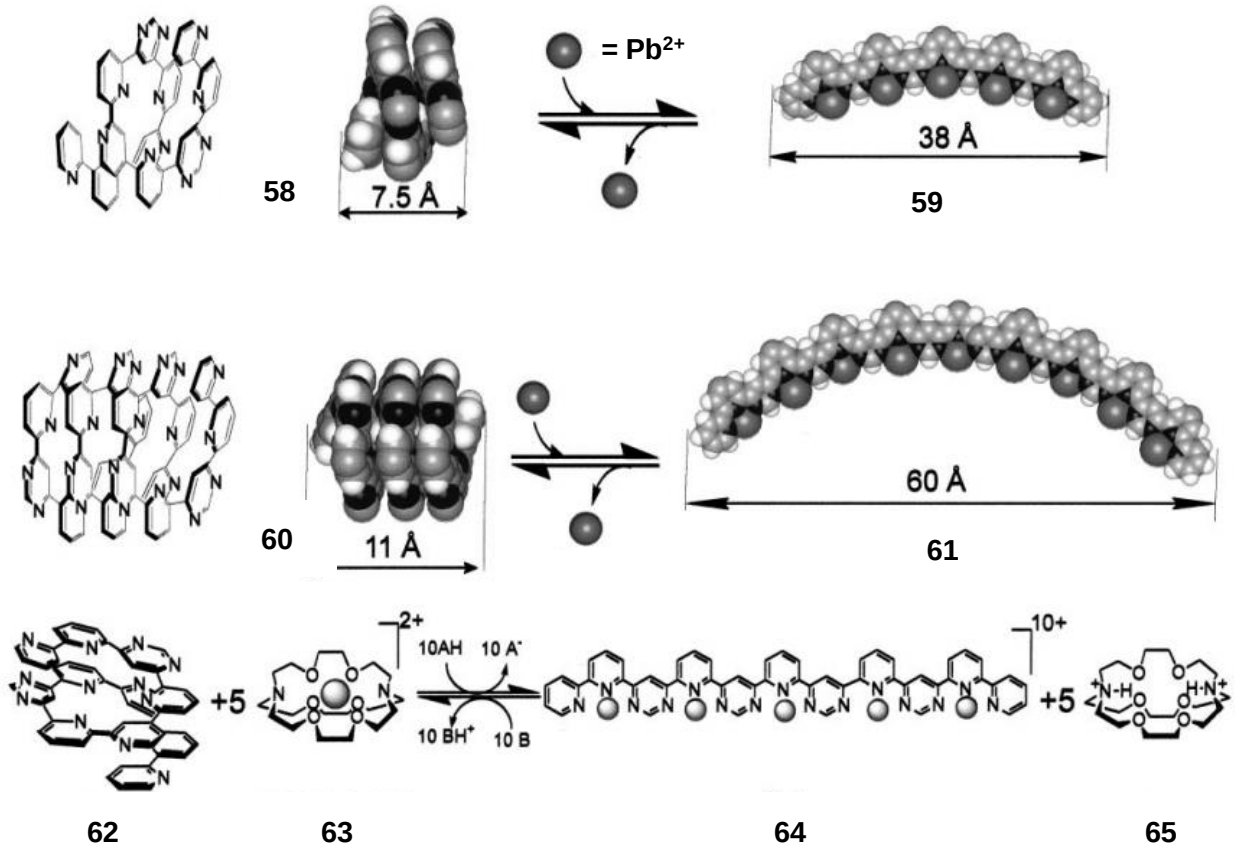

Figure 26. The coordination of metal ions to organic helical ligands to effect significant structural change. Reprinted with permission from ref [56d]. Copyright (2002) National Academy of Sciences, U.S.A.

Within our group helicates formed via subcomponent self-assembly have been shown to interconvert via subcomponent exchange, whereby a more electron rich amine, such as **66**, substitutes for a less electron rich amine **73** within pyridylimine metal complexes.[57] The sensitivity of this exchange to the electronic effects of substituents on anilines has allowed the creation of networks of cascading interconversion between different helicates (**68**-**70**, **72**)[58] and other topologically complex architectures.[59]

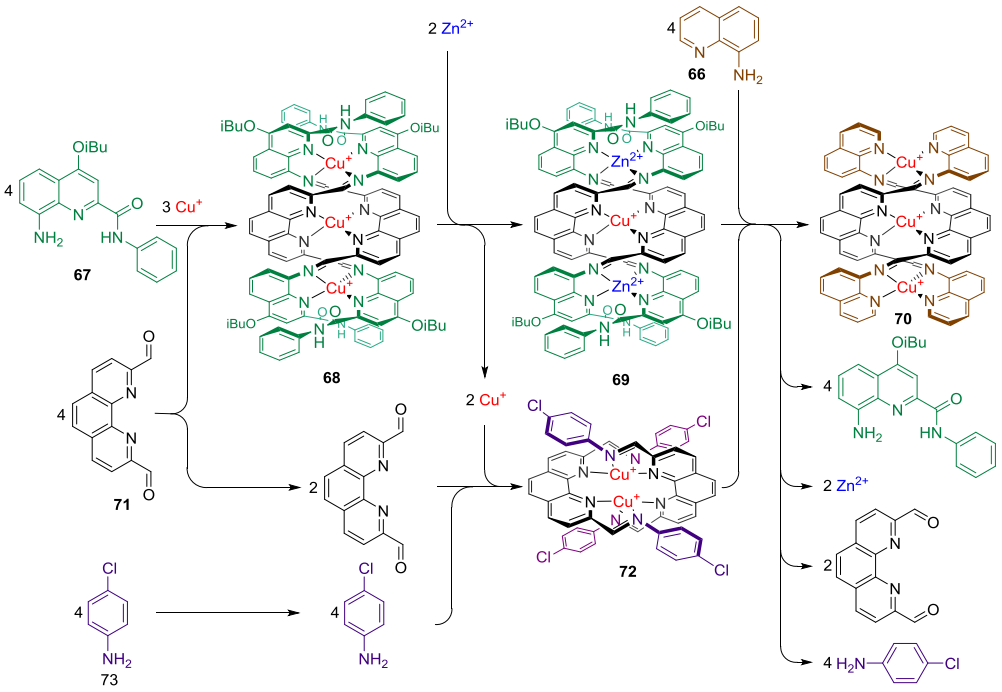

Figure 27. Cascading network of transformations via subcomponent substitution. Reprinted with permission from ref. [58].

A further method for converting between architectures exploits the differing pKa values of the associated amines. When acid is introduced to a system with two types of amine subcomponents, the more basic amines are preferentially protonated and thus do not form pyridyl imines. This effect can be exploited to bring about reversible transformations between helicates **76** and **77** (Figure 28).[60]

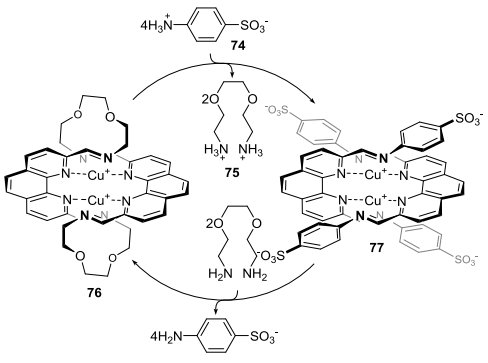

Figure 28. pKa dependent subcomponent exchange on Cu^{I} helicates. Reprinted with permission from ref. [60] Copyright 2006 Wiley-VCH.

The incorporation of functional groups into the ligands of a helicate that can undergo dynamic covalent exchange has also been used for chemical transformation. A collaboration between Otto's and our group has shown that helicates containing disulfide bonds re-equilibrate into a series of different products on addition of different disulfides.[61]

In order to make helicates that respond to an alkali or alkaline earth cationic signal, Rice *et al*. introduced crown ether macrocycles onto the periphery of a helicate. The binding of either Na^+ or Ba^{2+} cations into the receptor sites causes a structural reconfiguration from helicate **78** to a side-by-side structure **79** (Figure 29).[62]

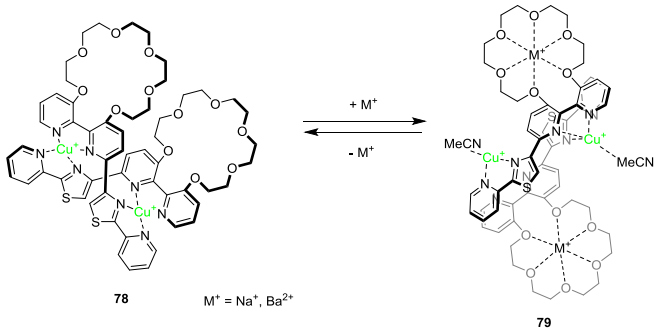

Figure 29. Cation-induced structural rearrangement of a Cu^I helicate.

Henry *et al.* observed the solvent-dependent formation of either a trinuclear circular helicate or a dinuclear double-stranded helicate when a ligand formed from two 3-phenyl-2,2'-biphenol units linked by a *p*-phenylene linker self assembled with $Ti(^iPrO)_4$. Upon self assembly in *n*-pentane, a triangular helicate was formed, but in toluene a dinuclear helicate was observed. When crystals of the triangular helicate were dissolved in DCM, the structure reconfigured into the dinuclear helicate.[63]

4.4 Mechanically Responsive Helicates

Deak *et al.* have reported a series of mechano-responsive Au_2L_2 helicates similar to the mononuclear complexes mentioned in Section 2. Both mechanical and chemical stimuli were found to alter the luminescent properties (Figure 30).[64] Solvent-assisted ball milling was shown to facilitate the anion-exchange of a $[Au_2L_2](NO_3)_2$ digold(I) helicate. Either

amorphous or crystalline forms of the complex were created depending on the nature of the grinding liquid (Figure 30).

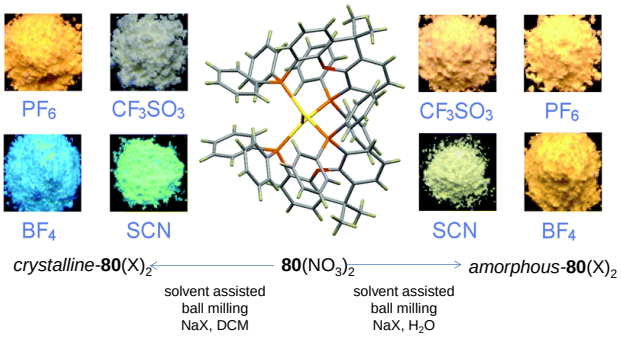

Figure 30. A mechanically responsive Au_2L_2 helicate. Adapted from ref [64a] with permission of The Royal Society of Chemistry.

5 Non-interlocked Molecular Machines, Switches and Mechanisms

The biological molecular machines found in nature, such as ATP synthase, are a source of inspiration for artificial molecular machines.[65] There are also examples of biomolecules, such as peptides, that contain metal centers and exhibit stimuli-responsive behavior.[66] Stimuli-responsive behavior is exploited to achieve molecular motion in molecular machines and switches, although the type of motion depends on the function of the system. The distinction between a molecular switch and machine goes beyond the scope of this review. However, the reader's attention is drawn to the reviews by Stoddart[67] and Leigh[68] for a more comprehensive discussion of the distinction. For ease of discussion, the topic of the responses of molecular machines and switches to stimuli will be divided into two sections; this section will focus on systems based on non-interlocked structures, while the next will discuss those based on interlocked structures, such as rotaxanes and catenanes.

5.1 Metal Ion Translocation Systems

Transition metal ions have been showed to move reversibly between inequivalent compartments of multitopic ligands using various stimuli. This concept has been the subject of a recent and comprehensive review.[69]

5.1.1 Chemically Responsive Systems

Sauvage and co-workers synthesized macrocycle **81** containing bidentate and tridentate chelating groups arranged in alternating fashion (Figure 31).[70] This macrocycle was found to bind either Fe^{II} or Cu^{I}, resulting in the formation of metal complexes having a figure-of-eight geometry. In the octahedral Fe^{II} complex **82**, the long axis was described as 'horizontal' with a height of ~11 Å, whereas in the tetrahedral Cu^{I} complex **83**, the long axis was 'vertical' with a height of ~30 Å. These complexes could be easily demetalated to afford the metal-free macrocycle, which could then be remetalated. By taking advantage of this metalation-demetalation-remetalation process, the compound could be switched between the contracted or elongated states. Similarly, electrochemical switching between Cu^{I} and Cu^{II} also generated the horizontal and vertical geometries, respectively, as inferred by cyclic voltammetry (CV).

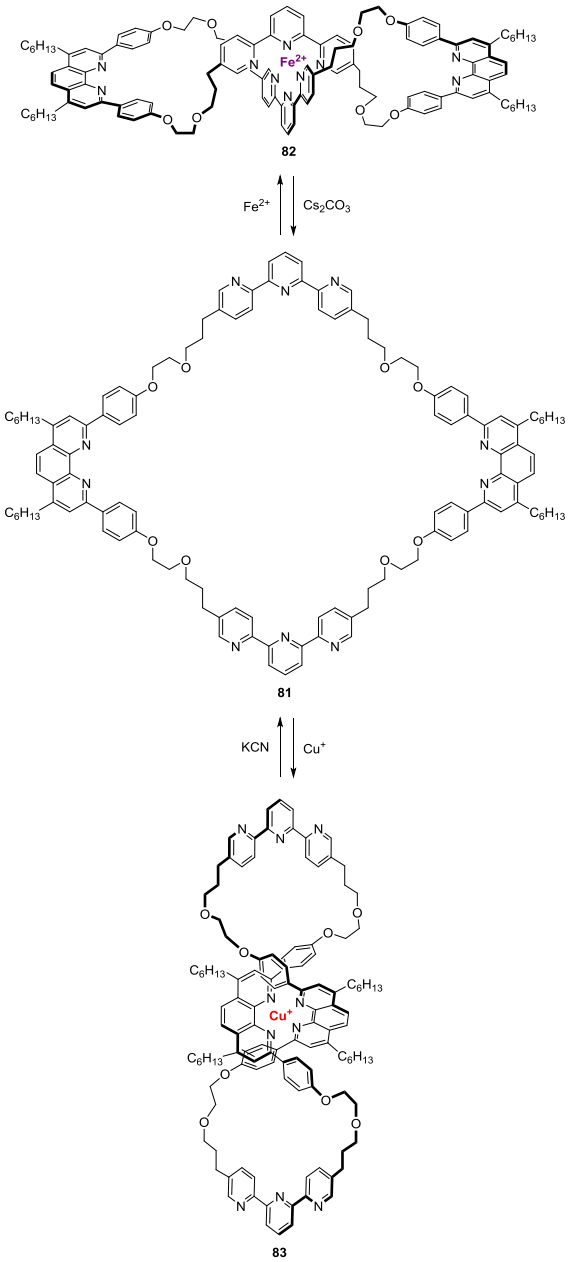

Figure 31. Metal-mediated switching between horizontal (top) and vertical (bottom) figure-of-eight geometries of macrocycle **81**.[70]

5.1.2 pH Responsive Systems

Fabbrizzi and co-workers synthesized ligand **84** (Figure 32) containing two metal coordinating compartments: (i) compartment B, consisting of two amine nitrogen atoms and two quinoline nitrogen atoms, and (ii) poorly coordinating compartment AH_2, consisting of two amine nitrogen atoms and two amide nitrogen atoms. Upon deprotonation of the two amide groups, however, AH_2 gave the strongly coordinating donor set A^{2-}.[71] At pH = 7.5, Ni^{II}

binds to compartment B (high-spin state, octahedral coordination) and at pH ≥ 9.5, Ni^{II} is located in the adjacent A^{2-} compartment, as a low-spin center, in a square planar arrangement. By varying the pH from 7.5 to 9.5, reversible translocation of the metal ion from one compartment to the other was demonstrated. Furthermore, when a fluorophore (anthracene, in **85**) was covalently linked to the AH_2 moiety, the Ni^{II} translocation switched the fluorescence on and off through a photoinduced electron transfer (PET) process.

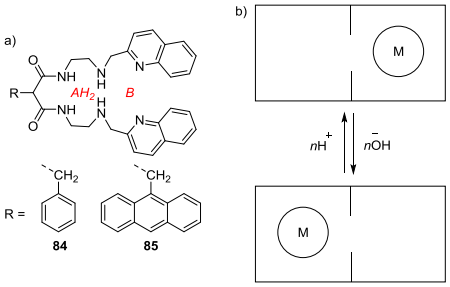

Figure 32. a) Chemical structure of receptors **84** and **85**, containing two metal binding compartments and b) schematic representation of the pH controlled translocation of Ni^{II} between the two compartments.[71]

5.1.3 Electrochemically Responsive Systems

Shanzer and co-workers have reported redox switches that interconvert between two distinct states.[72] A triple helicate ligand (**86**, Figure 33) containing two metal binding sites – an internal "hard" binding cavity functionalized with hydroxamate, and an external "soft" binding cavity functionalized with bipyridyl was employed for this study.[72a] Fe^{III} ions bind preferentially to the internal cavity. Upon reduction using ascorbic acid, the Fe^{II} ions translocate to the external cavity. This process was found to be reversible by re-oxidizing to Fe^{III} with ammonium persulfate. The translocation process could be readily followed based upon the difference in color between the Fe^{III}-hydroxamate (brown) and Fe^{II}-bipyridyl (purple) complexes. The achiral molecule **87**, which differed from **86** by lacking the L-alanyl acid moiety, exhibited the same behavior, but differed in the rate of reduction. Subsequently, the calix[4]arene derivative **88** functionalized with hydroxamate ("hard") and bipyridyl ("soft")

groups was reported.[72b] In the presence of Fe^{III}, the hydroxamates ("hard" binding groups) converge to embrace the "hard" metal ion and upon reduction, the ligand rearranges to engulf Fe^{II} with its "soft" bipyridyl groups. This process could also be reversed by oxidation. The switching process could be monitored in real time on the basis of the color change from orange to pink upon reduction.

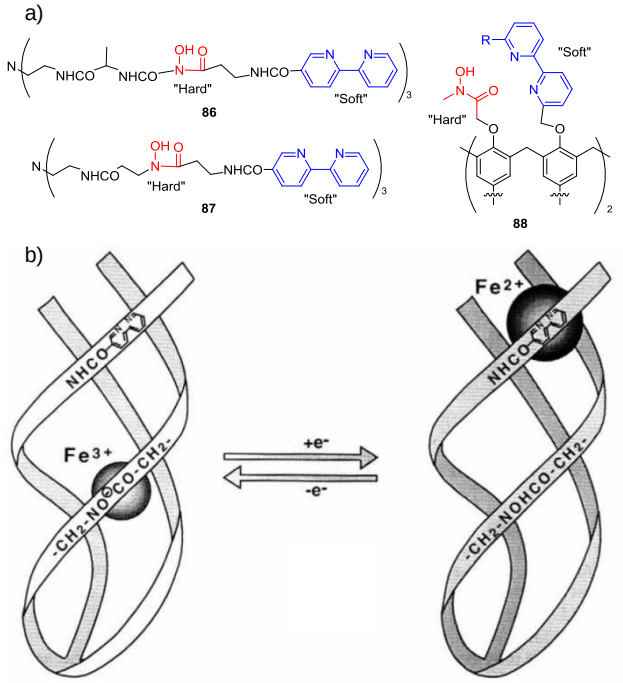

Figure 33. a) Chemical structures of mixed ligand binders **86-88**[72] and b) schematic representation of the triple-stranded metal complexes that function as molecular switches. Reprinted by permission from Macmillan Publishers Ltd: Nature [72a], copyright (1995).

Schmittel and co-workers have reported that the two heteroleptic complexes $[Cu(\mathbf{89})(\mathbf{90})]^{+}$ and $[Cu(\mathbf{89})(\mathbf{90})]^{2+}$, prepared from the ligands **89** and **90** (Figure 34), interconvert upon changing the oxidation state of their copper ions.[73] By incorporating these two ligands into the scaffold **91** and taking advantage of redox-triggered switching, translocation of ligand **90** and copper reversibly between two different stations has been demonstrated. In the presence of Cu^{I}, ligand **90** occupies the $PhenAr_2$ stations, whereas in the presence of Cu^{II}, the cargo molecules were found to occupy the $TerpyAr_2$ stations.

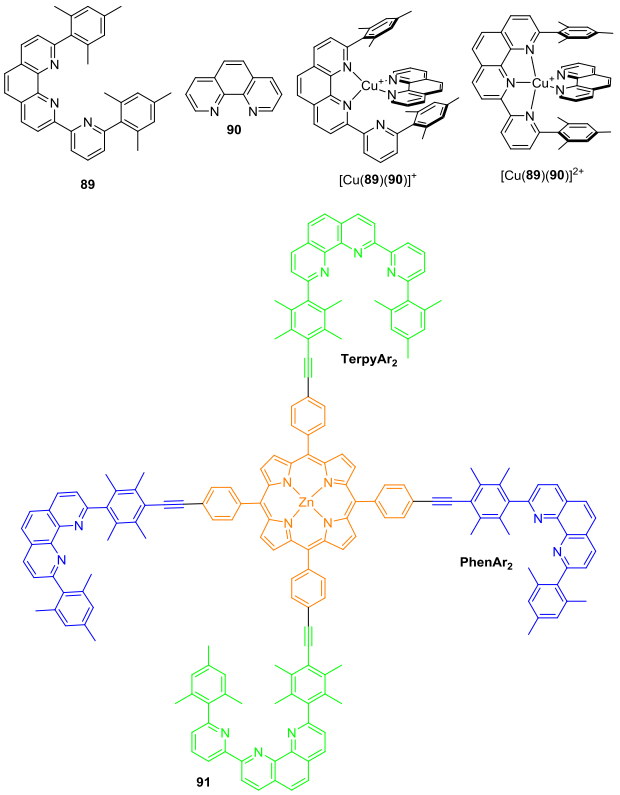

Figure 34. The building blocks of Schmittel's translocation system:[73] chemical structures of ligands **89** and **90**, the heteroleptic complexes formed from **89** and **90**, and the scaffold **91** incorporating these ligands.

5.1.4 Multi-stimuli Responsive Systems

Fabbrizzi, Pallavicini, Taglietti and co-workers have reported a polyaza macrocycle **92** which exhibits Cu^{II} translocation in response to pH changes and the presence of imidazoles (Figure 35).[74] The macrocycle consists of two metal binding compartments comprising of two diamide-diamine (DADA) tetradentate and two pyridine-diamine (PDA) tridentate binding sites. At pH > 10, the Cu^{II} ions bind to DADA sites. Upon lowering the pH, the amide groups are reprotonated, thus becoming non-coordinating. As a result, the two Cu^{II} ions translocate to the tridentate PDA units, with the other coordination sites being occupied by water molecules. In the presence of imidazole (Im), the formation of $[Cu_2(\mathbf{92}H_4)(Im)]^{3+}$ (Im⊂**92** in Figure 34) was observed, which predominates in the pH range of 6.0 to 10.0. This complex contains a bridging imidazolate anion (Im^-) and was stable below a pH of 10.2. Double cationic

translocation also occurs in the presence of imidazole and could be monitored *via* absorption spectroscopy. These spectroscopic changes were utilized to colorimetrically detect imidazole-containing biologically relevant substrates such as histidine and histamine.

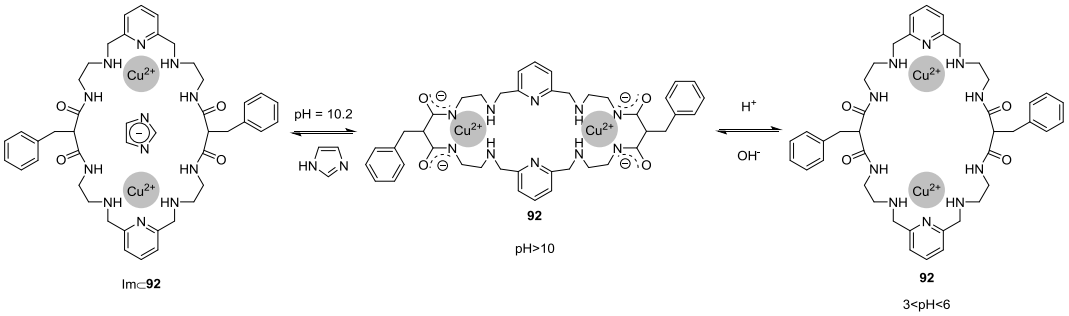

Figure 35. pH and guest induced intramolecular dislocation of the Cu^{II} ions within a receptor.[74]

5.2 Molecular Tweezers

Molecular tweezers are synthetic host molecules that are capable of binding guest molecules within a well-defined cleft. The nature of the arms defines the size and nature of the cleft, and facilitates binding of guests through non-covalent interactions. Since the arms are only connected at one end, the clefts are considered to be flexible, which is critical in determining the guest-binding properties. Molecular tweezers have received considerable attention in the past few decades and have been reviewed on several occasions.[75]

5.2.1 Chemically Responsive Molecular Tweezers

Lehn and co-workers have reported conformational switches that alternate between 'U' and 'W' shapes upon cation coordination and, as a consequence, bind or release a substrate.[76] The pyridine-pyrimidine-pyridine receptor (**93**, Figure 36) adopts a 'U'-shaped conformation in the absence of metal ions, and was found to bind planar aromatic guests through intercalation between the appended chromophores. The addition of Cu^{I} to the metal-free receptor brings about a conformational switching from a 'U' to a 'W' shape in order to incorporate the metal ion. This geometry was unsuitable for the intercalative binding of planar guests. The complex

may therefore be said to behave like a molecular tweezer, releasing the guest upon cation complexation. In contrast, the pyridine-pyridine-pyridine receptor (**94**) adopts a 'W' shape in the absence of metal ions and does not bind guest molecules. The addition of Zn^{II} results in a conformational change to a 'U' shape suitable for intercalative binding of guests.

Binding between receptors and guests involved charge-transfer interactions between the chromophores of the receptor and the guest molecule, and could be readily visualized through color changes. This work was followed up with the receptors **95** and **96** which exhibited metal-ion-induced shape switching, self-sorting and guest binding properties.[77] The metal complexes of ligand **95** have 'U' shapes, and upon reaction with a complementary diamine, resulted in bis(imine) macrocyclic structures. Similarly, ligand **96** could be converted from 'W' to 'U' shape through metal coordination. Planar aromatic guest molecules were found to intercalate into the cleft in the 'U' state, resulting in the formation of donor-acceptor complexes. Interestingly, the guest binding ability of this complex could be regulated by the nature of the metal ion. Complexation of M·**96** (wherein M = Pb^{II}, Hg^{II} or Zn^{II}) with pyrene was found to be 10 times stronger in the case of Pb^{II} than for Hg^{II} and negligible for Zn^{II}.

The behavior of a dynamic library consisting of ligands **95** and **96** with two different metal ions was also investigated. It was observed that these systems at thermodynamic equilibrium exhibited a self-sorting behavior, where the composition of the library could be modulated by the absence and presence of an intercalating guest. On the other hand, addition of metal to ligand **97** leads to the formation of a ML_2 complex and MLL-type heteroleptic complexes.[78]

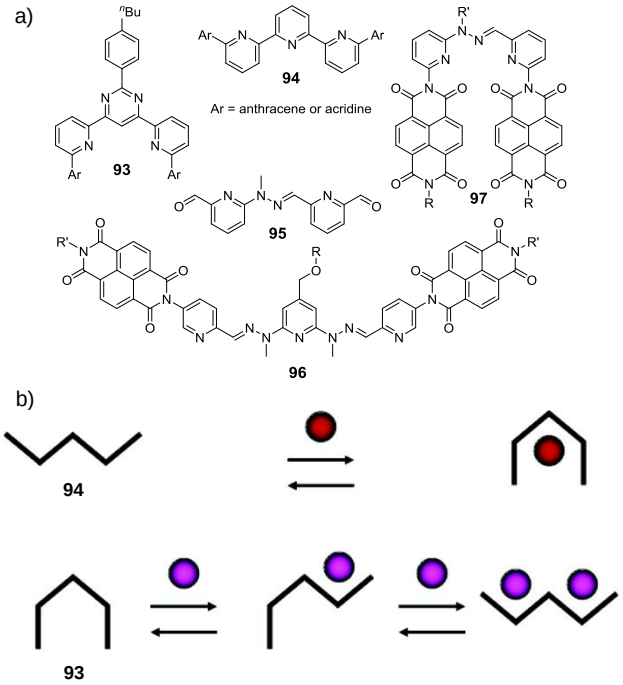

Figure 36. a) Structures of the conformational switches **93-97**,[76-78] and b) schematic representation of the two-stage (top) and three-stage (bottom) molecular shape switching processes induced by binding of metal ions to **94** and **93**, respectively.[76] Reprinted with permission from ref [76]. Copyright 2004 American Chemical Society.

Kim, Jang and co-workers have reported a porphyrin-based molecular tweezer **98** in which the direction of PET could be switched on the basis of guest binding (Figure 37).[79] This goal was achieved by utilizing a pair of zinc porphyrins connected by a bisindole bridge. In its native state, excitation energy flows from the bisindole moiety to the zinc porphyrins with high efficiency. The addition of Cu^{II} results in its complexation at the bisindole bridge, leading to significant quenching of its fluorescence. As a consequence, the direction of excitation energy flow reverses, i.e. the excitation energy of the zinc porphyrins flows to the Cu^{II}-coordinated bisindole. Subsequent addition of a bidentate ligand, such as pyrophosphate (PPi), results in a change in the coordination geometry of Cu^{II} from square planar to octahedral, thereby leading to decrease in the energy transfer efficiency from the zinc porphyrins to the Cu^{II}-coordinated bisindole.

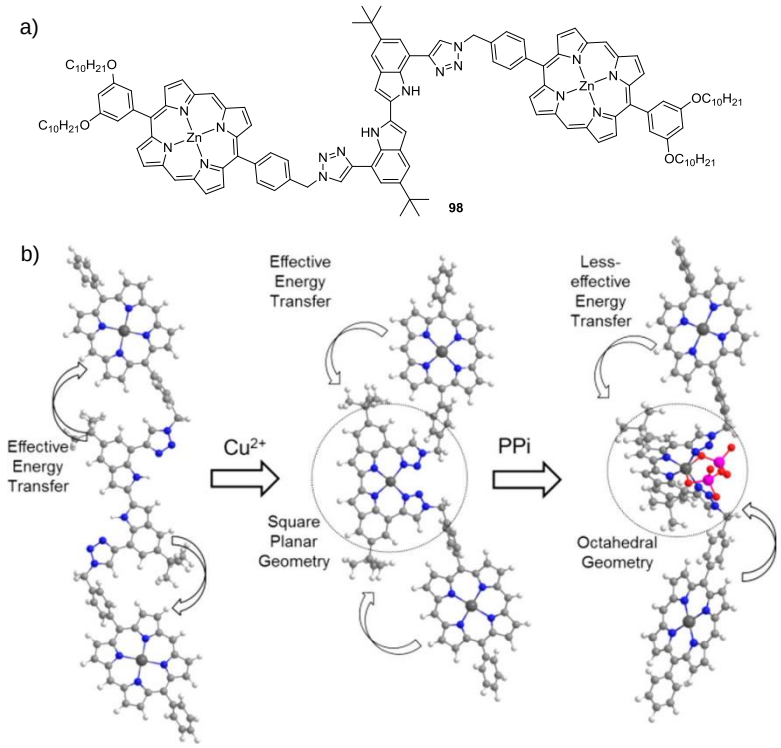

Figure 37. a) Chemical structure of bisindole-bridged-porphyrin tweezer **98** and b) representation of guest induced switching of excitation energy transfer.[79] Reprinted with permission from ref [79]. Copyright 2014 American Chemical Society.

Mirkin and co-workers have reported the solvent and temperature induced switching between the structural isomers of Rh^{I}-phosphinoalkyl thioether complexes (**99**, Figure 38).[80] These complexes could be switched between the *closed*- and *semiopen*-isomers, wherein the chloride counterion occupied the outer or inner coordination sphere of the metal ion, respectively. The preference for either isomer was found to be dependent on the solvent polarity, with more polar solvents favoring the *closed*-isomer. The isomer preference also depended on the electron donating ability of the R group, with electron donating groups favoring the *closed*-isomers and electron withdrawing groups favoring the *semiopen*-isomers.

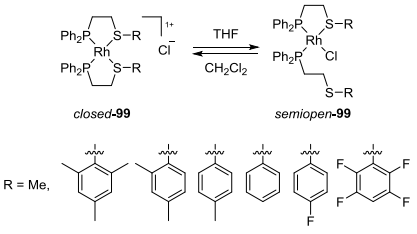

Figure 38. Switching between *closed*- and *semiopen*-isomers of Rh^{I}-phosphinoalkyl thioether complexes **99**.[80]

Mirkin and co-workers have also synthesized a triple-layer complex **100** composed of two transition metal nodes, two chemically inert blocking exterior layers, and a single catalytically active interior Al^{III}-salen complex (Figure 39).[81] The *semiopen* structure could be converted to the *closed* triple-layer structure through reaction with NaBArF (BArF = tetrakis[(3,5-trifluoromethyl)phenyl]borate) or $LiB(C_6F_5)_4$, whereas the reaction of the *closed* structure with Cl^- or CD_3CN resulted in the reverse reaction (to form the *semiopen* complex). The *semiopen* complex quantitatively catalyzes the ring opening polymerization of ϵ-caprolactone to polycaprolactone, whereas the *closed* form was inactive. The switching between the *semiopen* and *closed* structures was thus utilized to regulate the catalytic activity of the triple layer complex. The catalyst could be deactivated by the addition of NaBArF, which abstracts chloride and leads to the formation of the *closed* complex. Addition of acetonitrile to the *closed* complex yields the *semiopen* structure again and reactivates the catalyst, thereby allowing polymerization.

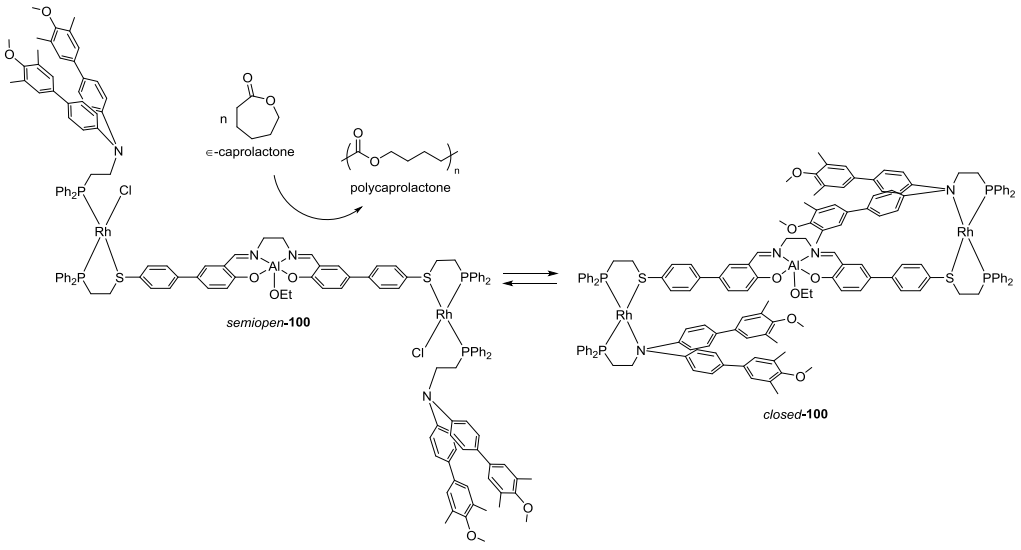

Figure 39. Switching between *closed* and *semiopen* isomers of the triple layer complex **100** for the regulation of the catalytic living polymerization of ϵ-caprolactone.[81]

5.3 Molecular Scissors

Angular motion of the cyclopentadienyl rings about the metal center in ferrocene has been utilized for developing molecular machines.[82] Kinbara, Aida and co-workers have reported chiral molecular scissors that performed a light-induced open-close motion.[83] Molecule **101** (Figure 40) consists of two phenyl groups (A) as the blade moieties, a ferrocene unit (B) as the pivot part, and two phenylene groups (C) as the handle parts, which are linked together by an azobenzene unit. In its native state, the azobenzene adopts a *trans*-configuration which keeps the blades in a 'closed' state. Upon irradiation with UV light (λ = 350 nm), the *trans*-azobenzene is converted to the *cis*-isomer, thereby inducing an angular motion of the ferrocene unit, which opens the blade moieties. Subsequent irradiation with visible light (λ > 400 nm) results in the *cis*- to *trans*-isomerization, which closes the blades. Later investigations established that upon changing the oxidation state of the ferrocene, the reversible open-close motion of molecular scissors could be actuated only by UV light.[84]

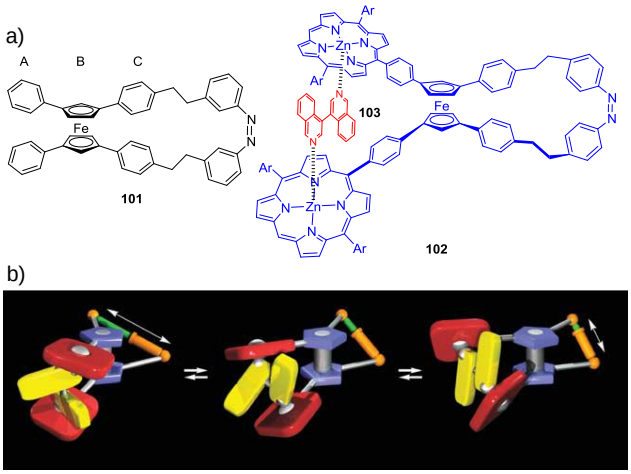

Figure 40. Chemical structures of light driven molecular scissors **101**[82] and **102**,[83] and schematic representation of a sequence of interlocked motions of **102**·**103** triggered by light. Reprinted by permission from Macmillan Publishers Ltd: Nature [85], copyright (2006).

Subsequently, Aida and co-workers attached zinc porphyrin units to the blades (**102**), which provided a binding site for guest molecules wherein bidentate ligands were found to coordinate in a 1:1 fashion with a high binding affinity.[85] Reversible photoisomerization of the

azobenzene strap in response to irradiation with UV and visible light induced a scissor- or pedal-like conformational change of the zinc porphyrins, which was translated into a twisting motion of the rotary guest **103** repeatedly in clockwise and counterclockwise directions. The rotary motion of the bound guest was monitored through circular dichroism (CD) spectroscopy: In isolation, the guest **103** is not optically (CD) active because of the free rotation about the C-C bond connecting the two bicyclic rings. However, upon binding to the host **102**, the guest **103** loses this freedom and becomes optically active. Upon irradiation with UV light, the CD intensity decreased, which suggested that the *trans*-to-*cis* isomerization of the azobenzene induced a conformational change (twist) in guest **103**.

Subsequently, the Aida group devised a signal transmission system (Figure 41) consisting of three different movable components; a chiral "scissoring" unit (**104**; red), an intermediate "bridging" unit (**105**; blue/purple), and a photochromic "signaling" unit (**106**; green).[86] These components were mechanically interconnected through coordinative interactions. Signaling unit **106** is a pyridine-appended dithienylethene (DTE) derivative, and can undergo switching between *open* and *closed* forms through irradiation. Scissoring component **104** involves a chiral tetra-substituted ferrocene core bearing two pyridyl groups, capable of coordinating to the zinc porphyrin handles of bridging module **105**. Bridging module **105** is a biaryl derivative bearing two sets of zinc porphyrin handles. Upon irradiation, **106** undergoes an opening or closing motion. As the bridging module is coordinated to the signaling unit, the opening/closing motion induced an angular motion in the bridging unit. This rotary motion translated into a scissoring motion of **104**. As in the previous examples, the scissoring motion was monitored through CD measurements.

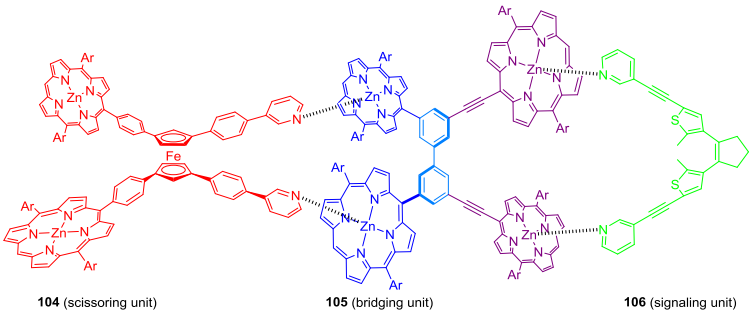

Figure 41. Ternary system utilized to demonstrate long-distance mechanical communication.[86]

5.4 Self-locking Systems

Within self-locking systems, non-covalent interactions between two or more functional groups generate the locked state, which can be unlocked by application of a stimulus that exposes previously hidden chemical functionality. Thus, self-locking systems can be switched between the locked and unlocked states, which have different properties.

5.4.1 Chemically Responsive Self-locking Systems

Durola and Rebek recently coined the term "*ouroborand*" (after the Greek "*ouroboros*", the symbol of a snake eating its own tail) to describe a structure that includes part of itself.[87] The resorcinarene-based ouroborand (Figure 42), functionalized with an arm containing a bipyridine and cyclohexane group, can be switched reversibly to control guest binding through the addition and removal of zinc ions. In the absence of zinc, the cyclohexyl arm is included within the cavity of the resorcinarene (**107a**). However, coordination of zinc to the bipyridine unit causes a conformational change (**108a**) that prevents inclusion of the cyclohexyl arm, allowing an external adamantane-based guest to bind (**108b**). Removal of zinc regenerates the original self-included conformation via **107b**, releasing the external guest.

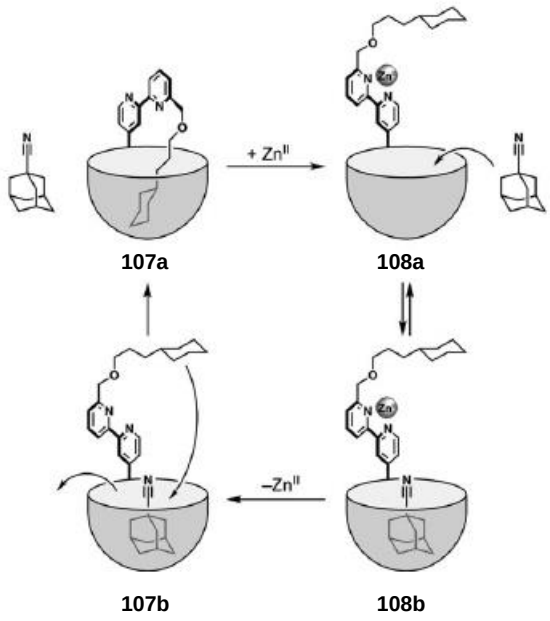

Figure 42. Rebek's ouroborand, where Zn^{II} complexation/decomplexation controls reversible guest release. Reprinted with permission from ref [87]. Copyright 2010 Wiley-VCH.

Schmittel and co-workers reported a self-locking nanoswitch where the activity of a Knoevenagel catalyst was regulated by chemical stimuli (Figure 43).[88] In the locked state (**110**), the 4-(2-pyridyl)pyridimidine unit is coordinated to the zinc porphyrin and the Knoevenagel reaction catalyzed by piperidine is active. Upon addition of Cu^{I} and anthracene-functionalized phenanthroline **111**, the 4-(2-pyridyl)pyridimidine decoordinates from the zinc porphyrin, forming a tetrahedral complex with Cu^{I} and phenanthroline **111**. The unlocked state **109** is thus generated, switching off the catalytic reaction as the piperidine catalyst coordinates to the vacant site on the zinc porphyrin. The locked state can be regenerated and catalytic activity switched back on by addition of phenanthroline **111**, which forms a stable homoleptic complex with Cu^{I}. It was possible to switch reversibly between the locked/catalysis ON and unlocked/catalysis OFF states through the sequential addition of Cu^{I} and ligand **111** with no loss of catalytic activity over three cycles. Recently, the Schmittel group has extended this work by incorporating the external phenanthroline ligand into the self-locking system through

functionalization at the bromo position of **109**. They have demonstrated bidirectional chemical communication between two[89] and three[90] nanoswitches using one electron redox inputs.

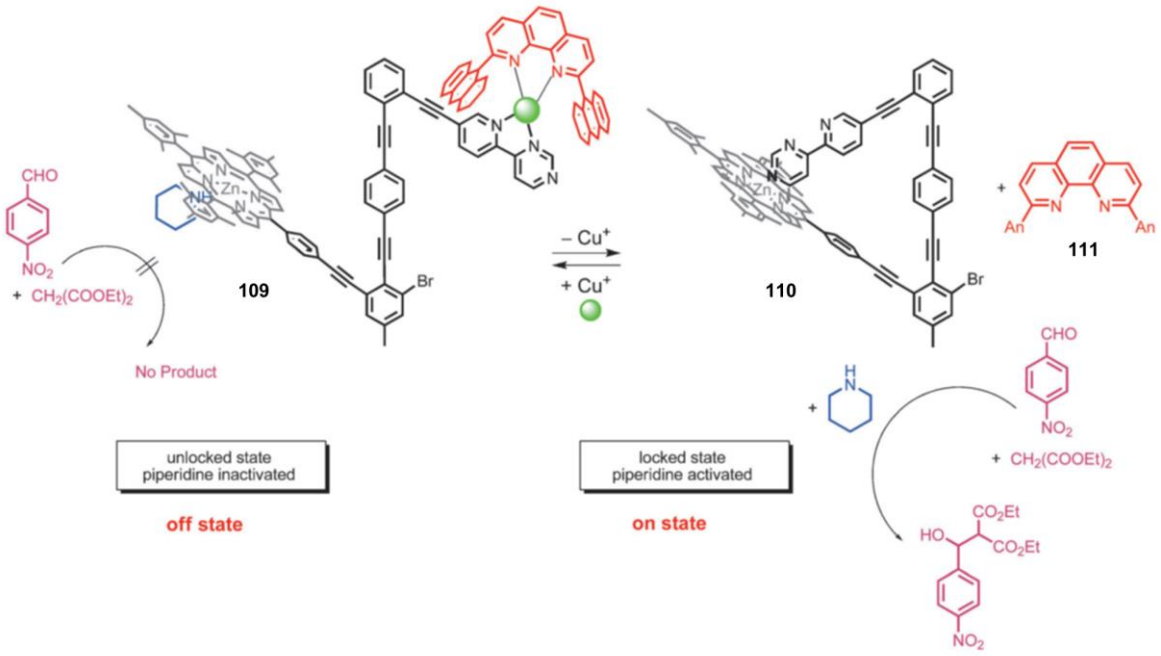

Figure 43. Schematic representation of the reversible locking and unlocking of Schmittel's nanoswitch for triggering catalysis (An = 9-anthracenyl). Reprinted with permission from ref [88]. Copyright 2012 Wiley-VCH.

5.4.2 Light Responsive Self-locking Systems

Aida's photo-responsive self-locking system is shown in Figure 44.[91] Host **112** consists of a ferrocene unit functionalized with a zinc porphyrin and aniline unit on each cyclopentadienyl ring. In non-polar solvents such as benzene, the host is internally double-locked, with intramolecular coordination of the aniline units to the zinc porphyrins. The self-locked system can be unlocked using 1,2-bispyridylethylene (**113**) as a photoresponsive key. In the presence of *trans*-**113**, the host remains self-locked, however, upon photoisomerization to *cis*-**113** the intramolecular locking interactions are broken. Instead, the two pyridine units of *cis*-**113**

coordinate to the zinc porphyrins, generating the externally locked state. Photoisomerization back to *trans*-**113** regenerates the self-locked state.

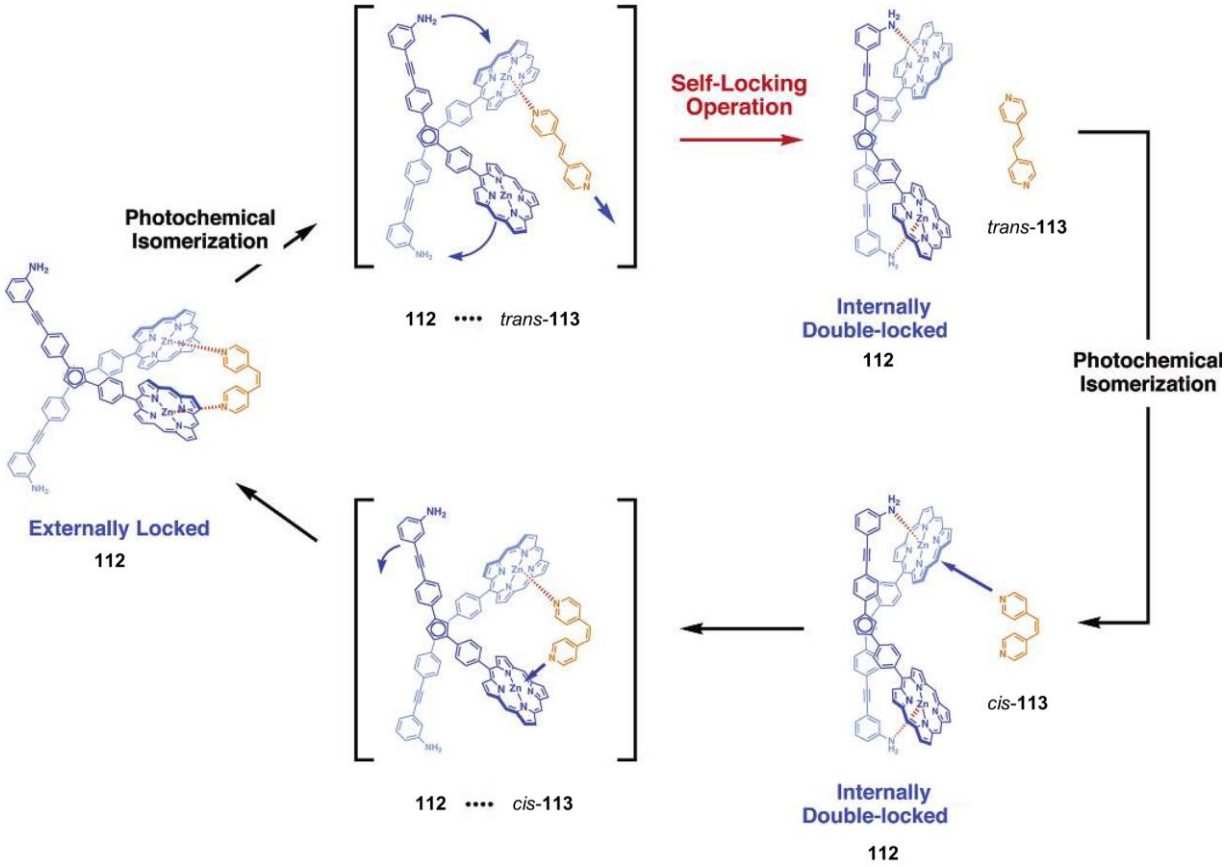

Figure 44. Molecular structures of internally double-locked and externally locked host and schematic representation of the self-locking operation in response to photochemical isomerization of 1,2-bispyridylethylene. Reprinted with permission from ref [91]. Copyright 2006 American Chemical Society.

5.5 Molecular Rotors

Molecular rotors consist of two parts that rotate relative to one another. These types of molecular machine have been the subject of several reviews.[92]

5.5.1 Chemically Responsive Molecular Rotors

Kelly and co-workers reported the first example of a molecular brake, consisting of a bipyridine derivative connected to a triptycene wheel (Figure 45).[93] When the brake is 'off', (**114**), the triptycene unit freely rotates. However, coordination of a metal ion such as Hg^{II} to the bipyridine unit switches the brake 'on' (**115**) and slows the rotation of the triptycene wheel. The brake can be switched 'off' again through addition of EDTA to remove the mercury ion.

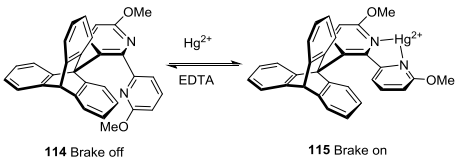

Figure 45. Kelly's molecular brake operated by addition and removal of a chemical stimulus, Hg^{II}.[93]

More recently, Tian and co-workers reported a dual-ion-switched ferrocene-based molecular brake (**116**) consisting of a ferrocene unit as a rotatable pivot, and photoactive benzo[*e*]indoline units as cranks (Figure 46).[94] Rotation about the ferrocene unit is braked through complexation of Zn^{II} to the two cranks, resulting in a U-type conformation. Protonation of the benzo[*e*]indoline units, in contrast, leads to an N-type conformation due to repulsion between the two cranks.

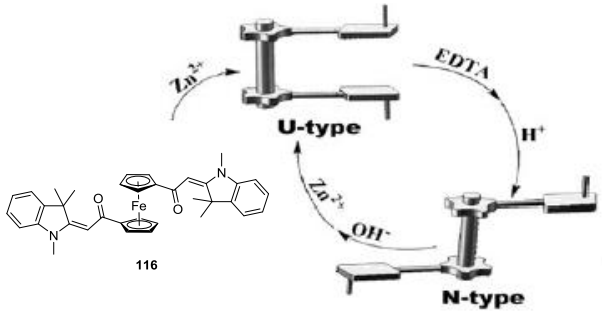

Figure 46. Schematic illustration of the molecular brake. Adapted from ref [94] with permission of The Royal Society of Chemistry.

The Shinkai group has demonstrated that chemical stimuli can be exploited to modulate the rotation of double decker porphyrins.[95] In one example, the addition Ag^I ions speed up the rotation of the porphyrin rings in cerium(IV) double decker complex **117**,[96] thereby acting as molecular "grease" (Figure 47).[92a] The rotation rates were found to be 200 s^{-1} and 220 s^{-1} at 20 °C and -40 °C, without and with Ag^I respectively. The acceleration in the presence of silver ions was attributed to conformational changes in the porphyrin due to three silver ions binding in the π cleft.

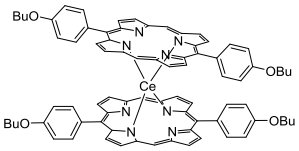

117

Figure 47. Shinkai's Ag^I-greased cerium(IV) double decker porphyrin.[95]

Tetraaryl-substituted cerium(IV) double decker porphyrins were also found to respond to chiral chemical stimuli, leading to properties that could be exploited for molecular memory applications.[95,97] Due to rotation of the porphyrin rings, double decker complex **118** exists as slowly interconverting enantiomeric rotamers. Chiral guests, such as **119** or **120**, bind cooperatively to the pyridyl substituents, suppressing porphyrin ring rotation. Thereby, the stereochemistry of the ensemble is influenced through the selective formation of the most thermodynamically stable diastereomer. Interestingly, this chiral information can be retained (following removal of the chiral guest by treatment with pyridine) when the meso phenyl groups of the porphyrin are substituted with bulky groups, such as 3,5-dimethoxyphenyl.[97a] This memory effect is due to the bulky substituents slowing porphyrin ring rotation and thus, racemization, in the absence of the chiral guest. It was estimated that the stereochemical information could be retained for 3 days at 0 °C, one year at -37 °C and 1.9×10^6 years at -100 °C.

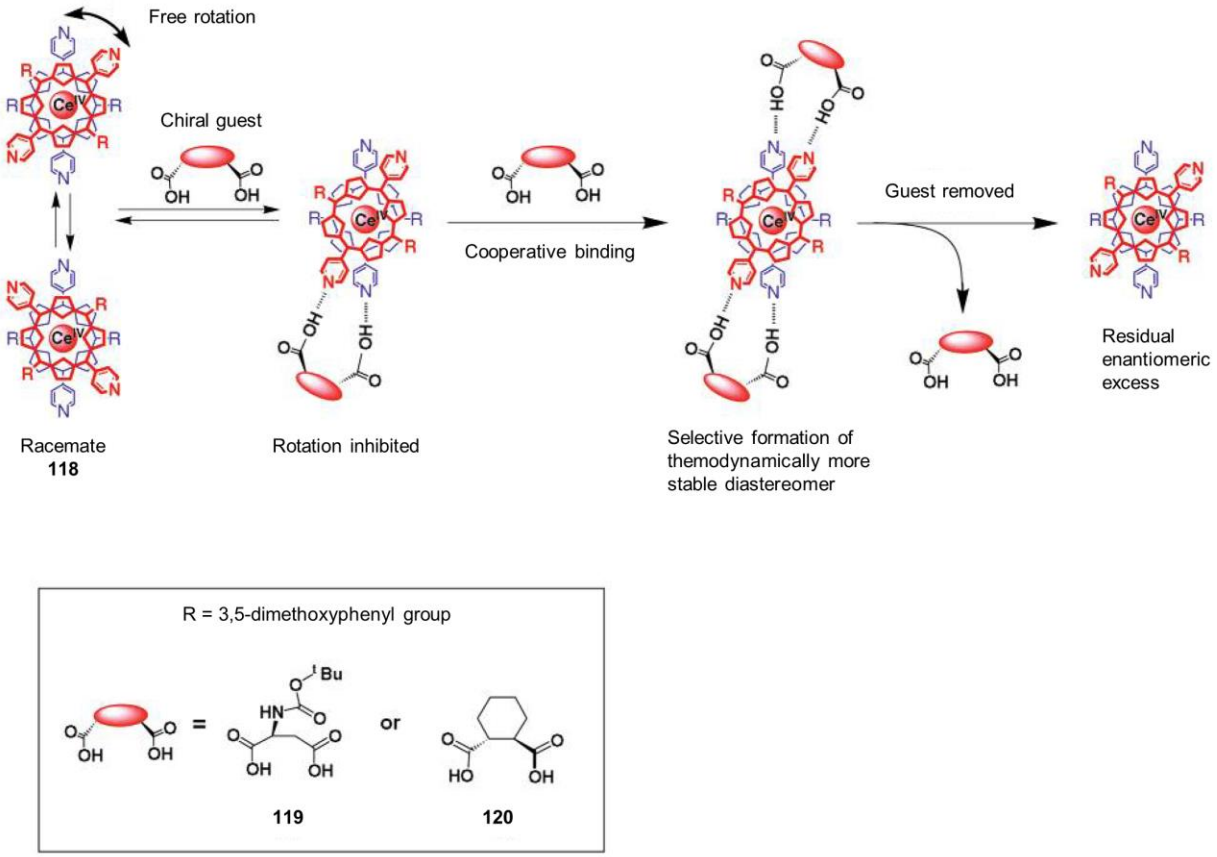

Figure 48. The response of Shinkai's cerium double decker porphyrin to chiral chemical stimuli. Reprinted with permission from ref [95]. Copyright 2001 American Chemical Society.

Schmittel and co-workers have also exploited double-decker porphyrin assemblies as nanorotors.[98] In their design, DABCO is used as a dynamic hinge between two different zinc porphyrins, one of which corresponds to the rotor and the other to the stator. The rotor and stator are linked together in such a way as to ensure the formation of a heteroleptic supramolecular assembly, by coordination of phenanthroline units attached to the stator with pyridine/pyrimidine units linking the rotor to Cu^{I} centers.

Chemical stimuli have been demonstrated to affect the behavior of the hinge and rotor. When one equivalent of DABCO is present between the two porphyrin rings, rotation about the N-N axis is observed but random tumbling is not, even at elevated temperatures (**121**, Figure 49).[98a] In the presence of excess DABCO, however, tumbling of the inside DABCO was observed (**122**). The excess DABCO coordinates to the outside sites of the zinc

porphryins, labilizing the inner DABCO. Variable temperature NMR spectroscopy indicated the tumbling could be frozen by cooling to -50 °C. Other coordinating ligands, such as quinuclidine or 4-bromopyridine, could also trigger tumbling of the inner DABCO.

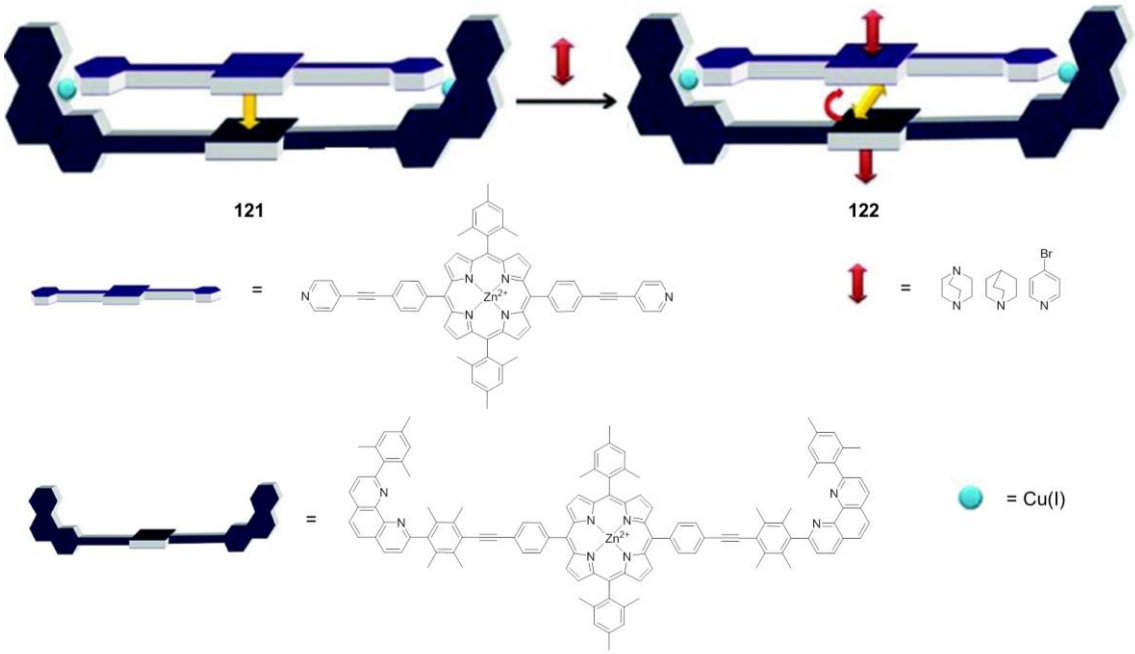

Figure 49. Chemically triggered tumbling of inside coordinated DABCO (yellow double-headed arrow) by coordination of ligands to external zinc porphyrin sites in Schmittel's nanorotor. Reprinted with permission from ref [98a]. Copyright 2011 American Chemical Society.

More recently, the effect of Cu^{I} on the rate of rotation of nanorotors containing symmetric and asymmetric rotors and a four-station stator was investigated.[98b] In nanorotor **123**, having an asymmetric rotor, the two Cu^{I} ions are coordinated to phenanthroline units on opposite sides of the stator, leading to two sets of signals in the ^{1}H NMR spectrum. These signals correspond to rotor-loaded and -unloaded phenanthroline units (Figure 50a). As a result, these nanorotors rotate in 180° steps. The rotational frequency for **123** at 25 °C was determined to be 97000 s^{-1}. When two additional equivalents of Cu^{I} are added to **123**, the remaining two phenanthroline units are loaded with Cu^{I}, generating **124**. The set of signals corresponding to

the unloaded phenanthroline units disappeared and several resonances broadened. This observation suggested oscillation between mixed 90°/180° steps among the four Cu^{I}-loaded phenanthroline units. Furthermore, the rotational frequency was observed to decrease to 81300 s^{-1}. Removing the added Cu^{I} by adding two equivalents of cyclam regenerated the pure 180° oscillation and higher rotational frequency of **123**. Thus, the speed and mode of rotation of the nanorotors could be tuned through the addition and removal of Cu^{I} ions.

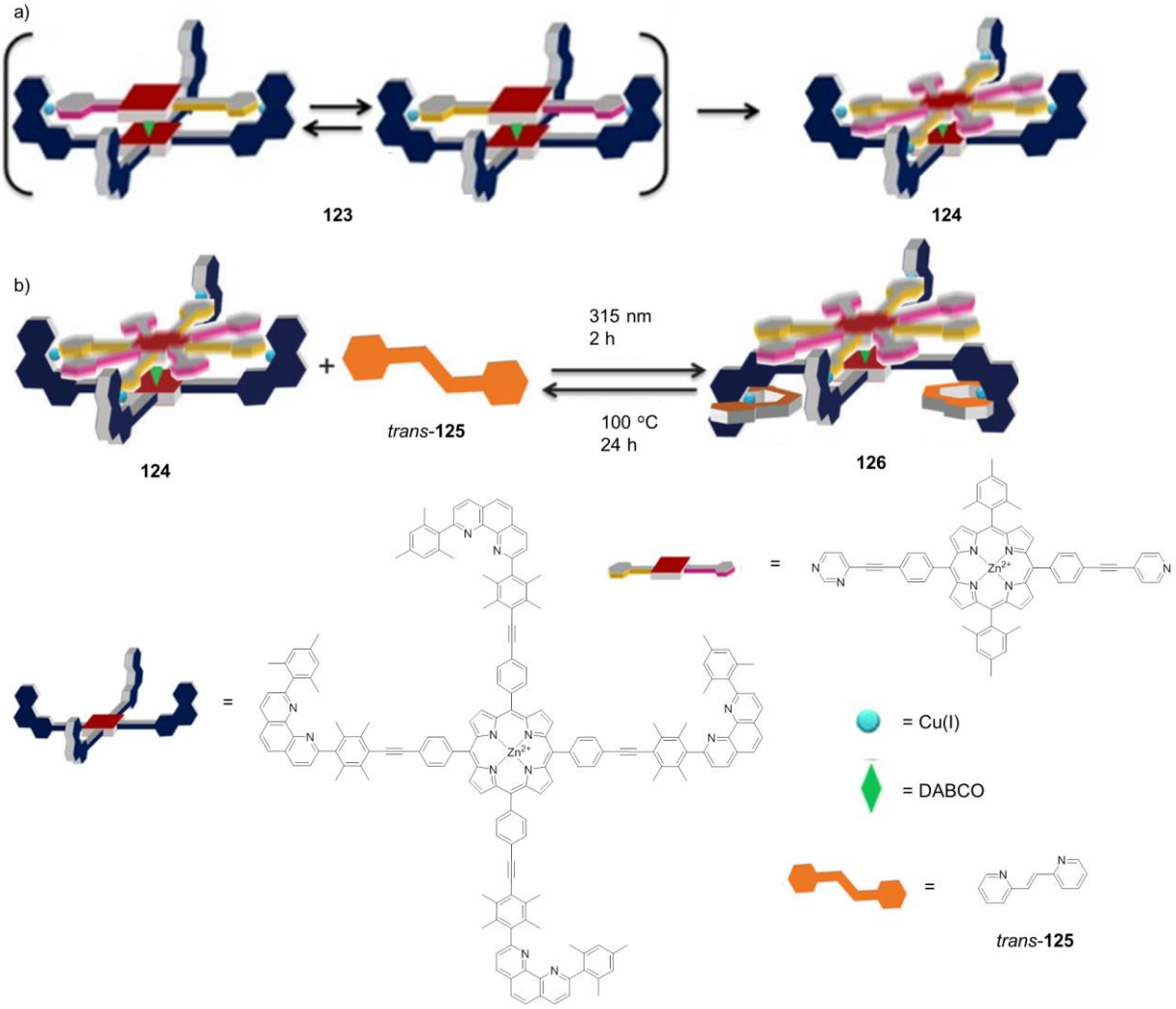

Figure 50. Schmittel's a) four component and b) five component nanorotors. Adapted from refs [98b] and [98c] with permission of American Chemical Society and The Royal Society of Chemistry.

5.5.2 Light Responsive Molecular Rotors

In an extension of this work, Schmittel and co-workers designed a five component nanorotor based on **124**, where the fifth component, 2,2'-diazastillbene (**125**), acts as a reversible brake (Figure 50b).[98c] 2,2'-Diazastillbene can be switched reversibly between its *cis* and *trans* isomers by light and heat, thereby acting as a signal transducer to regulate the speed of rotation of the nanorotor. The rotation speed of **124** in the presence of *trans*-**125** is slightly higher than the free nanorotor (86200 s^{-1} vs 81300 s^{-1} at 25 °C), however, it significantly slows to 38200 s^{-1} upon isomerization to *cis*-**125** following irradiation at 315 nm. The *cis* isomer, unlike *trans*-**125**, is a chelating ligand, and can therefore coordinate to the two phenanthroline units that are not coordinated to the rotor. Heating the ensemble in 1,1,2,2-tetrachloroethane to 100 °C switches the rotation speed back to 86200 s^{-1}, due to *cis* to *trans* isomerization.

Schmittel and co-workers have proposed a model to rationalize the reversible speed regulation by **125**. As discussed above, the rotor in **124** oscillates in mixed 90°/180° steps about the stator. As the rotator moves from one set of phenanthroline units to the orthogonal set, the Cu^{I} becomes coordinatively unsaturated. As a result, free rotation about the alkynyl groups of the stator is possible, leading to multiple conformations, which can affect the rotator's rotation in **126** when *cis*-**125** is coordinated to the phenanthroline units of the stator. Rotation is slowed in conformations where the complexed stator is in the path of the rotator, whereas it is unaffected when the complexed stator is rotated out of the path of the rotator. Thus, on average, the speed of the nanorotor is slower in the presence of *cis*- than *trans*-**125**. The increased rotation speed in the presence of *trans*-**125**, relative to the free nanorotor, was attributed to competitive displacement of the rotator's pyridine/pyrimidine nitrogen donor from Cu^{I}.

Nishihara and Kume have reported a series of copper complexes where the rotation of a 4-methyl-2-(2'-pyridyl)pyrimidine derivative around a bulky ligand can be exploited to switch from the stable (equilibrium) to the metastable state.[99] In one example, the light stimulus is

converted into an electrochemical potential shift without an accompanying color change.[100] In the dark, the complex exists as the inner and outer isomers (Figure 51a), which have different redox potentials ($\Delta E°' = -0.14$ V). Irradiation generates a metastable state due to rotation of the pyrimidine ligand from the inner to the outer isomer. It is proposed that this rotation occurs via a Cu^{II} state generated from PET to a redox mediator (decamethylferrocenium) or partial oxidation oxidation of the complex. The original equilibrium state can be regenerated by heating.

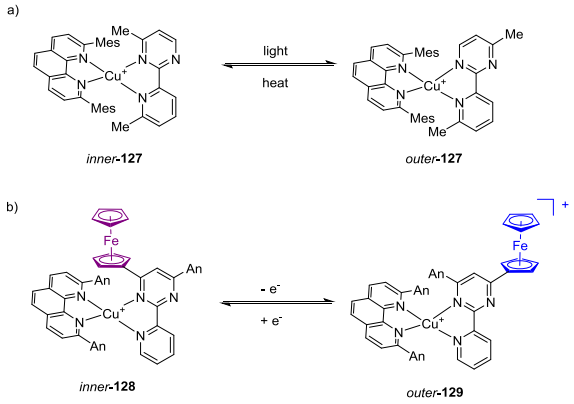

Figure 51. Nishihara and Kume's Cu^{I} complexes where rotation of the 4-methyl-2-(2'-pyridyl)pyrimidine ligand is induced by a) light and b) electrochemical stimuli.[100]

5.5.3 Electrochemically Responsive Molecular Rotors

In related examples, rotation of the pyrimidine ligand is induced by an electrochemical stimulus.[101] In the absence of an electrochemical stimulus, complex **128** exists as a mixture of isomers with *inner*-**128** as the major isomer (Figure 51b).[101c] Oxidation triggers rotation of the pyrimidine ligand and electron transfer to the ferrocene unit generating *outer*-**129** as the major isomer.

5.5.4 Acid-base Responsive Molecular Rotors

Building on their earlier work (Section 5.5.1), the Shinkai group has reported a series of pH-responsive bevel-geared rotors (**130**), consisting of two moving elements: a lanthanum(III) double decker (LaDD) porphyrin and a Rh^{III} porphyrin coordinated to the pyridine group of

the lanthanum porphyrin (Figure 52).[102] The motion of the side Rh^{III} porphyrin can be affected through altering the rotation rate of the lanthanum top rotor, by protonation and deprotonation of the pyrrole NH that is not coordinated to the lanthanum center;[103] deprotonation leads to slower rotation due to greater π–π stacking interactions between the porphyrins.

The pH response of the bevel-geared rotors is affected by the orientation of the side Rh^{III} porphyrin rotors. The bevel-geared rotor with one side Rh^{III} porphyrin behaved similarly to the rotor with two side Rh^{III} porphyrins 180° apart upon deprotonation and protonation by triethylamine and trifluoroacetic acid, respectively (Figure 52a).[102a] In the absence of base, rotor meshing was observed, where the frequency of rotation of the side and top rotors was equal. Deprotonation switches to a state where the rotation of the two rotors is independent; rotation of the side Rh^{III} porphyrin is much faster than that of the top lanthanum rotor since the side rotor slips out of gear, most likely due to a conformational change of the lanthanum double-decker porphyrin. Addition of trifluoroacetic acid switches back to the meshed state, where the rotation rates of both rotors are similar.

Two different meshed states are observed by changing the basicity of the solvent, when the two side Rh^{III} porphyrin rotors are orthogonal to one another (Figure 52b).[102b] The rotation of the top and side rotors is faster in CD_2Cl_2 than pyridine-d_5.

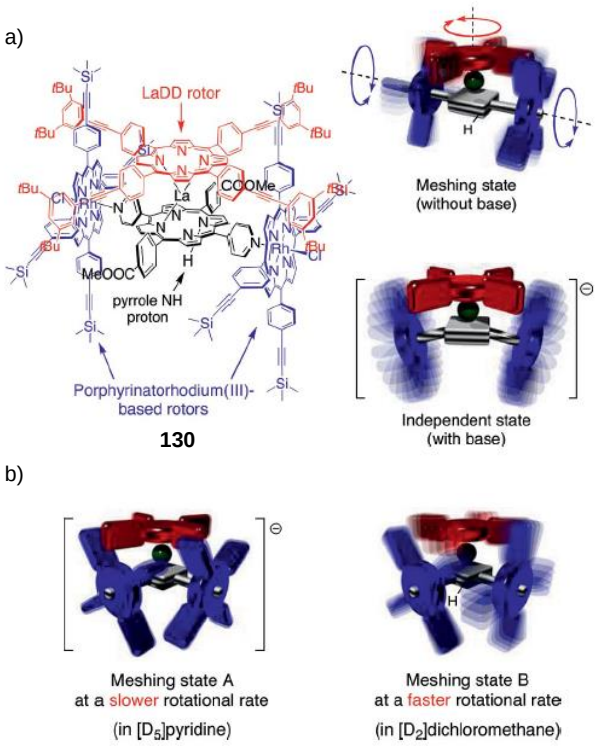

Figure 52. Shinkai's bevel-geared rotors, where the side Rh^{III} porphyrin rotors are a) 180° and b) 90° apart, leading to different responses to pH stimuli. Adapted and reprinted with permission from ref [102b]. Copyright 2011 Wiley-VCH.

6 Molecular Machines, Switches and Mechanisms Based on Interlocked Structures

Mechanically interlocked structures have played a central role in the development of molecular machines.[68,104] In contrast to the examples in the previous section, these molecular machines consist of two or more molecular components interlinked by a mechanical bond, so that the components cannot be separated without breaking a covalent bond.

The two most common forms of interlocked structures are [n]catenanes and [n]rotaxanes, where n refers to the number of interlocked components. Catenanes (from the Latin *catena*, meaning chain) consist of two or more interlocked rings, whereas rotaxanes (from the Latin *rota* and *axis,* meaning wheel and axle) consist of mechanically interlocked macrocycle and stoppered axle components. Stimuli can be exploited to manipulate the relative orientations and positions of the interlocked components to switch between states, and thus generate

molecular motion. It should also be noted that while this review only deals with metal-based interlocked structures, there have also been significant contributions to the field by groups working on systems containing no metal ions.

6.1 Catenane-based Molecular Locks

Fujita and co-workers have demonstrated that the lability of the Pd^{II}-pyridine coordination bond can be exploited to prepare [2]catenanes from pre-formed macrocycles via a 'magic ring' synthesis (Figure 53a).[105] However, due to this lability an equilibrium exists between the [2]catenane and macrocycle, where the concentration of the Pd^{II} species and solvent polarity influence which species predominates. The catenane is the major species at high Pd^{II} concentrations or in polar solvent systems. When Pt^{II} was used in place of Pd^{II} in the magic ring synthesis, a kinetic mixture of products, including the [2]catenane and macrocycle, was obtained because the Pt^{II}-pyridine coordination bond is inert at room temperature.[105a] Metal-ligand bond reversibility is therefore crucial for obtaining the [2]catenane, however, this reversibility also introduces an equilibrium between the catenane and macrocycle. To overcome this reversibility problem, Fujita proposed the use of the Pt^{II}-pyridine bond as a "molecular lock" to access irreversibly locked [2]catenanes. Under normal conditions the Pt^{II}-pyridine bond is inert and therefore "locked," however, upon exposure to a stimulus – heat or light – the bond becomes labile, introducing the reversibility required to form the [2]catenane structure (Figure 53b). Once the [2]catenane has formed, dissociation into two macrocycles can be stopped by cooling to room temperature so that the Pt^{II}-pyridine bond is again locked. This concept has been demonstrated using both heat and light as the stimulus to release the molecular lock.

6.1.1 Heat Responsive Molecular Locks

In the first example of a molecular lock, the Pt^{II}-pyridine bond of macrocycle **131**, was unlocked by heating in water at 100 °C in the presence of $NaNO_3$ (Figure 53c).[106] Under these

polar conditions, the equilibrium between the macrocycle and [2]catenane favors the catenane, which was locked by removing the salt and cooling to room temperature.

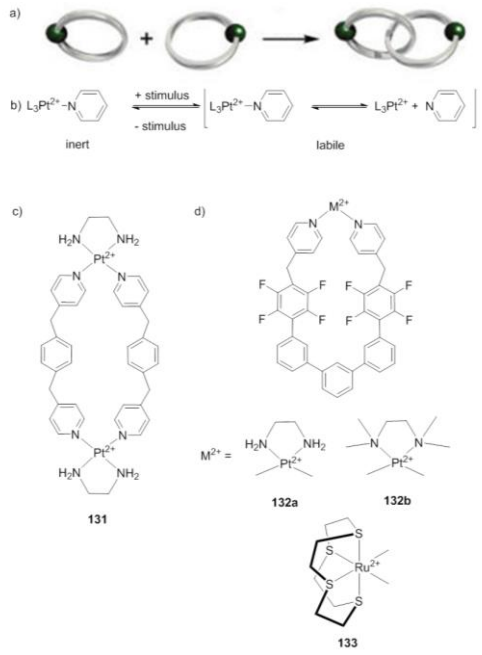

Figure 53. Fujita's stimuli-responsive molecular locks. a) Magic ring synthesis of a [2]catenane from pre-formed macrocycles; b) strategy for exploiting Pt^{II}-ligand bonds as molecular locks; c) heat and d) light responsive molecular locks. Adapted and reprinted with permission from ref [107]. Copyright 2007 American Chemical Society.

6.1.2 Light Responsive Molecular Locks

An alternative unlocking strategy was investigated since operation of the thermally responsive molecular lock was not clean and straightforward, due to the necessity of removing the salt. Instead, a light switchable molecular lock was developed where UV irradiation unlocked the Pt^{II}-pyridine bond of macrocycles **132a** and **132b** to form [2]catenanes (Figure 53d).[107] Upon irradiation, the macrocycles were cleanly converted into catenanes within 15 minutes. The catenanes were locked in the absence of irradiation. This light unlocking strategy was also extended to Ru^{II}-pyridine bonds to prepare a [2]catenane from Ru^{II} macrocycle **133**.

6.2 Catenane-based Molecular Pirouettes

Molecular machines based on catenanes exploit the rotation of one of the interlocked rings to switch between bistable states; this pirouetting motion can be triggered by different stimuli. Sauvage and co-workers demonstrated that catenanes provided a good framework to explore pirouetting molecular machines in the first example of a metal templated catenane synthesis.[108] The [2]catenane could be prepared in high yield by using Cu^{I} as a metal template to coordinate the phenanthroline groups of different rings, thereby fixing the orthogonal orientation of the two rings. Upon demetalation, there was a significant geometrical change as the two rings were no longer held together by the metal ion. As the two macrocycles in the [2]catenane were identical, the metalated and demetalated catenanes cannot be described as bistable states. In order to achieve bistability for operation of catenanes as molecular machines, it is necessary to incorporate different stations into at least one of the rings of the catenane.

6.2.1 Chemically Responsive Molecular Pirouettes

In a collaboration between the Sauvage and Stoddart groups, a switchable hybrid catenane was designed exploiting both transition metal complexation and π-electron donor-acceptor interactions (Figure 54).[109] Each ring contains a phenanthroline ligand to coordinate a tetrahedral metal ion. However, the second station in each ring is not identical; one ring contains electron deficient bipyridinium units while the other ring has an electron rich 1,5-dioxynaphthalene unit. In the presence of Cu^{I}, tetrahedral complexation results in catenane **134**; however, upon demetalation the two rings rotate so that the bipyridinium units of one ring π–π stack with the 1,5-dioxynaphthalene unit of the other ring. Addition of Li^{+} to the metal-free catenane **135** rapidly switched the catenane to a conformation with the lithium tetrahedrally coordinated to the two phenanthroline ligands. However, it did not prove possible to switch back to the conformation with π-electron donor-acceptor interactions by removing Li^{+}. Acid and base could also trigger switching between the conformations in the metal-free catenane.

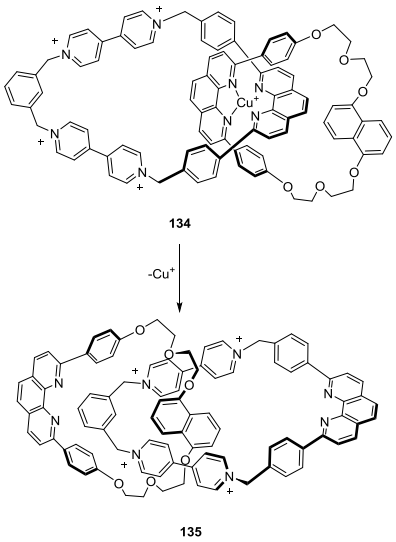

Figure 54. Sauvage and Stoddart's switchable hybrid catenane.

Yashima and co-workers reported a catenane where a salt bridge between amidine and carboxylate functionalities on different macrocycles prevents the free rotation of the two macrocycles (**136**, Figure 55).[110] Addition of one equivalent of Zn^{II} breaks the salt bridge to generate catenane **137**. An accompanying fluorescence enhancement and red-shift in emission was observed, which could be reversed by addition of [2.2.1]cryptand to remove the Zn^{II}. The breaking and formation of the salt bridge could also be achieved by addition of acid and base, respectively.

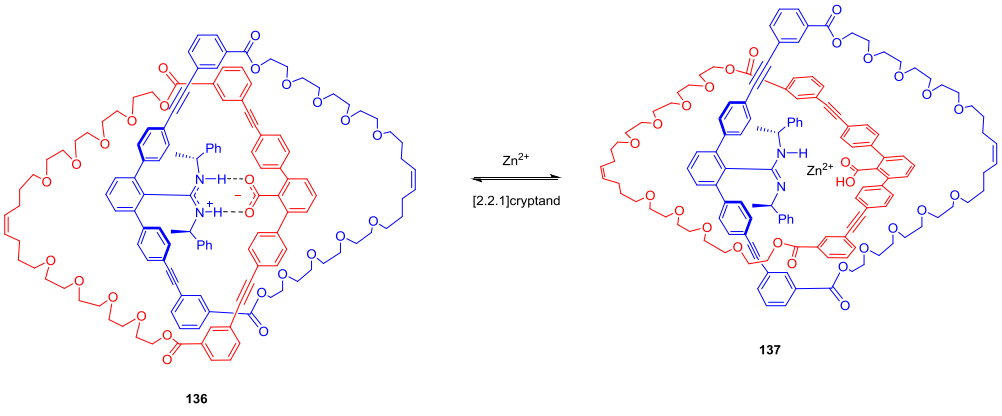

Figure 55. Yashima's catenane where free rotation of the two rings is locked by a salt bridge between the carboxylic acid and amidine and unlocked by addition of Zn^{II}.

6.2.2 Electrochemically Responsive Molecular Pirouettes

The redox state of the metal center(s) in the catenane can also be modulated to achieve switching between bistable states. Two examples from the Sauvage group exemplify how the different geometrical preferences of Cu^{I} and Cu^{II} may be used to this effect.[111] In the earliest and simplest example, a [2]catenane has one ring with a phenanthroline ligand and another with both a bidentate phenanthroline and tridentate terpyridine ligand (Figure 56a).[111a] A tetrahedral complex results from complexation of Cu^{I} to the two phenanthroline ligands (**138a**), and upon oxidation to Cu^{II}, this complex rearranges from the transient 4-coordinate Cu^{II} complex **139a** to the more stable 5-coordinate complex **139b**. Reduction back to Cu^{I} regenerates the initial 4-coordinate complex **138a** via the transient 5-coordinate Cu^{I} complex **138b**. The kinetics of the rearrangement process depends on the oxidation state of the metal center as the pirouetting motion relies on metal decoordination; the rearrangement of the Cu^{II} complexes, **139a** to **139b**, was much slower (several minutes to several hours depending on the experimental conditions) than that of the Cu^{I} complexes (seconds), **138b** to **138a**. Similar rearrangement kinetics are also observed with analogous pirouetting rotaxanes, discussed in more detail in Section 6.3.1.

Systems containing more than two stimuli-accessible states are less common than bistable systems, but they are promising for application in molecular devices since they have the potential to store and process more information than binary bistable systems.[104e] Building on the previous example, three different geometries can be accessed in response to an electrochemical stimulus by incorporating both phenanthroline and terpyridine ligands into each ring component of the catenane (Figure 56b).[111b] Thus, it is possible to access 4 (**140a**), 5 (**140b**) and 6-coordinate (**140c**) copper complexes, where the stability of each complex is dependent on the oxidation state of the metal. For Cu^{I}, the stability of the complexes is **140a** > **140b** > **140c** whereas this order is reversed for Cu^{II}. Of the six possible species, only the 4-coordinate Cu^{I}, 4-coordinate Cu^{II} and 6-coordinate Cu^{II} species could be observed by

UV/visible spectroscopy. However, using CV three distinct redox waves were observed at 0.63, -0.05 and -0.41 V, which were assigned to the Cu^{I}/Cu^{II} couples within **140c**, **140b** and **140a**, respectively.

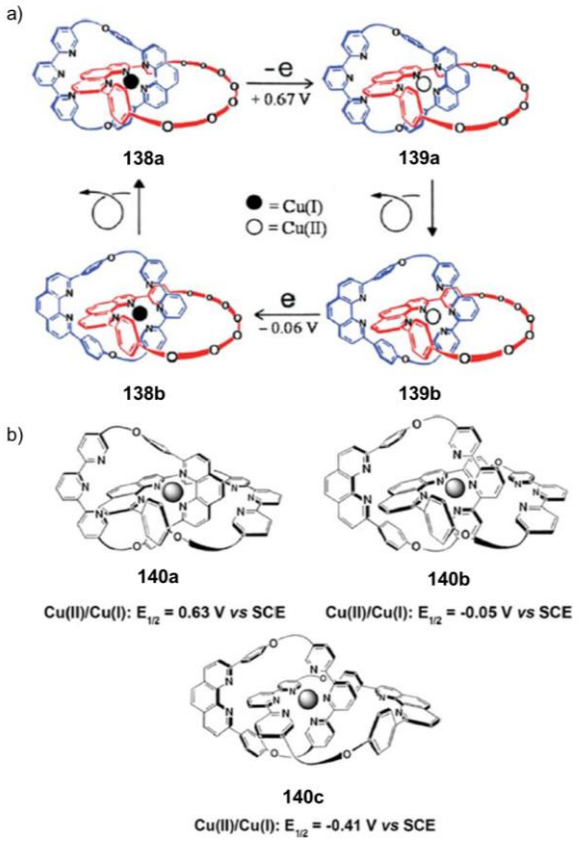

Figure 56. Sauvage's a) two stage and b) three stage pirouetting catenanes. Reprinted from ref [104e] with permission of The Royal Society of Chemistry.

In another example of a multistage system, Korybut-Daszkiewicz and co-workers exploited the redox potential of different metal centers to drive pirouetting in a heterodinuclear bismacrocyclic transition metal complex (Figure 57).[112] The dibenzo[24]crown-8 macrocycle (DBC8) can interact with the copper or nickel station of the other ring by π–π stacking interactions. In the initial state **141**, the macrocycle resides on the Ni^{II} station in preference to the Cu^{II} side; however, oxidation to Cu^{III} switches the electron rich macrocycle from Ni^{II} to the more electron deficient Cu^{III} station, generating **142**. Increasing the potential oxidizes the Ni^{II} center returning the DBC8 macrocycle to the now-nickel(III) station, to give **143**. By

Osteryoung square-wave voltammetry, a splitting of the nickel oxidation signals was observed which was attributed to different microenvironments of Ni^{II} in the presence and absence of the DBC8 macrocycle; at shorter time scales and lower temperatures, movement of the macrocycle from the Ni^{II} to Cu^{III} station upon oxidation was slowed, leading to a splitting of the peaks. More importantly, it was possible to control the movement of the macrocycle from one station to the other by controlling the redox potential and reversibly oxidizing the Ni^{II}, Cu^{II}, or both metal centers.

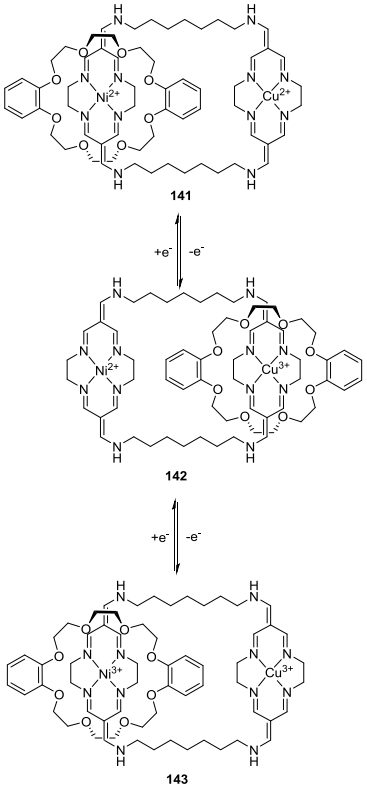

Figure 57. Korybut-Daszkiewicz's pirouetting catenane based on a heterodinuclear bismacrocyclic transition metal complex.[112]

6.2.3 Light Responsive Molecular Pirouettes

Light can be employed as a stimulus to labilize ligands, as discussed in Section 6.1.2. There are many examples of photosubstitution reactions of ruthenium(II) complexes.[113] Complexes based on $[Ru(diimine)]^{2+}$ are suitable for developing light driven molecular machines, as they absorb light strongly in the visible region, and it is possible to tune the steric and electronic

properties of the ligands to effect photolabilization. Sauvage and co-workers prepared [2]catenanes **144** and **146,** where an octahedral Ru^{II} metal center complexed two macrocycles; one ring contained two phenanthroline ligands, while the other ring was based on a bipyridine ligand (Figure 58).[114] Exposure to light triggers quantitative decomplexation of the bipyridine ligand, replacement with two monodentate ligands (chloride or acetonitrile for **145** and chloride only for **147**) and a geometrical change. Heating at elevated temperature regenerates the initial [2]catenane in quantitative yield. The size of the bipyridine functionalized macrocycle affected the decomplexation and complexation reactions; the photoreaction was 40 times slower for the smaller macrocycle in **146** and substitution only occurred with chloride ligands, however, the thermal regeneration of **146** was 2-3 times faster than for **144**. These results could be understood by invoking steric and concentration effects, highlighting the importance of subtle structural factors in the control of motion in molecular machines.

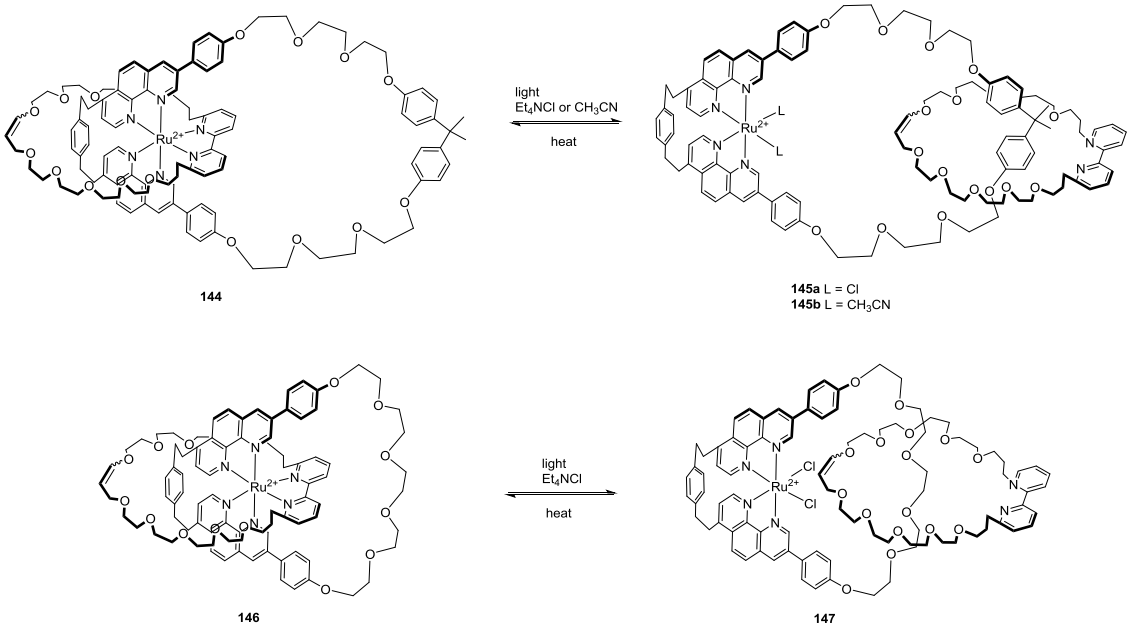

Figure 58. Sauvage's light responsive catenanes.[114]

6.3 Rotaxane-based Molecular Pirouettes

The macrocycle component of rotaxanes can rotate, or pirouette, around the axle, triggered by both chemical and electrochemical stimuli, as with the catenanes described in the previous section.

6.3.1 Electrochemically Responsive Molecular Pirouettes

Building on their work investigating catenane-based molecular pirouettes, Sauvage and co-workers have reported a series of rotaxane-based devices where oxidation of Cu^{I} to Cu^{II} triggers rotation of the macrocycle from a bidentate ligand, such as phenanthroline or bipyridine, to a terpyridine station (Figure 59a), and in which the rotation can be reversed by reduction back to Cu^{I}.[115] Switching between the two stations proceeded via 4-coordinate Cu^{II} and 5-coordinate Cu^{I} intermediates to give the more stable 5-coordinate Cu^{II} complex **149** and 4-coordinate Cu^{I} complex **148**, respectively. As with the catenanes discussed in Section 6.2.2, the oxidation state and subtle structural differences significantly affect these rearrangement rates. Electrochemical studies revealed that pirouetting in rotaxanes is faster than for catenanes; the rearrangement rates around Cu^{II} and Cu^{I} were 0.007 s^{-1} and 17 s^{-1}, respectively, for the original and slowest pirouetting rotaxane **148**/**149**.[115a] Rearrangement of the Cu^{II} complex is slower than for the Cu^{I} due to stronger metal-ligand bonding in Cu^{II} complexes. Steric bulk around the metal center also plays a role, as the rearrangement process relies on decomplexation and access of other ligands, such as solvent and counteranions, to the metal. By shortening the axle and replacing the diphenylphenanthroline ligand with the sterically less bulky bipyridine ligand, rearrangement rates were increased dramatically to 5 s^{-1} and > 500 s^{-1} for axle **150a**.[115c] They could be accelerated further to 12 s^{-1} and > 1200 s^{-1} by lengthening the distance between the bipyridine ligand and stoppers in axle **150b**.[115e] Recently Gaviña and Tatay reported the related [2]rotaxane **151** as the most rapidly pirouetting rotaxane to date by replacing the terpyridine station with a pyridine bisamine one (Figure 59b).[116]

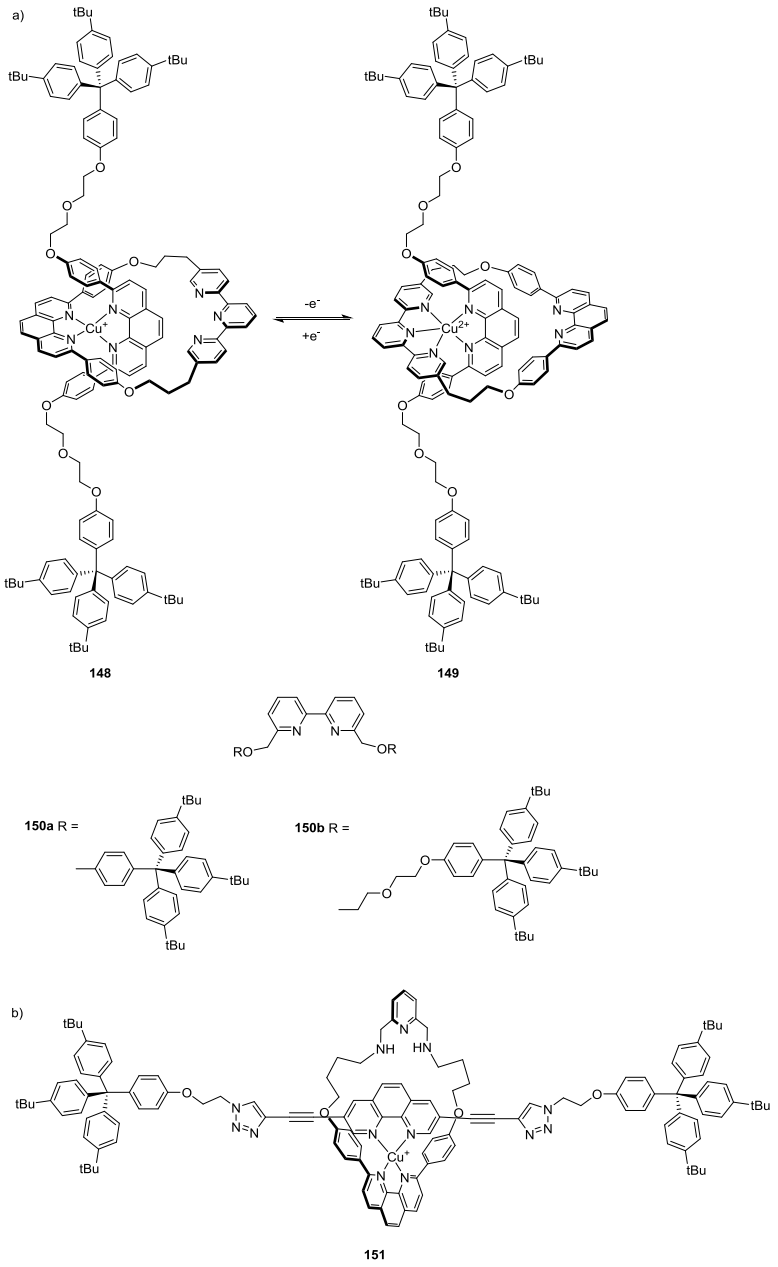

Figure 59. a) Sauvage's[115] and b) Gaviña and Tatay's[116] pirouetting rotaxanes.

Sauvage and co-workers proposed using their rotaxane with axle **150b** in a set-reset machine, switching between 4-coordinate Cu^{I} (state 0, **148** in Figure 59) and 5-coordinate Cu^{II} (state 1, **149**) species electrochemically.[115d] They demonstrated that when a set potential is applied to state 0, an anodic peak is observed and when the reset potential is applied to state 1, a cathodic peak is observed. In order to fabricate devices using the pirouetting rotaxanes, the rotaxanes were deposited on electrode surfaces. In one example, a [3]rotaxane was prepared in solution containing a disulfide linker. Cleavage of this linker converted the [3]rotaxane into

two [2]rotaxanes having a gold electrode as one stopper.[115b] CV confirmed that in solution the [3]rotaxane undergoes fast pirouetting motion. However, no evidence was found of pirouetting for the [2]rotaxane immobilized on the gold surface. Similarly, a series of pseudorotaxanes showed fast pirouetting behavior in solution[117] but not on a gold electrode. The authors attribute the lack of motion to steric interference by the gold surface.[117b]

6.3.2 Chemically Responsive Molecular Pirouettes

Multi-porphyrinic rotaxane **152** also exhibits pirouetting motion triggered by metalation and demetalation (Figure 60).[118] The [2]rotaxane consists of a macrocycle containing a Au^{III} porphyrin and an axle stoppered by two Zn^{II} porphyrins. In the presence of Cu^{I}, a tetrahedral complex forms between the phenanthroline ligands of the axle and macrocycle leading to the orientation of the gold and zinc porphyrins shown in rotaxane **152**. However, demetalation induces pirouetting of the axle component to give rotaxane **153** where the gold porphyrin is stacked between the two zinc porphyrin units, as shown by ^{1}H NMR spectroscopy. These conformational changes affect the mechanism and kinetics of PET between the zinc(II) porphyrin donor and gold(III) porphyrin acceptor.[118b] Recomplexation with silver or lithium cations regenerates **152**.

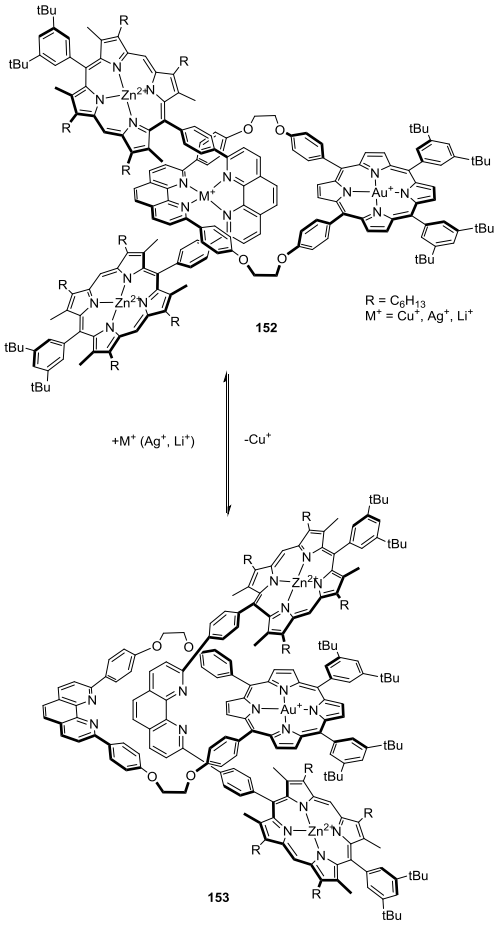

Figure 60. Sauvage's multi-porphyrinic pirouetting rotaxane.[118b]

6.3.3 Multi-stimuli Responsive Molecular Pirouettes

Recently, Sauvage and co-workers reported a [3]rotaxane where the two rings rotate like flapping wings, in a motion triggered by a chemical or electrochemical stimulus (Figure 61).[119] As with previous examples, switching between 4-coordinate (**154**) and 5-coordinate (**155**) metal complexes, by oxidation of Cu^{I} or exchange of Cu^{I} for Zn^{II}, induces rotation of the rings; however, in this case the two rings are parallel in the 4-coordinate complexes, whereas they are at an angle to each other in the 5-coordinate complexes.

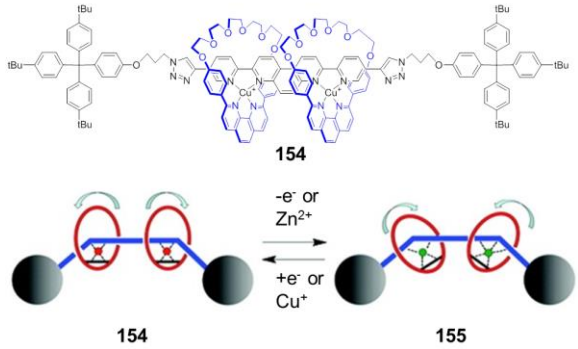

Figure 61. Sauvage's multi-responsive rotaxane, whose macrocycles act as flapping wings. Reprinted with permission from ref [119]. Copyright 2012 American Chemical Society.

6.4 Rotaxane-based Molecular Muscles

In nature the extension and contraction of muscles is achieved by two types of filaments; thick myosin filaments move along thin actin filaments in one direction or the other. Three classes of rotaxanes, daisy chains, presses and cages, have been identified as candidate artificial muscles.[120] Examples of each type of architecture will be presented in this section, so as to illustrate how different stimuli can be exploited in metal-based rotaxanes to achieve extension and contraction molecular motion reminiscent of muscles. For a more detailed description of the different types of architectures and non-metal-containing rotaxane-based molecular muscles, the reader's attention is drawn to recent reviews on rotaxane-based molecular muscles.[120-121]

6.4.1 Chemically Responsive Molecular Muscles

Sauvage and co-workers have reported examples of daisy chain and press rotaxanes, where chemical stimuli control the molecular motion.[122] In an example of a daisy chain rotaxane muscle, two identical macrocycle-axle components were mechanically interlocked by threading the axle component through the macrocycle of the other component and vice versa (Figure 62).[122c] The different coordination preferences of metal ions were exploited to switch between the bidentate phenanthroline and tridentate terpyridine stations of the axle, leading to

extended or contracted conformations. The extended conformation **156** was observed in the presence of Cu^{I} as this metal bound between two bidentate phenanthroline sites of the macrocycle and axle. Upon demetalation by potassium cyanide and subsequent metalation with Zn^{II}, the rotaxane switched to the contracted conformation **157** by forming five coordinate metal complexes between the phenanthroline and terpyridine sites of the macrocycle and axle, respectively. This contraction was reversible, as the addition of excess Cu^{I} regenerated the extended conformation.

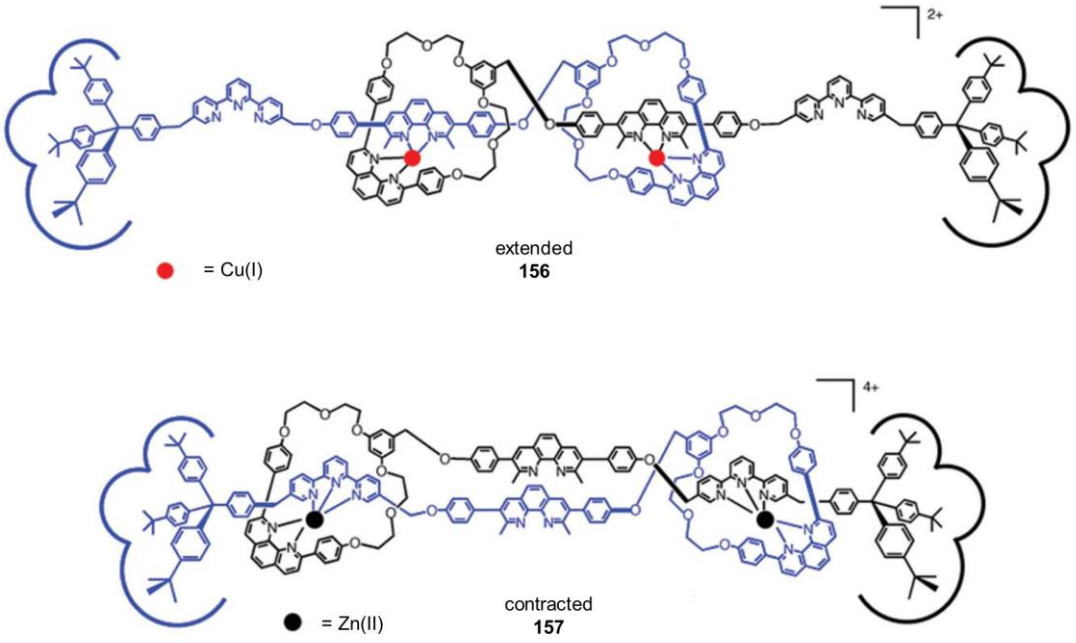

Figure 62. Sauvage's daisy chain rotaxane muscle. Reprinted from ref [104e] with permission of The Royal Society of Chemistry.

This metalation/demetalation strategy was also successfully employed by Sauvage to develop a switchable molecular receptor based on a cyclic bisporphyrin [4]rotaxane as an example of a press rotaxane.[122b] Previously, this group had reported [3]rotaxanes where two porphyrinic plates define the antipodes of an extensible space, adapting to guest binding between these plates (Figure 63a).[122a,122d,e] In the dicopper(I) [3]rotaxane **158**, the position of the macrocycles is fixed by coordination to copper centers, whereas the macrocycles are free

to move along the stoppered axle in the demetalated [3]rotaxane **159**. Therefore, the dicopper(I) and demetalated [3]rotaxanes are able to respond differently to chemical stimuli in the form of ditopic guests bearing pyridyl or amine groups that bind to the zinc porphyrin plates. The demetalated rotaxane **159** is adaptable and can accommodate different sized guests, in contrast to the dicopper rotaxane, which only binds small guests strongly because the distance between the porphyrinic plates is fixed. Interestingly, different guest binding behavior was observed with the cyclic bisporphyrin [4]rotaxane (Figure 63b). While the dicopper rotaxane **160** binds guests, such as DABCO and 1,4-diaminobutane, demetalation with potassium cyanide switches off binding of these guests, in contrast to the behavior of the [3]rotaxanes described above. This loss of guest affinity is attributed to a conformational change, whereby the demetalated [4]rotaxane **161** collapses and the zinc ions of the porphyrin coordinate to two of the four triazole groups in the axle. This internal competition prevents binding of ditopic guests between the zinc porphyrin plates. Re-metalation restores guest affinity and switches the rotaxane back to its initial conformation **160**.

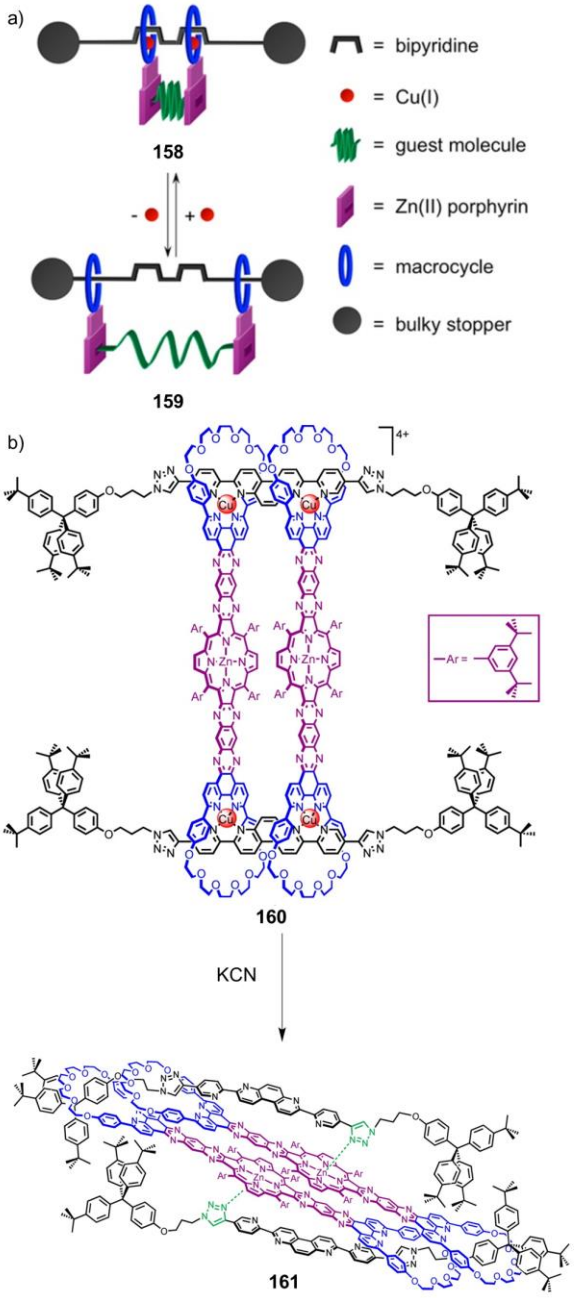

Figure 63. Sauvage's a) [3]rotaxane and b) [4]rotaxane molecular compressors. Adapted and reprinted with permission from ref [122a]. Copyright 2014 American Chemical Society.

6.4.2 Acid-base Responsive Molecular Muscles

Tanaka's fourfold rotaxane is another example of a press rotaxane, and in this case the molecular motion mimics a molecular elevator upon changing the pH (Figure 64).[123] The rotaxane consists of a porphyrin functionalized with four phosphoramidate and four alkylammonium groups, which thread through the four crown ether macrocycles appended to a

phthalocyanine. Both the porphyrin and phthalocyanine units contain a Cu^{II} metal center. pH can be used as a stimulus to alter the distance between the two units, resulting in switchable spin-spin communication. Under acidic conditions, the crown ethers encircle the protonated alkylammonium groups, resulting in isolated spins (**162**). Upon addition of base, the phosphoramidate groups are deprotonated, followed by the ammonium groups (**163**). This brings the porphyrin and phthalocyanine units closer together, resulting in antiferromagnetic coupling between the Cu^{II} centers. The protonation and deprotonation events were reversible for multiple cycles without degradation of the complex.

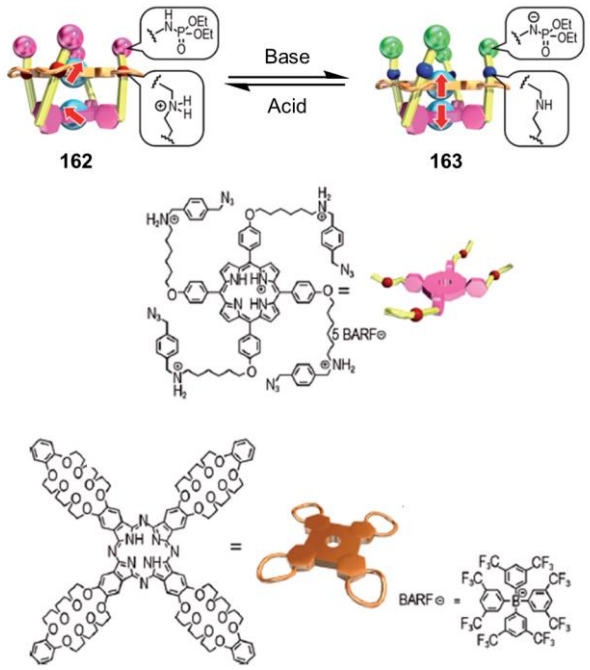

Figure 64. Tanaka's four fold rotaxane with switchable intermolecular communication. Adapted and reprinted with permission from ref [123]. Copyright 2012 Wiley-VCH.

Qu's [2](2)rotaxane, where (2) refers to the axle threaded twice through the macrocycle of a [2]rotaxane, is an example of a cage rotaxane (Figure 65).[124] The axle consists of a ferrocene unit symmetrically functionalized with both a dibenzylammonium and N-methyltriazolium station on each arm, while the macrocycle consists of an anthracene substituted with two dibenzo[24]crown-8 groups. In the stretched state **164**, the crown ether units reside on the

dibenzylammonium stations. Deprotonation switches the macrocycles to the N-methyltriazolium stations in the contracted state **165**. Molecular dynamics simulations of the two states, as well as an intermediate state where one dibenzylammonium is deprotonated, revealed that rotation of the ferrocene unit accompanies the stretching and contraction. Furthermore, the calculated length change of the rotaxane between the two states (~48%) exceeds the percentage length change in human muscle (~27%). Buhler and Giuseppone demonstrated that molecular contractions and extensions can result in micrometer scale changes by integrating thousands of molecular muscles into a [c2] daisy chain rotaxane.[125]

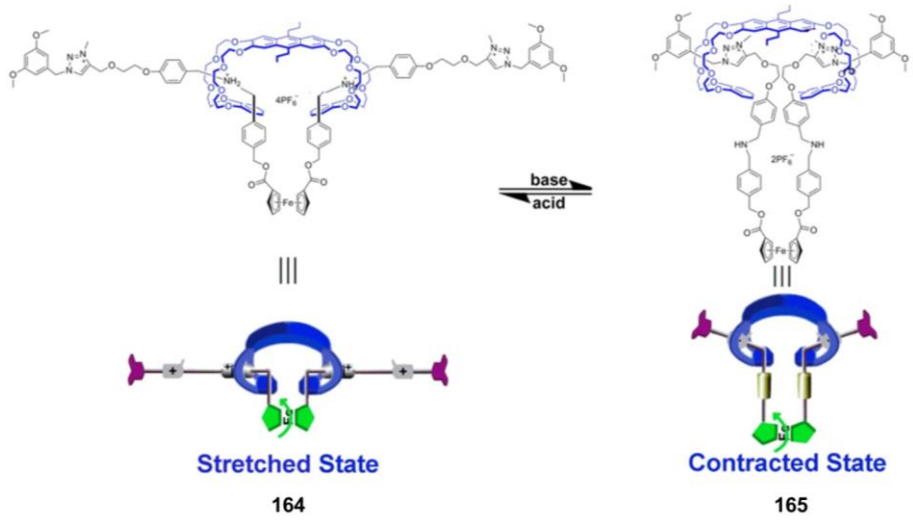

Figure 65. Qu's [2](2)rotaxane, where rotation of the ferrocene unit accompanies the stretching and contraction. Reprinted with permission from ref [124]. Copyright 2014 American Chemical Society.

6.4.3 Light Responsive Molecular Muscles

Light-switched rotaxanes can also be exploited to achieve muscle-like movement by contraction and extension. Tian's [1]rotaxane is one example where light was used to drive the molecular motion (Figure 66).[126] The [1]rotaxane consists of a cobalt(III) salen unit bridging two β-cyclodextrins functionalized with azobenzene moieties. Photoisomerization of the azobenzene units from *trans* (**166**) to *cis* (**167**) occurs upon irradiation at 365 nm, leading to a

contraction that brings the two cyclodextrins closer together. This contraction was accompanied by chemical shift changes in the ^{1}H NMR spectrum, the observation of a new set of NOE cross-peaks, and changes in the UV/visible and induced circular dichroism spectra due to the cyclodextrins residing closer to the metallosalen unit. The motion showed good photoreversibility; photoswitching was reproducible for 5 cycles even after storage in aqueous solution for one month.

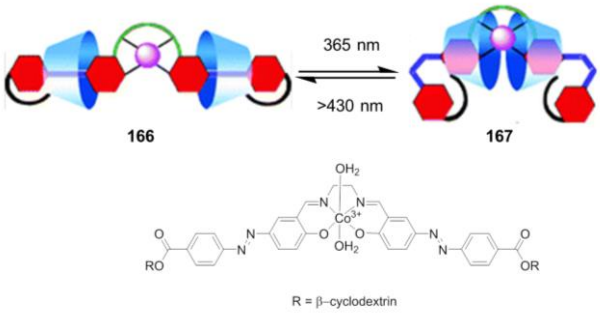

Figure 66. Tian's light responsive [1]rotaxane. Reprinted from ref [126] with permission of The Royal Society of Chemistry.

6.4.4 Multi-stimuli Responsive Molecular Muscles

Qu and co-workers reported the dual mode operation of a bistable [1]rotaxane, where pH and potential can be exploited as stimuli to operate an INHIBIT logic gate (Figure 67).[127] The [1]rotaxane design has a ferrocene unit covalently tethered to both a macrocycle and a stoppered axle, which is threaded through the macrocycle. The stoppered axle contains dibenzylammonium and N-methyl-triazolium stations for the macrocycle, and 4-morpholin-naphthalimide (MA) as both a stopper and fluorescent reporter. Fluorescence can be turned on and off by PET depending on the distance between the ferrocene and MA units. The macrocycle can be switched reversibly between the dibenzylammonium (**168**) and N-methyl-triazolium (**169**) stations by the addition of base and acid, respectively. Base leads to contraction and the fluorescence switching off due to PET, whereas acid leads to extension and restoration of the fluorescence in "active" mode. Oxidation of the ferrocene unit by

$Fe(ClO_4)_3$ switches operation from "active" to "silent" mode, where the fluorescent signal is unaffected by acid/base switching between the two stations (**170** and **171**). Ascorbic acid reduction returns the rotaxane to the "active" mode, where the fluorescence can be switched on and off by chemical stimuli. Through different combinations of base and $Fe(ClO_4)_3$, the fluorescence response of the rotaxane behaves like an INHIBIT logic gate and the authors propose that this type of system could be developed into a component of a complicated logic circuit.

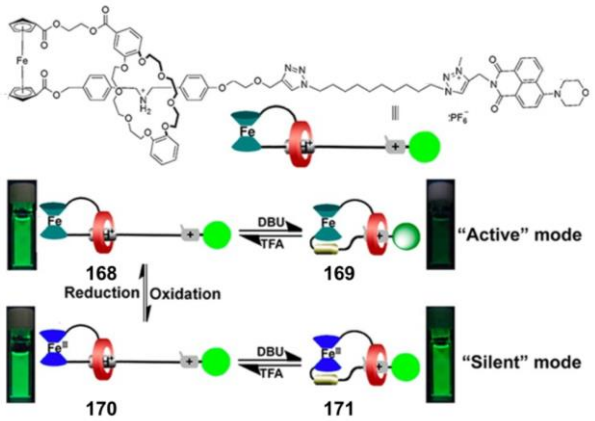

Figure 67. Qu's bistable [1]rotaxane, where addition of acid/base and reduction/oxidation controls the fluorescence response. Reprinted with permission from ref [127]. Copyright 2013 American Chemical Society.

6.5 Rotaxane-based Molecular Shuttles

6.5.1 Chemically Responsive Molecular Shuttles

Otera reported an intermittent molecular shuttle as a binary switch, which responds to metalation and demetalation (Figure 68).[128] The rotaxane contains two identical stations bridged by a bipyridine unit. In the dynamic mode (**172**) of the switch, the macrocycle shuttles between these stations. However, complexation of Cu^{I} between two rotaxanes results in a color change from orange to dark red and generates the static mode **173**, where shuttling is prevented between the two stations. Decomplexation was achieved by exposing the rotaxane

to an ion-exchange resin to regenerate the dynamic mode. Thus, it was possible to switch reversibly between the two states.

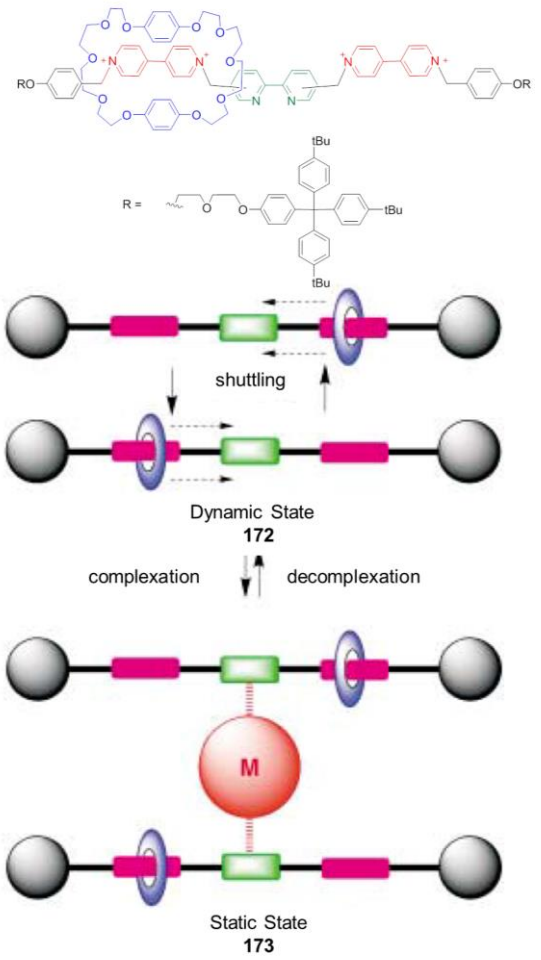

Figure 68. Otera's intermittent molecular shuttle. Reprinted with permission from ref [128]. Copyright 2004 Wiley-VCH.

6.5.2 Electrochemically Responsive Molecular Shuttles

Sauvage has reported a series of molecular shuttles where an electrochemical stimulus switches a copper-complexed macrocycle between the phenanthroline and terpyridine stations of an axle (Figure 69).[129] As with the pirouetting catenanes and rotaxanes in Sections 6.2 and 6.3, the rearrangement rates of Cu^{II} 4-coordinate (**175a**) and Cu^{I} 5-coordinate (**174b**) intermediates are affected by the steric bulk around the metal center. Their first reported example suffered from slow translation between the stations;[130] however, replacement of

macrocycle **176**, containing a 2,9-diphenyl-1-10-phenanthroline (dpp) unit, with **177**, containing the sterically less hindered 8,8'-diphenyl-3,3'-biisoquinoline (dpbiiq) unit, increased the speed of translation by at least four orders of magnitude.[129b,c] The flexibility of the linker between the stations also impacted the switching kinetics, with the more flexible linker **178** enabling faster translation than the rigid aromatic **179**. It was expected that increasing the distance between stations would slow translation. However, by introducing a third bipyridine station between the phenanthroline and terpyidine stations in axle **180**, it was possible to lengthen the axle considerably while maintaining a fast switching rate.[129a] It is not known whether the bipyridine unit acts as a real intermediate station, or if it simply helps stabilize the copper center between the two end stations.

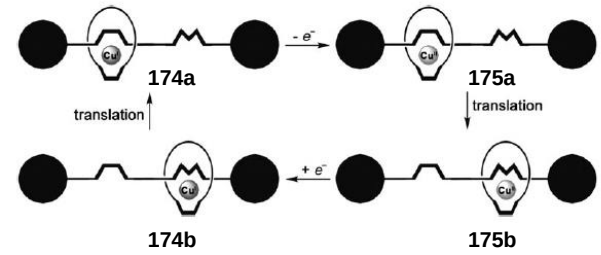

174a **175a**

174b **175b**

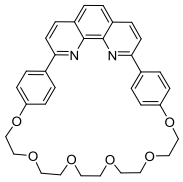

176

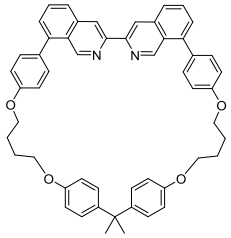

177

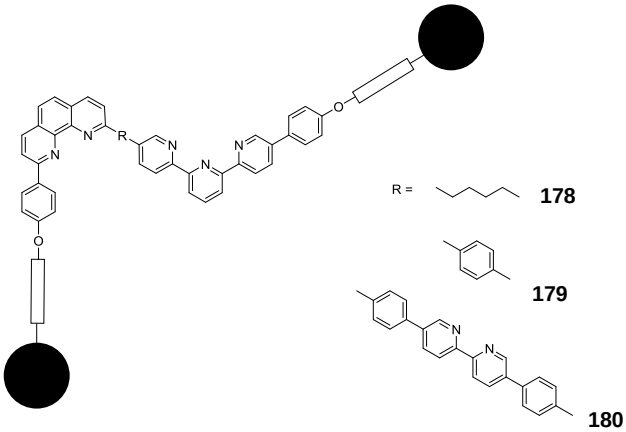

178

179

180

Figure 69. Sauvage's electrochemically responsive molecular shuttles. Adapted and reprinted with permission from ref [129c]. Copyright 2009 Wiley-VCH.

In an unusual example where switching does not involve co-conformational changes and where the rotaxane contains equivalent stations, Woźny and co-workers recently reported the potential-controlled reversible folding and unfolding of a rotaxane (Figure 70).[131] The rotaxane consists of a DBC8 macrocycle threaded onto an axle containing two nickel(II) tetraazamacrocyclic (TAM^{2+}) units as stoppers. When a flexible linker joins the two stopper units, a folded conformation is adopted due to π–π stacking interactions between TAM^{2+} and the benzene rings of the crown ether macrocycle, and shuttling between the TAM^{2+} stations occurs at room temperature. Interestingly, the rotaxane exhibits time-dependent electrochemical behavior: At fast scan rates, peaks at 1.31 V and 1.45 V are observed in the square wave voltammogram, corresponding to sequential oxidation of the two TAM^{2+} units (**181** to **182a** and **183a**) with the unit enclosed by the macrocycle oxidized first. Due to electrostatic repulsion between the TAM^{3+} units, the rotaxane unfolds to give structure **183b**. As the scan rate is decreased, the peak at 1.45 V decreases until there remains only a single broad peak at 1.31 V. Decreasing of the scan rate thus provides is enough time for structure **182a** to unfold to give structure **182b**, in which oxidation of the second TAM^{2+} unit also occurs at 1.31 V to give structure **183b**, leading to the broad single peak observed in the square wave voltammogram at slow scan rates. The unfolding process can be reversed when the potential is less than 1.31 V, as π–π stacking interactions drive the formation of the folded conformation. This unusual switching mechanism between identical stations is not always observed; replacing the flexible linker with a rigid one prevents adoption of the folded conformation, and thus only shuttling between the two stations is observed. More recently, the authors reported a molecular shuttle with an asymmetric axle containing Ni^{II} and Cu^{II} TAM units, where the potential-controlled switching involves not only unfolding of the rotaxane but also translocation of the DBC8 macrocycle.[132]

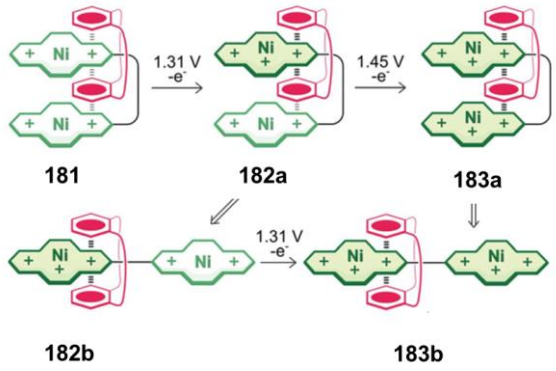

Figure 70. Mechanism of the dynamic behavior of a folding and unfolding rotaxane. Reprinted from ref [131] with permission of The Royal Society of Chemistry.

6.5.3 Light Responsive Molecular Shuttles

Stoddart, Balzani and co-workers have reported several examples of molecular shuttles driven by light, where ruthenium(II)tris(2,2'-bipyridine) is exploited as a photosensitizer to reduce 4,4'-dialkylbipyridinium units.[133] One example is rotaxane **184**, consisting of a ruthenium(II)tris(2,2'-bipyridine) stopper (P^{2+}), an electron rich macrocycle, and electron-deficient 4,4'-bipyridinium (A_1^{2+}) and 3,3'-dimethyl-4,4'-bipyridinium (A_2^{2+}) stations (Figure 71). In the ground state, the macrocycle resides on the more electron deficient A_1^{2+} station. Photoexcitation generates a long-lived, strongly-reducing excited state of the ruthenium complex. Photo-induced electron transfer from this excited state to the A_1 station results in the macrocycle shuttling to the A_2 station. Back electron transfer (BET) from the reduced A_1 station to the oxidized ruthenium complex restores A_1 as the more electron deficient station, and the macrocycle shuttles back from station A_2 to A_1. Initially, the proof of concept was demonstrated using a sacrificial switching mechanism, where triethanolamine (TEOA) and dioxygen were used as external reagents to reduce the P^{3+} and oxidize A_1^{+}, respectively.[133b] This approach does not generate an autonomous machine, which operates by itself as long as there is energy input, since alternate addition of fuels (TEOA and dioxygen) is necessary to achieve switching and waste products are generated. In order to operate

autonomously, an intramolecular rather than a sacrificial mechanism is necessary for the BET step. Several years later, the authors reported the autonomous operation of the system as a four stroke engine, although the competing BET (step 5) interfered with the shuttling reducing the quantum efficiency of the motor to 2%.[133a] However, this could be increased to 12% by using phenothiazine as an electron relay to slow down the BET step 5.

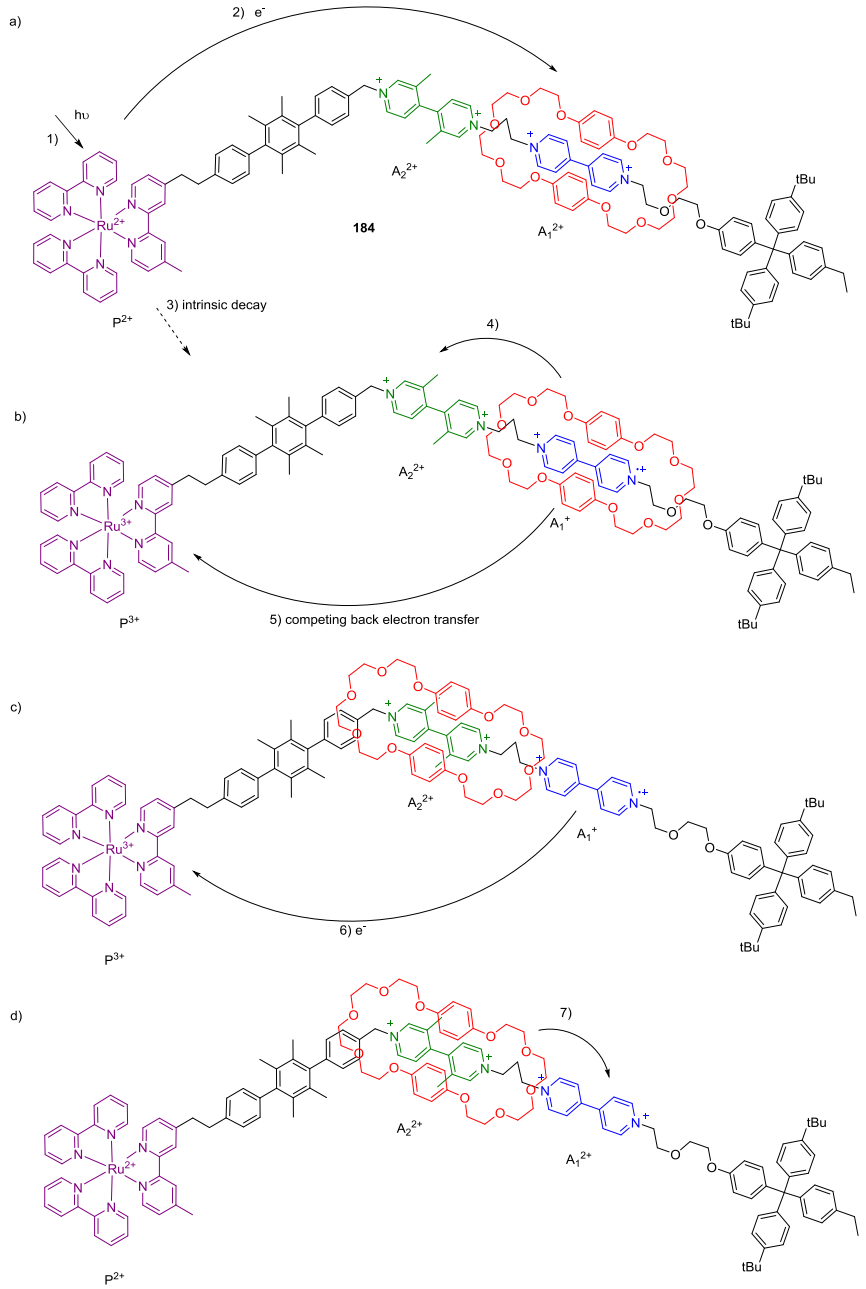

Figure 71. An autonomous artificial four-stroke engine powered by light.[133]

In a more recent example, light-driven switching in water was demonstrated by exploiting radical-radical interactions (Figure 72).[133c] In the ground state of rotaxane **185**, the cyclobis(paraquat-*p*-phenylene) macrocycle resides on the electron rich 1,5-dihydroxynaphthalene (DNP) unit rather than the electron deficient 4,4'-bipyridinium unit. In the presence of the sacrificial reducing agent TEOA, photoexcitation of the ruthenium complex transfers three electrons to reduce the 4,4'-bipyridinium units of the macrocycle station to generate radical cations. This results in shuttling of the diradical dicationic macrocycle from the DNP station to the radical cationic bipyridinium unit due to stabilizing radical pairing interactions, to generate rotaxane **186**. Upon oxidation of the radical cationic bipyridinium units by dioxygen, the macrocycle shuttles back to the DNP station.

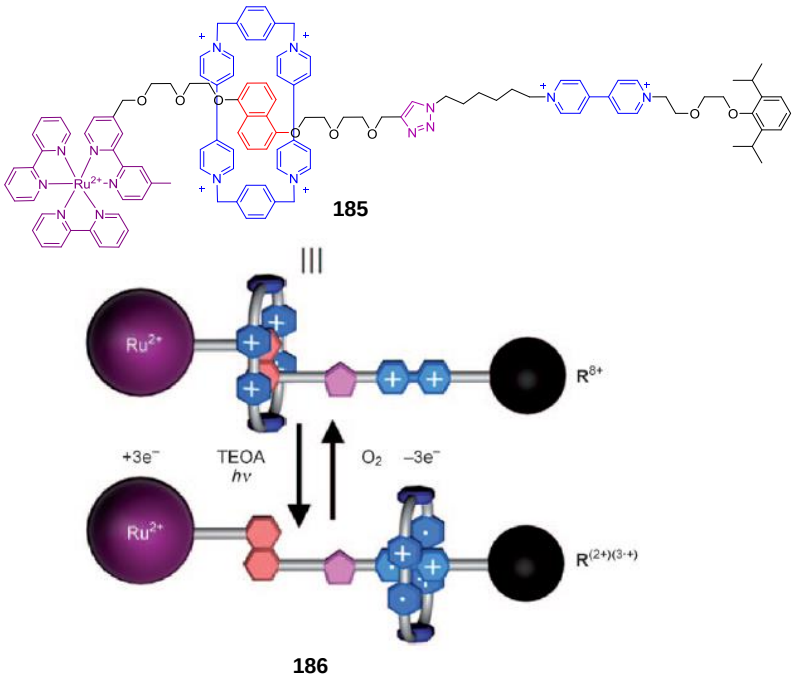

Figure 72. Sauvage and Stoddart's light responsive molecular switch driven by radical-radical interactions in water. Adapted and reprinted with permission from ref [133c]. Copyright 2011 Wiley-VCH.

6.5.4 Multi-stimuli Responsive Molecular Shuttles

Leigh and co-workers have reported a multi-stimuli responsive molecular shuttle where pH changes initiate shuttling of a Pd^{II}-complexed macrocycle between 4-dimethylaminopyridine

and pyridine stations (Figure 73a).[134] However, the macrocycle does not immediately translocate to the second station due to the substitution pattern of the ligands and kinetic inertness of the Pd-N bond. Instead, a second stimulus (heat and/or a coordinating solvent/anion) is required, and as a result, four states of the shuttle can be isolated and characterized (**187a-b, 188a-b**). Through extension of this work, a molecular walker **189** was designed by replacing the Pd^{II} macrocycle with a Pd^{II} acyclic component (the Pd^{II} foot) and including a kinetically inert Pt^{II} complex between the 4-dimethylaminopyridine and pyridine stations (Figure 73b).[135] The Pt^{II} complex acts as a pivot for the Pd^{II} foot to step between the two stations.

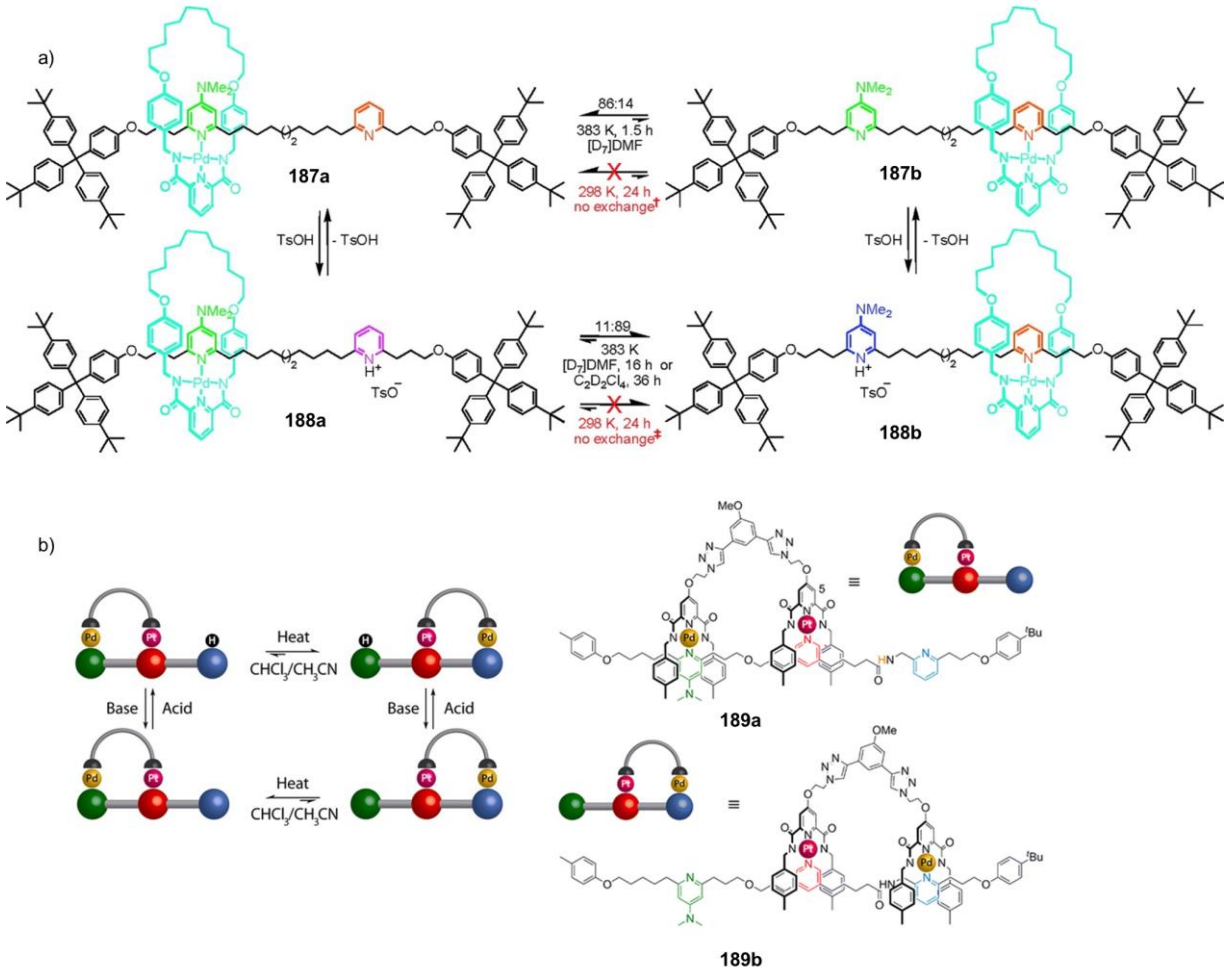

Figure 73. Leigh's multi-stimuli responsive a) molecular shuttle and b) molecular walker. Adapted and reprinted with permission from refs [134] and [135]. Copyright 2007 and 2014 American Chemical Society.

Zhu's molecular shuttle consisting of amide and dialkylammonium stations operates as a multilevel fluorescence switch, where the fluorescence emission was tuned by pH and metal complexation/decomplexation (Figure 74).[136] In the absence of a stimulus, the macrocycle resides on the dialkyammonium station and fluorescence was completely quenched due to strong PET from the aniline subunit of the macrocycle to the anthracene stopper (**190**). Addition of base caused the macrocycle to shuttle from the dialkylamine to the amide station (**191**). In this state, PET from the macrocycle was weakened, but the fluorescence only increased slightly due to PET from the dialkylamine to the anthracene stopper. In contrast to pH, metal ion complexation had a more significant effect on fluorescence; lithium complexation to the amide station of the macrocycle (**192**) further increased the fluorescence, as PET from the macrocycle was completely blocked, however, Zn^{II} complexation induced the highest level of fluorescence emission. Coordination of Zn^{II} to the macrocycle and dialkylamine station caused the macrocycle to shuttle (**193**) and as a consequence, all PET processes were blocked. The operation of the multilevel fluorescence switch was reversible over 6 cycles by alternate addition of Li^+/[12]-crown-4 or Zn^{II}/EDTA.

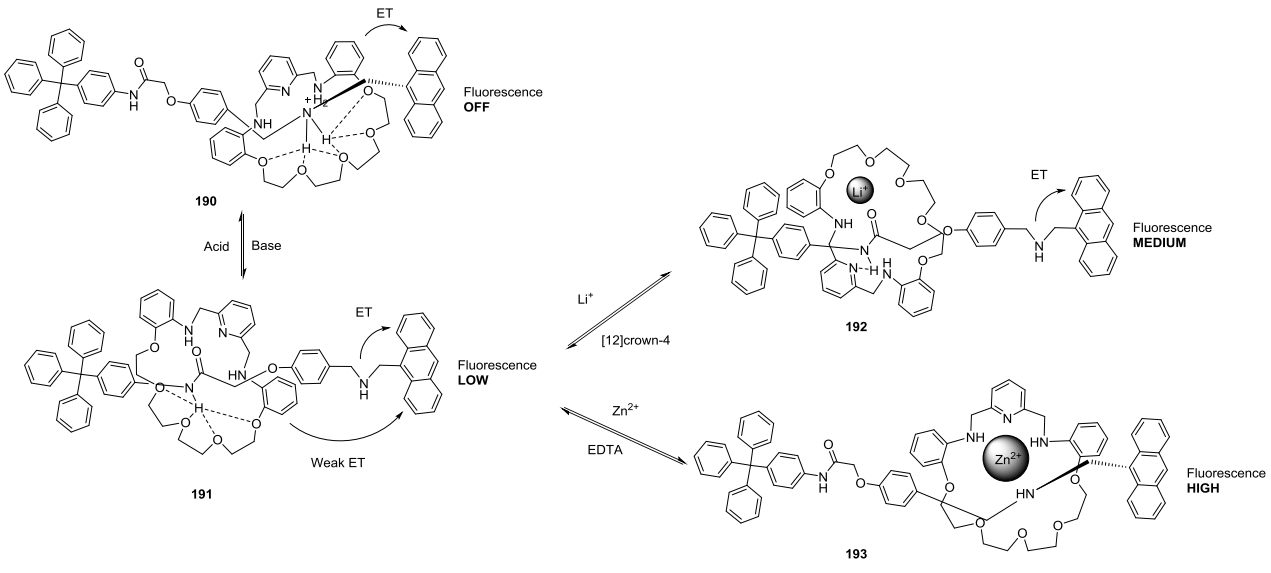

Figure 74. Zhu's multilevel fluorescence switch tuned by pH and complexation.

7 Metal Organic Cages

Metal organic cage assemblies have attracted much interest in recent years because their enclosed internal voids provide an environment isolated from bulk solution, into which guest molecules may bind. As chemists have grown adept at designing and synthesizing these 3D assemblies, greater control has been gained over the structure of this internal environment. Consequently, the number of functions performed by these cage assemblies now range from catalysis[137] to acting as protecting groups[138] (for both reagents and catalysts) and as potential drug delivery systems.[139]

These functions make it desirable to introduce stimuli-responsiveness into cage assemblies. If a response can be designed to affect the environment of the internal void or the rate at which molecules pass into it, further control over host-guest chemistry may be envisaged.

A plethora of complex three-dimensional complexes have been prepared through the thermodynamically-controlled self-assembly of smaller components. The dynamic nature of these assemblies and the number of interactions involved in their formation often means that stimuli have the potential to invoke complex responses, including multiple structural rearrangements.

7.1 Light Responsive Metal Organic Cages

It is challenging to create cage assemblies that respond in a complex way to a light stimulus. A large body of work demonstrates the selective uptake of photoresponsive guests,[140] the modulation of an assembly's physical properties with photo-responsive counterions,[141] and different photo-reactions involving bound guests,[142] all of which are beyond the scope of this review. To affect the architecture itself requires the introduction of functional groups that can both absorb light and modulate a strong chemical response, so that structure is modified. To

date the most striking example of this behavior is found in recent studies by the Clever group.[143]

7.1.1 Light-driven Structural Reconfiguration

Clever *et al.* introduced a DTE photoswitch into pyridine-based bis-monodentate ligand **194** that, upon addition of stoichiometric amounts of Pd^{II}, self-assembles to form complex **195** (Figure 75). When pre-formed (**195**) is irradiated at 365 nm, the DTE photoswitch cyclizes, causing the ligands to rigidify and cease isomerizing by bond rotation. The cyclized (***closed*-195**) and non-cyclized (***open*-195**) forms of the complex both bind a $[B_{12}F_{12}]^{2-}$ guest, but with different affinities ($K_{closed} = 6.7 \times 10^2\ M^{-1}$ vs $K_{open} = 3.2 \times 10^4\ M^{-1}$). Thus, a light signal has been used to cause a structural change in an architecture that modulates guest binding.

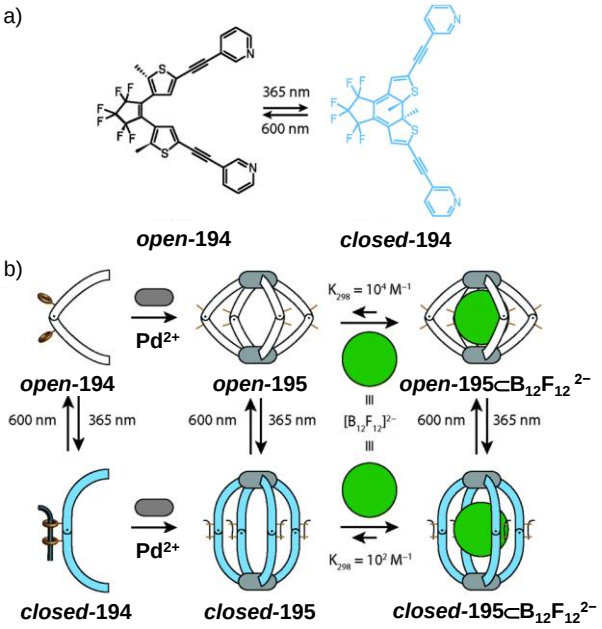

Figure 75. a) Clever's DTE-containing bismonodentate ligand and b) the light driven modulation of guest binding of a derived Pd_2L_4 cage. Adapted from ref [144] with permission of The Royal Society of Chemistry.

Previous to this, there have been examples of a cage's properties being modulated by light without affecting the overall structure of the cage itself. This strategy was first achieved by Fujita *et al.* by incorporating endohedral azobenzene units into a $Pd_{12}L_{24}$ spherical complex.[145]

These inward-facing photoresponsive groups were shown to alter the hydrophobicity of the complex's cavity, through isomerization between the *trans* and *cis* isomers of azo-benzene, which in turn modulated the binding of a 1-pyrenecarboxaldehyde guest (Figure 76).[146]

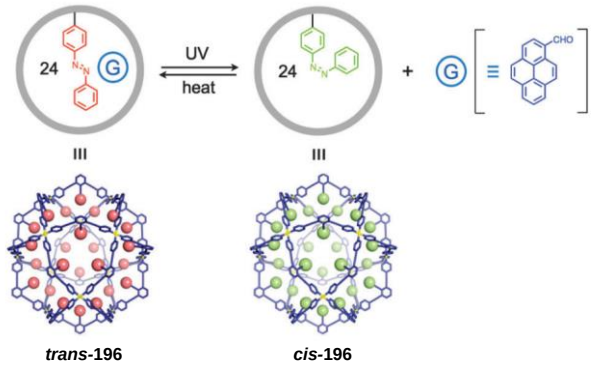

Figure 76. Control of the interior hydrophobicity of a $Pd_{12}L_{24}$ spherical complex by the *cis*/*trans* photoisomerisation of 24 azobenzene units within its cavity. Reprinted from ref [145] with permission of The Royal Society of Chemistry.

More recently Zhou *et al.* added outward-facing azobenzene chromophores to a copper(II) "paddle-wheel"-based cuboctahedron.[147] These groups did not affect guest binding within the cavity of the host within solution. However, solid state studies under conditions where both *trans* and *cis* forms of the cage were present showed that guests, bound in interstitial binding sites between the cage units in the solid state, were released upon irradiation with UV light (Figure 77).

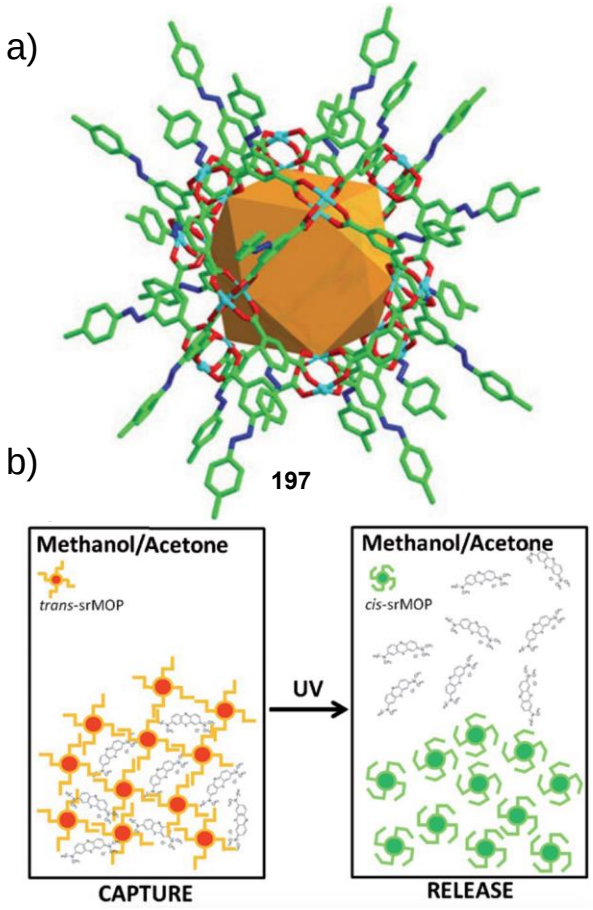

Figure 77. a) Crystal structure of **197** an azobenzene-functionalized cuboctahedral cage, as determined by single-crystal X-ray diffraction analysis. b) Schematic illustration of the capture of methylene blue by *trans*-**197** and its release from *cis*-**197.** Adapted and reprinted with permission from ref [147]. Copyright 2014 Wiley-VCH.

7.1.2 Photo-active Hosts

The photo-reaction of a bound guest that involves the reduction, oxidation or energetic excitement of the host, in the context of this review, is classed as a stimuli-responsive system in which a light stimulus acts on the assembly.

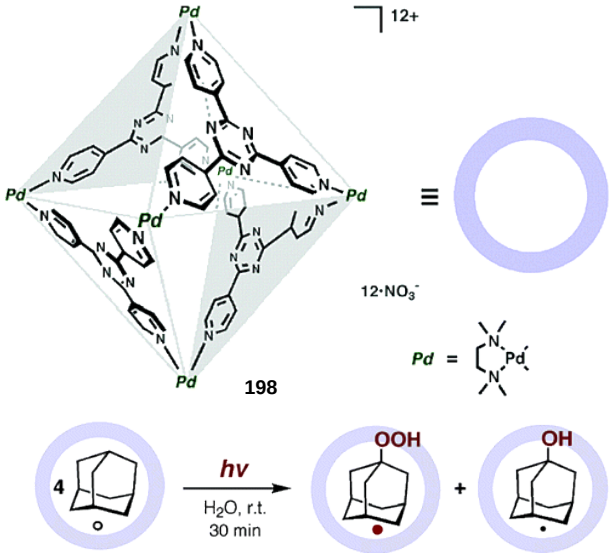

Figure 78. Cage **198**, which photo-oxidizes the encapsulated adamantane guest through PET. Adapted and reprinted with permission from ref.[148] Copyright 2004 American Chemical Society

Fujita *et al.* provided the first example of a self-assembled cage photo-sensitizer. A M_6L_4 coordination cage, constructed from four tritopic pyridine based ligands and six cis-protected Pd^{II} cations, bound an adamantane guest. Upon photo excitation of the cage by UV light in the presence of oxygen the bound adamantane was regioselectively oxidized.[148] Further experiments showed linear hydrocarbons which could bind in the cage (C_nH_{2n}, n = 6-8) were also photo-oxidized, but longer linear hydrocarbons and guests that were not bound by the cage, e.g. decalin and perhydrofluorene, were not changed, demonstrating that encapsulation was essential to the oxidation process. This host has further been used in the photooxidation of triquinacene[149] and in the photo-driven anti-Markovnikov hydration of 1-phenyl-1-hexyne.[150] In initial studies there was little evidence for the proposed mechanism of PET from guest to host. However, a follow up publication[151] used in situ IR spectroscopy, electrochemical measurements and calculations to show that the mechanism involves the generation of a host radical anion species, where the electron-deficient triazine panel acts as the electron acceptor.

Further investigations into host-guest energy transfer were also undertaken using picosecond time-resolved fluorescence spectroscopy by Tahara *et al.*[152]

The strategy of host sensitization has been expanded upon further by Duan *et al.* in the creation of a supramolecular system capable of inducing light-driven water splitting.[153] They designed a cerium-based metal-organic basket-like complex that binds a [FeFe]-hydrogenase mimic. Carbazole fragments contained within the linear chelating ligand were used as the photosensitizer, as their reduction potential of ca. -2.3 V was sufficient to allow PET to the iron cluster. Light-driven H_2 production occurred in the presence of $^{i}Pr_2EtNH{\cdot}OAc$ as a sacrificial electron donor; control experiments showed both host and guest needed to be present in order for H_2 evolution to take place. To confirm whether the H_2 production occurred in the host cavity, a non-photoactive guest adenosine triphosphate (ATP) was introduced to the system. The ATP outcompeted the [FeFe] cluster for the host central binding pocket and subsequently inhibited H_2 production.

7.2 Electrochemically Responsive Metal Organic Cages

Beyond photo-oxidation, metal organic cage assemblies have also been designed to exhibit electrochemically responsive behavior either through the incorporation of redox-active ligands, or through electrochemistry on the metal ions themselves. So far, coupling an electrochemical stimulus to a complex response has yet to be realized but remains an attractive target due to the potential coupling of these systems into conventional electronics. Recently Sallé *et al.* designed a series of tetrathiafulvalene-containing ligands that form a variety of cages upon complexation with palladium(II), platinum(II) or ruthenium(II) (Figure 79).[154]

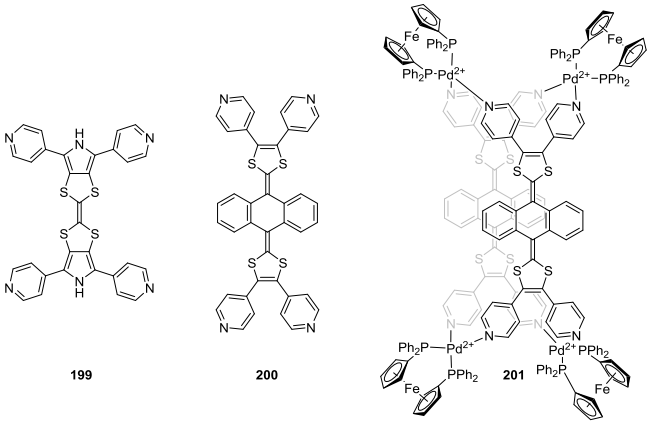

Figure 79. Tetrathiafulvalene containing ligands **199** and **200** and an example Pd^{II}-based cage **201**.[154]

An M_6L_3 prism formed from Pd^{II} and ligand **199** has been shown to bind tetrafluoro tetracyano-*p*-quinodimethane ($TCNQF_4$) in acetonitrile. This electron-poor guest interacted with the electron rich ligands to form a charge transfer complex, as observed by the increase in new absorption bands corresponding to the progressive formation of the $TCNQF_4$ radical anion, and the ligand based radical cation.

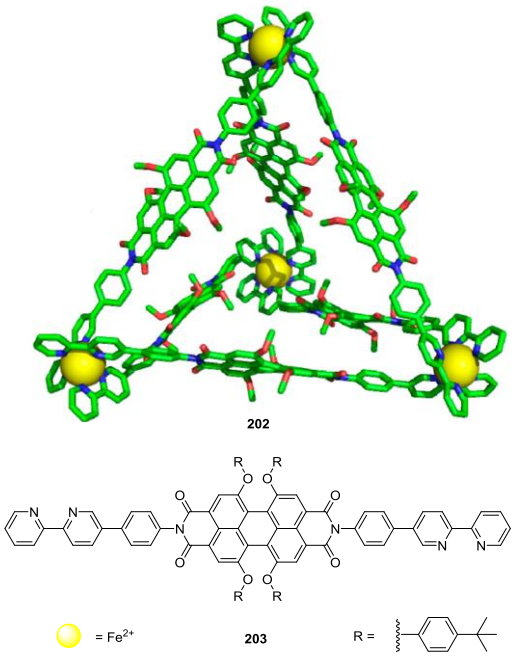

Figure 80. An electroactive host tetrahedron **202** formed from perylene bis imide containing ligand **203.** Adapted and reprinted with permission from ref.[155] Copyright 2013 American Chemical Society.

Würthner *et al.* have employed a similar strategy to create an electroactive host tetrahedron formed from Fe^{II} ions and ligand **203**, consisting of a linear perylene bisimide with two 2,2'-bipyridine groups covalently attached at each end (Figure 80).[155] The cyclic voltammogram of the cage is complicated, featuring seven reversible electrochemical oxidation and reduction waves spanning a 3.0 V range. The cage is also shown to bind one or two equivalents of the fullerene C_{60}.

Clever *et al.* have also created a phenothiazine-based banana-shaped[144] ligand that upon self-assembly with Pd^{II} ions creates an interpenetrated $(Pd_2L_4)_2$ coordination cage.[156] The ligand can be successively chemically oxidized to its S^{IV}=O and O=S^{VI}=O forms. Both forms can be obtained free in solution or as part of the interpenetrated cage assembly. However, apart from observing some structural changes in the solid state (a 5% reduction in the Pd-Pd distance on oxidation), the ligand oxidation has not yet been coupled to a more intricate response.

7.3 Chemically Responsive Metal Organic Cages

Chemical stimuli can take a range of forms, from changes in pH to the addition of coordinating ions or guest molecules. In order to effect a significant structural response, the stimulus must substantially alter the thermodynamic landscape of the system to cause the destruction of the assembly or the formation of a new structure. The mode of action may be obvious (e.g., the protonation of coordinating pyridine ligands or addition of a competing reagent that reacts with cage components) or more subtle, where multiple weak interactions act to favor one structure over another of similar thermodynamic stability (e.g., guest induced structural rearrangement).

7.3.1 pH Responsive Metal Organic Cages

Despite the ability of metal organic cage assemblies to bind guests, there are currently few examples of reversible destruction and reformation of a host as a method of guest capture and release.[139] Because protons can compete for Lewis-basic ligand binding sites, pH is a stimulus that may often be used to induce a host's disassembly and, depending on the stability of the components, reassembly.

One example from our group that illustrates this strategy uses the reversible protonation of metal-coordinating ligands, and the pH-dependence of the Schiff base formation equilibrium to deconstruct a metal organic cage into its protonated sub-components. The reaction of 4,4'-diaminobiphenyl-2,2'-disulfonic acid and 2-formylpyridine with iron(II) sulfate and base generates water-soluble metal-organic tetrahedron **204**. This cage was shown to bind a range of hydrophobic guests, including cyclohexane, P_4 and sulfur hexafluoride. Release of these guests through host disassembly could be effected by reducing the pH. A subsequent pH increase was shown to cause the reformation of the host and re-encapsulation of the guest (Figure 81).[157] Likewise, a related subcomponent-based cage synthesized by Kaifer *et al.* has also be shown to disassemble and reassemble on varying pH, enabling the capture and release of sulfate.[158]

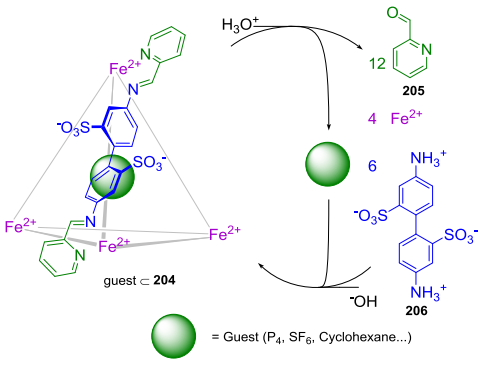

Figure 81. Water soluble tetrahedral cage **204** and its reversible assembly/disassembly and accompanied guest release on changes of pH.

Shionoya *et al*. have observed that a mixed metal Ti^{IV} and Pd^{II} based $Pd_2Ti_2(HL_2)_2(acac)_2Cl_4$ (acac = acetylacetone) ring that could be converted into a $[Pd_3Ti_2(L_6)\ Cl_6]^{4-}$ cage through the addition of base. This conversion was found to be reversible.[159]

Lusby *et al.* have also exploited pH as a stimulus to form responsive coordination complexes, metalla-cycles and polyhedra.[160] They exploit the fine balance between the formation of a Pt-C bond between metal and ligand and the resulting Pt-X C-H bonds formed from HX insertion into a square-planar carboplatinum complex [LPt(X)] (H_2L = 2,6-diphenylpyridine). Using this responsive system, they have demonstrated the inter-conversion between a $[(HLPt)_6(4,4'\text{-bipyridine})_3(tpt)_2](PF_6)_6$ (tpt = 2,4,6-tri-4-pyridyl-1,3,5-triazine **209**) trigonal prism **212**, $[(HLPt)_4(4,4'\text{-bipyridine})_4](PF_6)_4$ tetra-nuclear metallocycle **210** and two linear bimetallic coordination complexes $[(LPt)_2(4,4'\text{-bipyridine})]$ **211** and $[(HLPtX)_2(4,4'\text{-bipy})]$ **207** (Figure 82).

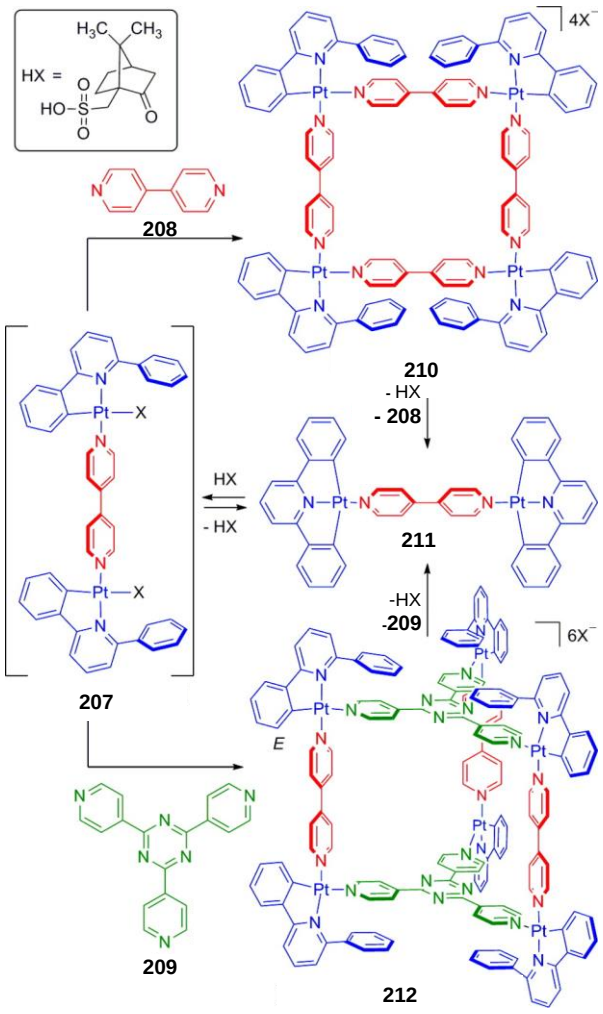

Figure 82. Interconversion between several Pt^{II} based structures through changes in pH. Reprinted with permission from ref [160b]. Copyright 2009 American Chemical Society.

In a different approach, Saalfrank *et al.* demonstrated a pH responsive assembly whose response is not linked to the destruction of the cage.[161] The system is based on a C_3-symmetric N-centered heptadentate tris(1,3-diketonate) ligand which self-assembles in the presence of indium(III) into a In_4L_4 tetrahedron. The nitrogen at the center of the ligand can be protonated or deprotonated, with the hydrogens of the protonated form pointing into the interior in the solid state. Only the non-protonated form is able to bind cesium ions.

7.3.2 Guest Responsive Metal Organic Cages

The binding of guests into the internal cavities of cage assemblies has been extensively studied.[137b,138b] All guest binding causes small perturbations in the structure of the host. For the guest to bring about a significant structural change, binding must template a new structure and the energetic barriers to the interconversion between those structures must be surmountable.

Raymond *et al.* provided an early example of a guest responsive assembly with a 2,4 diaminoanthracene based ligand. The ligand was used to form either M_2L_3 helicate or the entropically disfavored M_4L_6 tetrahedron (Figure 83). Introduction of Me_4N^+ templates the formation of the M_4L_6 tetrahedron, demonstrating that the enthalpic gain of binding the guest overcomes the entropic penalty of forming a larger assembly. Ti^{IV} analogues of the helicate and tetrahedron were synthesized, but Ga^{III} was chosen for the interconversion studies due to its greater lability.[162]

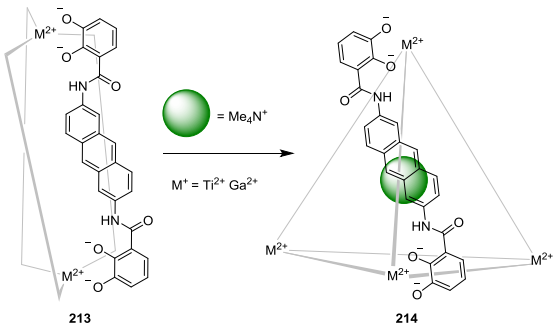

Figure 83. Interconversion between a Ga_2L_3 helicate and a Ga_4L_6 tetrahedron via guest binding.[162]

The Fujita group synthesized a guest-responsive trigonal prismatic host from three (3-pyridyl) functionalized porphyrins and six Pd^{II}(en) (en = ethylene diamine) corners. Each Pd^{II}(en) center can orient apically or equatorially with respect to the prismatic framework.[163] In the case of the empty host, only apically orientated Pd^{II}(en) centers were observed in the X-ray crystal structure. This observation was further corroborated via molecular modeling studies that predicted a 67.6 kcal mol^{-1} stabilization of the all-apical structure over the all-equatorial isomer. Upon addition of a pyrene guest, the simple ^{1}H-NMR spectrum of the host became more complicated, indicating a change in the structure of the host from a D_{3h}-symmetric species to one that is C_2-symmetric. Their proposed structure of the new C_2-symmetric species has two equatorial Pd^{II}(en) centers at either corner of the prism , reducing the distance between two of the porphyrins. This reduced distance provided a smaller binding pocket, with improved π-contact between the host and the pyrene guest.

Guest binding can also bring about the formation or change the physical properties of host cavities. Recently, we published a molybdenum-paddlewheel-based supramolecular cube whose guest binding properties could be modulated by the binding of guests into the interior of the cavity.[164] Guests such as ammonia, trimethyl ammonia and triphenylphosphine coordinate to the interior molybdenum sites of the paddlewheels, creating a binding pocket that encapsulates iodide with a greater affinity than that of the empty cube host. The binding of

triflate, a larger anionic guest, inhibits iodide binding. In addition, two forms of allosteric modulation of guest binding have also been observed to act on this cubic host.[165]

Anions are another class of guest used extensively to effect structural rearrangements. Shionoya *et al.* showed that a system consisting of tritopic ligands and Ag^{I} ions was capable of expressing either a tetrahedral $Ag_4L_4^{4+}$ species, when triflate was present to act as a template, or a disk-shaped $Ag_3L_2^{3+}$ species.[166] The $Ag_4L_4^{4+}$ species could be transformed into the $Ag_3L_2^{3+}$ through an increase in concentration of Ag^{I}, a stimulus that will be discussed below.

We have reported a chemical network that exists in three distinct states (Figure 84), comprised of aniline **215**, dialdehyde **216**, and cobalt(II).[167] The first state is a dynamic combinatorial library, **217**, of Co^{II} ions linked to varying numbers of coordinated ligands. The second state, formed on the addition of a triflate or hexafluorophosphate anion, is a more ordered $Co^{II}_4L_6$ tetrahedral capsule **218**. The third state is induced by the addition of an anion such as ClO_4^-. The anion brings about a structural rearrangement of the tetrahedron into a $M_{10}L_{15}$ pentagonal prism **219** assembled from 60 molecular components. Five interstitial binding pockets bind perchlorate and a sixth binding pocket in the center of the complex binds a chloride anion with high affinity. Further investigations found that the $M_{10}L_{15}$ architecture was not unique to Co^{II} and could be formed with Fe^{II}, Cd^{II} or Zn^{II} ions.[168] A related $M_{12}L_{18}$ hexagonal prism was also discovered, and found to convert into other structures upon application of an anionic signal.[169] The transformation from $M_{12}L_{18}$ to $M_{10}L_{15}$ was effected by the addition of a secondary template such as halide ions that bound into the sixth central binding pocket in the $M_{10}L_{15}$.[168a]

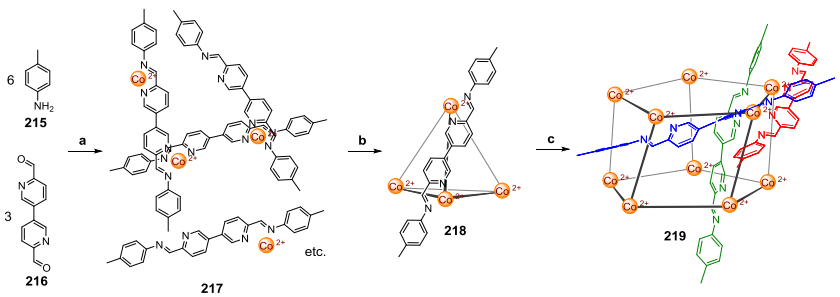

Figure 84. A molecular network transformed through various anionic guest stimuli. Adapted and reprinted with permission from ref [167]. Copyright 2012 Nature Publishing Group.

Clever *et al.* have observed structural reconfiguration of their $[Pd_2L_4]^{4+}$ coordination cages upon application of an anionic guest signal.[170] When cages were formed from ligand **220**, a transient thermodynamically unstable $[Pd_2L_4](BF_4)_4$ empty cage **221** was observed, which rapidly transformed into $[BF_4{\subset}Pd_4L_8](BF_4)_7$ interpenetrated cage **222**, with two secondary binding sites for chloride. Additionally, the related ligand **224** self-assembles in the presence of Pd^{II} ions to form empty monomeric $[Pd_2L_4](BF_4)_4$ cages **225** that can be isolated and subsequently transformed into an interpenetrated dimer $[Cl{\subset}Pd_4L_8]$ **226** upon addition of a chloride ion signal. This interpenetrated cage also contains two new binding pockets suitable for the encapsulation of perrhenate ions.

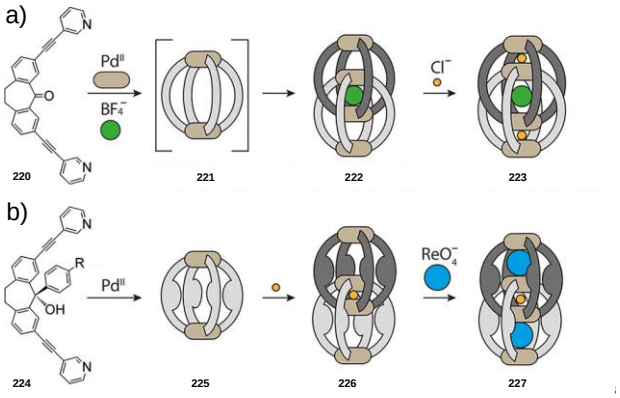

Figure 85. Interpenetrated cages **221** and **225** and their anion induced interpenetration and reconfiguration. Reprinted from ref [144] with permission of The Royal Society of Chemistry.

These hetero-anionic systems are similar to homo-anionic work by Kuroda *et al.,* where a similar Pd^{II}-based M_2L_4 cage transforms into the related interpenetrated dimer through the addition of nitrate. The reverse reaction is also possible; the addition of a naphthalene sulfonate anion causes the cleavage of the dimer into monomers.[171]

Our group has observed a subtle response to anionic signals in an $Fe^{II}_4L_6$ tetrahedral cage formed through the subcomponent self-assembly of 4,4-diaminobiphenyl, 2-formylpyridine and iron(II).[172] When the cage is formed from iron(II) bis(triflimide), the cage has no anion bound in its central cavity. It exists as a collection of diastereoisomers of *T*, C_3 and S_4 symmetry. Different anionic guests were found to bind more strongly to one diastereoisomer over the others, causing a shift in the equilibrium and an increase in population of the most strongly-binding species. The effect is particularly pronounced for the halides and BF_4^-, which template the *T*-symmetric diastereoisomer to such an extent that it is exclusively seen in solution.

7.3.3 Coordinatively Responsive Metal Organic Cages

Structural responses can be introduced into cage assemblies as a consequence of the dynamic nature of the metal-ligand interactions used to form them. Stimuli in the form of competing ligands or changes in stoichiometry can change the form of a cage, or completely disassemble it in solution.

Crowley *et al.* have used a competing ligand in the form of dimethylaminopyridine (DMAP) to disassemble a Pd_2L_4 cage **228** based on (2,6-bis(pyridin-3-ylethynyl)pyridine) ligands (**229**). This cage encapsulates the anticancer drug cisplatin **230** (Figure 86).[139] Their goal is to exploit the stimuli responsiveness of the cage in the targeted delivery of the encapsulated cisplatin to tumors, thus mitigating its side effects.

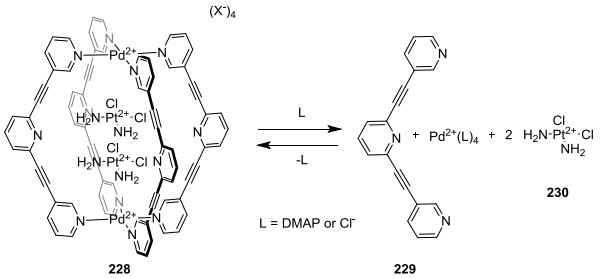

Figure 86. The capture and release of *cis*-platin on addition of competing ligands to cage **228**.[139]

Hardie *et al*. have also utilized the coordination of DMAP to Pd^{II} to induce the disassembly of homoleptic $[M_6L_8]^{12+}$ stella octangula cages. This process was reversible, and reassembly could be induced by the protonation of DMAP by TsOH. Furthermore, the addition of DMAP to a solution of $[Pd_6L_8]^{12+}$ cages composed of two different ligands was used to induce ligand exchange, resulting in a library of heteroleptic stella octangula cages.[173]

Competing ligands have been used not to only induce the disassembly of cages, but also to bring about their structural reconfiguration into new species. Zhou *et al.* used this strategy in the reconfiguration of 2D metallocycles to interconvert between a series of homo- and hetero-leptic 3D cage architectures.[174] They developed a network of Cu^{II}-paddlewheel based architectures built from a library of di-carboxylate ligands. An initial Cu^{II}-paddlewheel monomer **236** could be transformed first into homoleptic cages (e.g. **235**, Figure 87), then into heteroleptic cages (e.g. **241** Figure 87) or finally dissembled into new Cu_2 paddlewheel monomers (e.g. **238** Figure 87). In each case the transformation from one structure to another is driven by the addition of competing ligands.

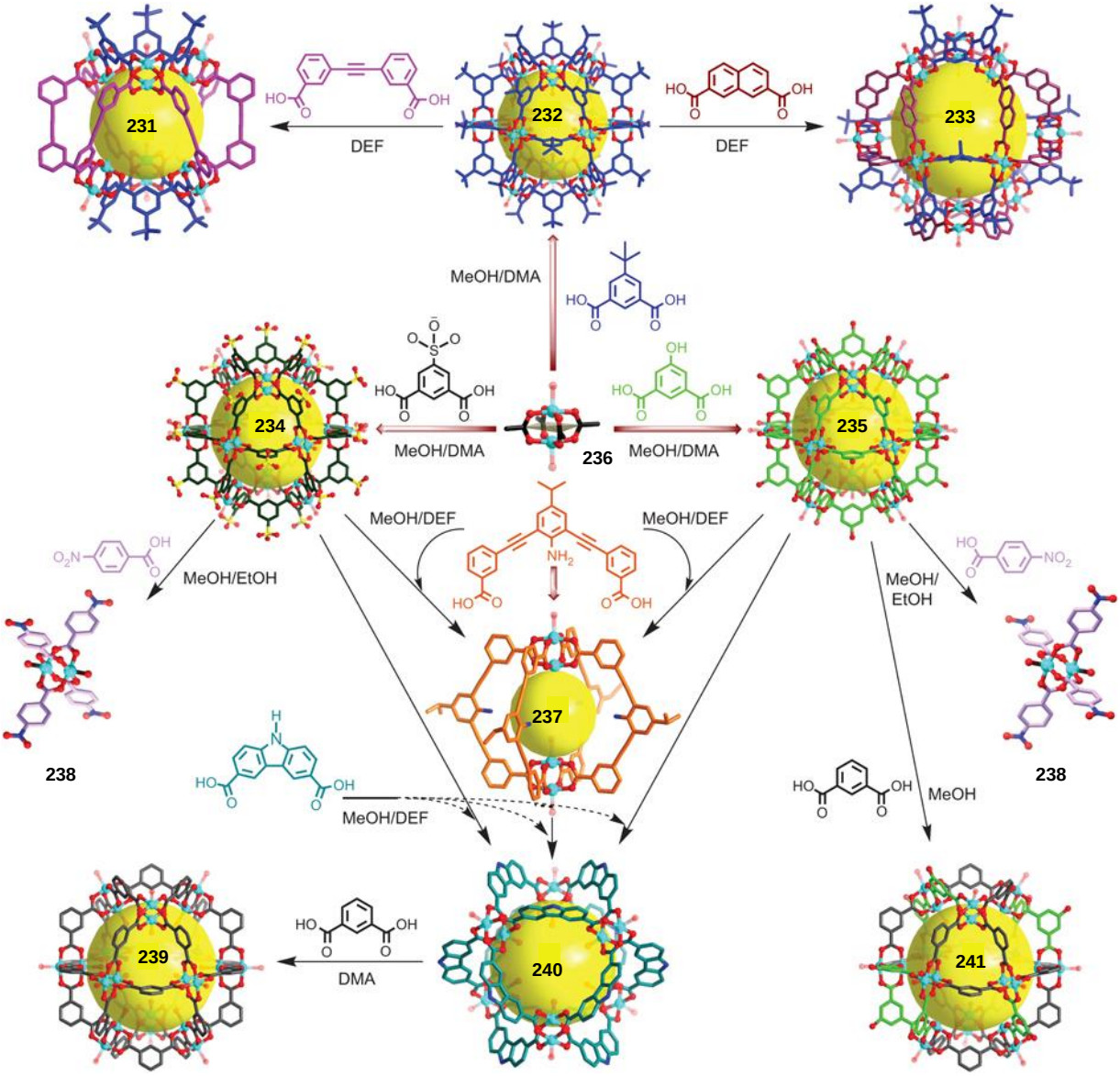

Figure 87. A series of homo and heteroleptic 3D cage architectures synthesized via ligand exchange on a Cu_2 paddlewheel building block. Reprinted by permission from Macmillan Publishers Ltd: Nature Chemistry[174], copyright (2010)

Stang *et al.* have also applied this strategy to the post assembly modification of cages, and have developed a system of molecules capable of ligand exchange based on the preferential coordination of one carboxylate and one pyridyl ligand to Pt^{II}. Early work showed the conversion of two homoleptic cages into two related heteroleptic polyhedra.[44] Further studies

demonstrated that homoleptic $Pt^{II}_4L_6$ species could be converted into a series of heteroleptic cages that have both different structures and incorporate new chemical functionality.[175]

Mirkin *et al.* have applied the "weak-link" approach, discussed above, to the formation of a calix[4]arene based cage which exhibits host guest chemistry that could be reversibly modulated either through the addition or removal of chloride, or through the irreversible coordination of cyanide to the Pd^{II}- based effector (Figure 88).[176]

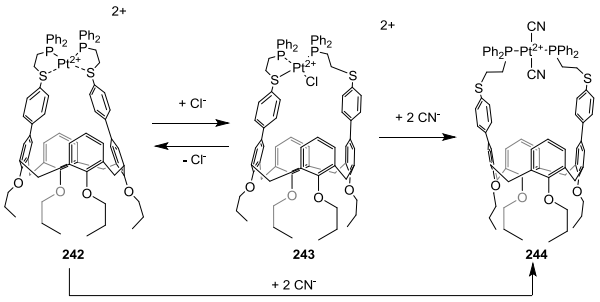

Figure 88. The weak link approach to modulation of host guest chemistry of a calix[4]arene.[176]

The above examples highlight how the incorporation of different ligands can bring about significant structural changes to cages. However, it is not necessary for a new ligand to be incorporated for a significant response to be generated. Even alteration of the ratio of metals to ligands in solution can cause large structural transformations in dynamic systems. In addition to the example in Section 7.3.2 where cage formation can be both templated by anions or induced with increased metal ion concentration, Shionoya *et al.* have observed this effect in two other systems based on similar pyridine-containing C_3 symmetric ligands. Altering the ratio of ligand to metal can bring about the transformation between fluorescent Hg_6L_8 capsule **246** and non-fluorescent Hg_6L_4 cage **248** (Figure 89),[177] or transformations between two similar Ag^+ based architectures, one of which binds an adamantane guest which can be released on transformation to the other.[178]

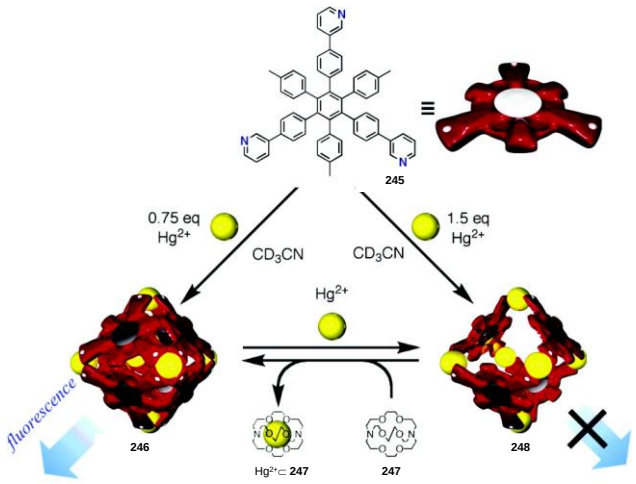

Figure 89. Transformation between a fluorescent Hg_6L_8 capsule and non-fluorescent Hg_6L_4 cage through changes in metal to ligand ratio. Reprinted with permission from ref [177]. Copyright 2007 American Chemical Society

Similarly, Yoshizawa *et al.* reported a transformable porphyrin based capsule/cube assembly where the binding and release of fullerenes was effected by a stoichiometry dependent structural transformation.[179]

Fujita *et al.* have also achieved structural modification of an assembly by reversibly stellating a preassembled $Pd_{12}L_{24}$ cuboctahedron through the addition of Pd^{II} ions to vacant sites in the faces of the structure.[180] Chand *et al.* have also used this strategy to create a system capable of interconverting between a Pd_2L_4 and "double decker" Pd_3L_4 cages.[181]

Dynamic bond-forming reactions have also been used to induce structural transformations by modifying the ligands within complexes. Subcomponent substitution in the form of dynamic imine exchange allows for the modification of helicates in complex ways within networks.[57] Further research in our group extended this strategy to the formation of stimuli-responsive cage assemblies. A recent example uses subcomponent substitution to cause the reconfiguration of a Zn_3L_3 triple helicate structure into a Zn_3L_2 cage capable of binding planar aromatic guests (Figure 90).[182]

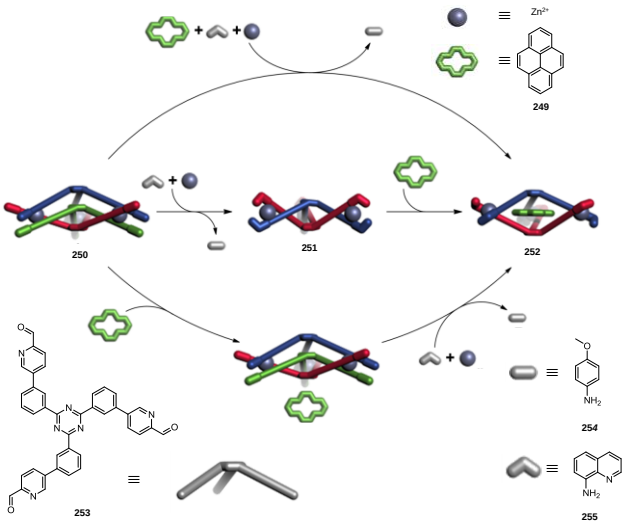

Figure 90. The transformation of a Zn_3L_3 triple helicate into a pyrene-binding Zn_3L_2 double helicate through subcomponent substitution. Reprinted with permission from ref [182]. Copyright 2013 Wiley-VCH

The substitution is driven by the greater metal affinity of an imine ligand derived from a more electron rich amine.[183] By choosing the correct sequence of amines, networks of interconverting architectures can be obtained,[169] the stereochemistry of cages can be manipulated,[184] and mixtures of cages with different guests bound inside can be selectively disassembled, allowing for the release of specific guests in sequence.[185]

Li *et al.* have also used subcomponent substitution in the structural transformation of a neutral cubic nickel(II)-imidazolate cages ($Ni_8L_{12}X_4$) into a rhombic dodecahedral cage $(Ni_{14}L_{24})^{4+}$ through the exchange of methylamine for 4-methoxy-benzylamine.[186]

Schmittel *et al.* exploited the formation of pyridylimines from pre-organized 2-formyl-pyridine based Cu^I precursors and *p*-phenylenediamine to form extended polymers consisting of stacked cages.[187] These could be capped, demetalated, and the imines reduced to secondary amines to form C_3 symmetric star-shaped polyamines.

7.3.4 Solvent Responsive Cage Assemblies

The finely-tuned energetic balance between different assemblies can be affected by the nature of the solvent. Some responses can be predicted e.g. the effects of coordinating solvents[188] while others are harder to predict but can lead to significant structural change.[189]

Fujita *et al.* observed a solvent-dependent structural transformation between a Pd_4L_8 cage generated in DMSO and a smaller Pd_3L_6 cage assembled from the same building blocks in MeCN.[190] They report that the addition of MeCN to the larger Pd_4L_8 structure followed by heating to 60 °C for 3 h brought about a conversion to the Pd_3L_6 structure, whereas evaporation of the MeCN reverses the process.

Severin *et al.* have reported a system where even slight differences in solvent properties, in this case the difference between DCM and chloroform, cause the interconversion between a ruthenium(II)-based octanuclear cage and a tetranuclear complex.[191] From studying the crystal structure they infer that strong hydrogen bonding between the CH's of DCM and the O atoms bound to Ru^{II} stabilize the tetranuclear complex with respect to the octanuclear cage, providing the driving force for the transformation.

Solvent dependent structural reconfiguration can also cause a second order response, as observed in the solvatochromic cage reported by Aida *et al*. The box-shaped tetrameric zinc bisporphyrin complex **257** exists in two isomeric forms (Figure 91), each of which has a different absorption spectrum. The ratio of isomers was found to be dependent on the solvent. This observation led to the solvatochromic response of the assembly. It was demonstrated that the response was sensitive enough to discriminate between the regioisomers of xylene even though they have very similar dielectric constants.[192]

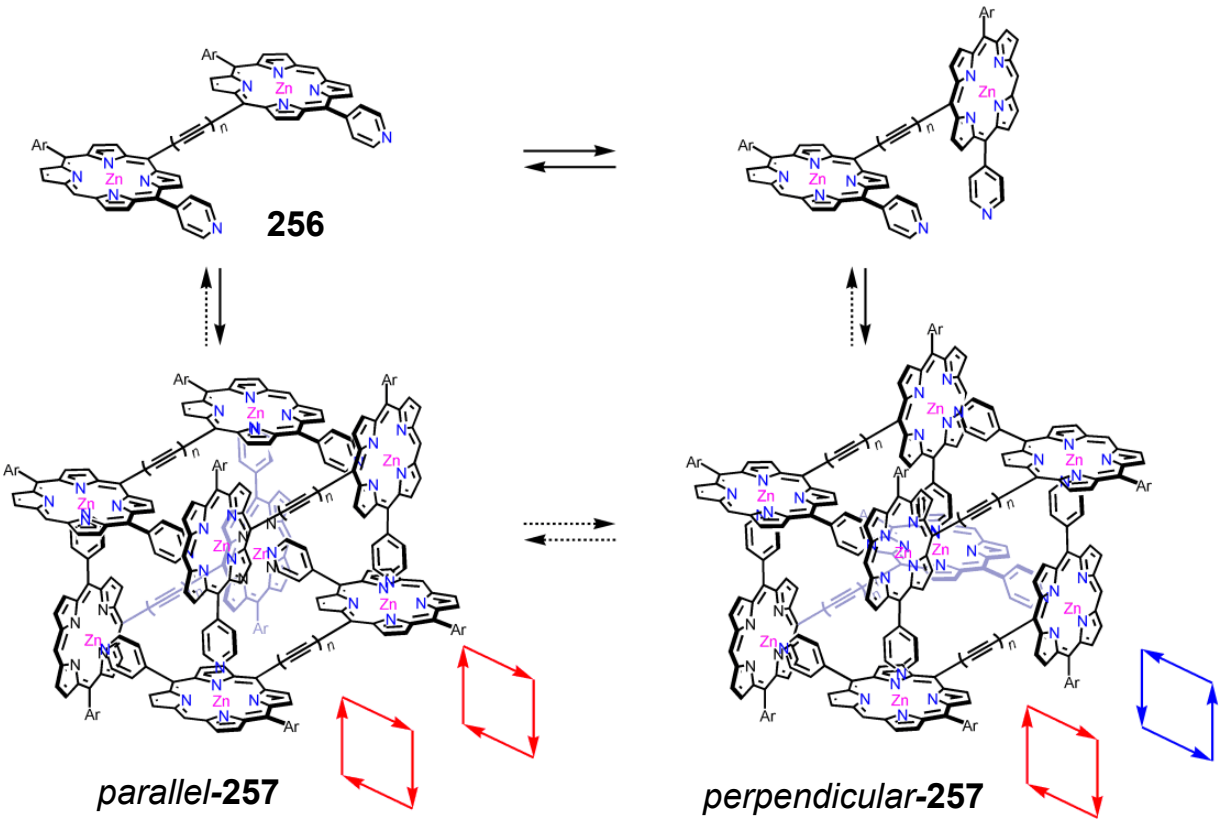

Figure 91. Potential isomers of zinc porphyrin containing cage **257**. Reprinted with permission from ref [192]. Copyright 2008 Wiley-VCH

Recently, we too have observed solvent-dependent structural transformation in a water-soluble $Fe^{II}_{10}L_{15}$ pentagonal prism.[193] A lower nuclearity $Fe^{II}_{4}L_{6}$ tetrahedral cage is observed to transform, following the addition of methanol, into a higher nuclearity $Fe^{II}_{10}L_{15}$ pentagonal prism, which appeared to be stabilized by the presence of methanol. This pentagonal prism could also be generated from the tetrahedron during crystallization from water at 20 °C for one month, and it was found to convert back into the tetrahedron after heating to 50 °C in water for one week.

Ward *et al.* have also observed that crystallization can cause structural reconfiguration.[189] A trigonal prismatic M_6L_9 assembly formed from a bis-bidentate pyrazolyl-pyridine containing ligand and either Zn^{II} and Cd^{II} was found to crystallize preferentially as a $M_{16}L_{24}$ tetracapped truncated tetrahedron. Redissolved crystals left for a period of one week were found to re-equilibrate to the solution-stable M_6L_9 product.

Similarly, Hong *et al.* reported the crystallization-driven formation of an infinite chain of polycatenated cages from an Ag_6L_4 monomer present in a supersaturated solution.[194] Interestingly, the polycatenated chain of cages was found to be a kinetic product. A non-interpenetrated cage polymer, where cages are linked by Ag-Ag contacts, crystallizes from a non-supersaturated solution.

Shionoya, Clever *et al.* reported the structural transformation of a Pd_2L_4 cage upon crystallization from a solution containing two equivalents of a hexamolybdate guest.[195] X-ray analysis found that that the product of crystallization was an L_3 triangle wrapped around one hexamolybdate anion, with the loss of the Pd^{II} ions. Two protons were found to have been scavenged from solution and coordinated to the pyridines of the ligands to cause the L_3 triangles to form hydrogen bonded dimers in the solid state.

Zhou *et al.* have observed the solvent-dependent aggregation of a 5-((triisopropylsilyl)ethynyl)isophthalate-Cu^{II}-based cuboctahedral cage.[196] On formation in a hydrophilic solvent mix of DMF and water, the hydrophilic triisopropylsilyl groups cause cages to aggregate in a linear fashion, creating a chain of cages where the bulky ligands are interdigitated and two of the metal vertices are further linked by two oxygen atoms from neighboring cages. This chain can be broken up on addition of a hydrophobic solvent, such as chloroform, and the process is reversible on addition of DMF:water and heating at 85 °C for three days.

8 Polymers and Gels

Over the last few decades metallo-supramolecular polymer (MSP) chemistry has grown steadily.[197] The presence of reversible metal-ligand interactions in MSPs enables the systematic tuning of their properties and endows them with unusual features. Because of their unique properties, MSPs and metallo-supramolecular gels (MSGs) have attracted considerable attention. Manipulation of their metal-ligand interactions has enabled stimuli-responsive MSPs

and MSGs to be utilized for different applications.[198] In many MSPs and MSGs, metal ions function as bridges to connect the organic ligands, thereby forming a polymer chain.

This section is divided into two parts: the first reviews systems comprised of discrete metallo-supramolecular assemblies that undergo further association, resulting in higher-order structures with useful properties. The second section treats those systems wherein metal ions bridge between organic ligands, leading to supramolecular polymers and gels.

8.1 Hierarchical Assembly of Discrete Structures

8.1.1 Chemically Responsive Systems

Yang and co-workers have synthesized an extensive series of building blocks for metallacycles. The self-assembly of 120° dendritic building blocks **258**-**260** (Figure 92) with 60° diplatinum(II) acceptor **266** yielded metallodendritic rhomboids **276**-**278** (Figure 93).[199] Second-generation metallodendrimers were observed to self-assemble hierarchically in pure and mixed organic solvents into stable supramolecular organometallic gels having discrete metallacycles as their backbones (Figure 93a). Reversible gel to sol transition could be achieved upon the addition and removal of bromide ions. Similarly, by employing the structurally similar 120° building block **261** in combination with a 120° diplatinum(II) acceptor **270**, the authors synthesized hexagonal metallacycle **279** (Figure 93b).[200] In mixed solvent systems, the metallacycle self-assembled into nanofibers and supramolecular organometallic gels, and exhibited bromide-induced reversible gel-sol phase transition *via* the disassembly and reassembly of discrete hexagonal metallocycles.

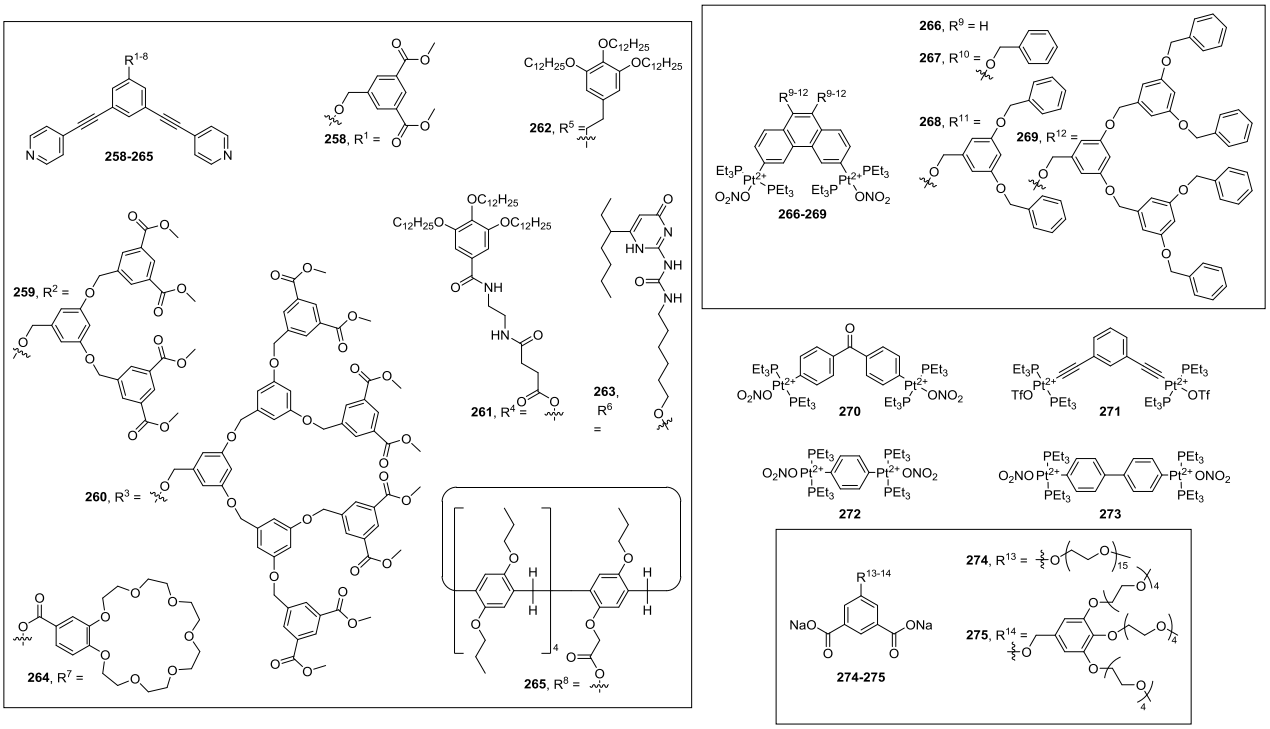

Figure 92. Building blocks synthesized by Yang, Stang and Huang for preparing metallacycles.

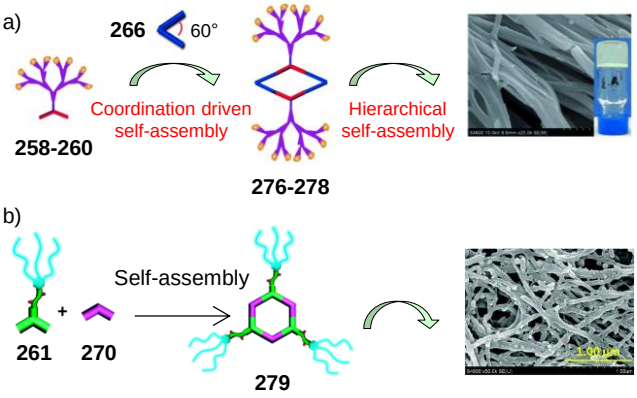

Figure 93. Self-assembly of dendritic donor ligands (**258-261**) in the presence of 60° and 120° diplatinum(II) acceptors **266** and **270** into a) rhomboid (**276-278**) and b) hexagonal metallacycles (**279**), and their subsequent self-assembly into supramolecular gels. a) Adapted with permission from ref [199b]. Copyright 2013 WILEY-VCH. b) Adapted from ref [200] with permission of The Royal Society of Chemistry.

Subsequently, using the metallo-dendritic ligands **258-260** and diplatinum(II) acceptor **270**, well-defined hexagonal metallodendrimers **280-282** were synthesized which underwent further hierarchical self-assembly into monodisperse vesicle-like structures (Figure 94).[201] The hexagonal metallodendrimers were shown to disassemble and reassemble controllably following the addition and removal of bromide ions, resulting in transitions between vesicles and micelles. This stimuli-responsive behavior was utilized for encapsulation and controlled release of fluorescence dyes.

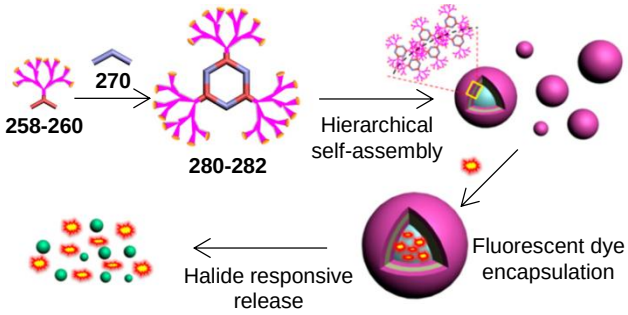

Figure 94. Synthesis of hexagonal metallodendrimers (**280-282**) from **258-260** and **270**, and their hierarchical self-assembly into vesicles and micelles and the subsequent halide-induced controlled release of guests. Adapted with permission from ref [201]. Copyright 2014 American Chemical Society.

Bonifazi, Yang and co-workers recently described the preparation of rhomboidal (**283**) and hexagonal metallacycles (**284** and **285**) and their hierarchical self-assembly to yield fibrillar and spherical aggregates (Figure 95).[202] The reaction of **262** and **266** (Figure 92) yielded a rhomboidal metallacycle (**283**) which aggregated into nanosized fibers. Hexagonal metallacycles **284** and **285**, synthesized by reaction of **262** with **270** and **272**, respectively, formed nanoparticles under the same conditions. All nanostructures displayed distinct morphologies from the one exhibited by ligand **262**, which formed an infinite entangled mesh. The differences in self-assembly behavior were attributed to the differences in the hydrophilic/lipophilic character of individual metallacycles, which in turn depended on the number and orientation of the alkyl chains.

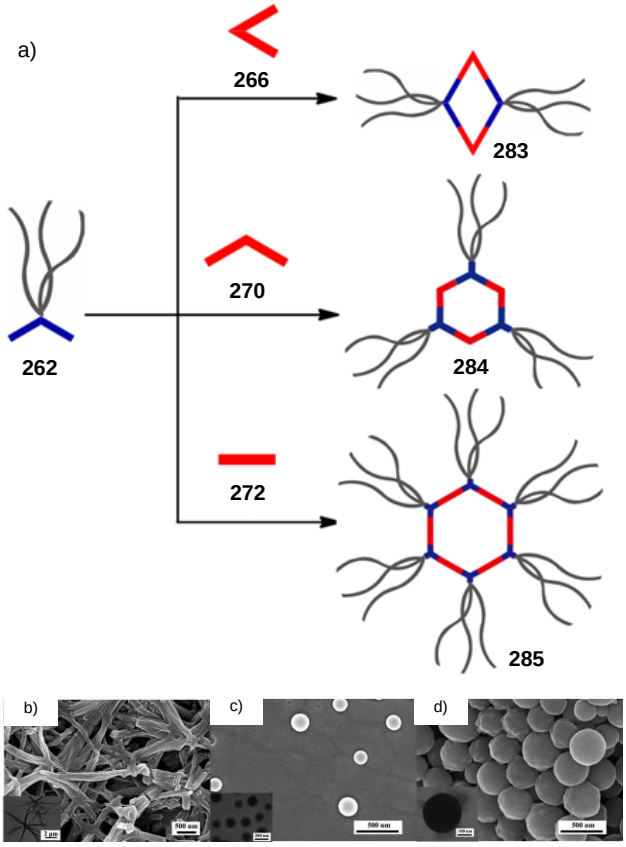

Figure 95. a) Schematic representation of the rhomboidal and hexagonal metallacycles (**283-285**). b-d) SEM and (inset) TEM images of **283-285** obtained by drop-casting a solution of the appropriate metallacycle onto Si (111) surfaces (SEM) and Cu grids (TEM). Adapted with permission from ref [202]. Copyright 2014 WILEY-VCH.

Similarly, Yang and co-workers synthesized platinum-acetylide metallacycles (**286** and **287**, Figure 96) functionalized with hydrophobic alkyl chains.[203] At low concentrations, discrete metallacycles were observed in solution, whereas ordered aggregates formed through hydrophobic interactions between alkyl chains and hydrogen bonding between amide groups was observed at higher concentrations.

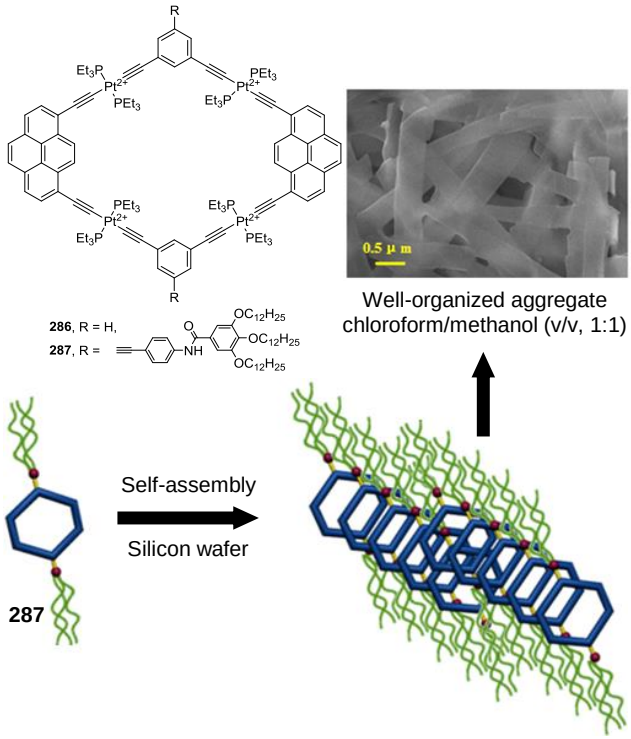

Figure 96. Chemical structure of metallacycles **286** and **287** and a schematic representation of the self-assembly of **287**, together with an SEM image of this assembly. Adapted from ref [203] with permission of The Royal Society of Chemistry.

Huang and Stang have reported the synthesis of supramolecular polymers consisting of discrete metallacycles.[204] The authors synthesized **263** (Figure 92) by functionalizing the dipyridyl ligand with 2-ureido-4-pyrimidinone (UPy) moieties, which enable self-complementary hydrogen bonding. Coordination-driven self-assembly of the UPy-functionalized dipyridyl ligand with metal acceptors (**266, 270, 271**) resulted in the formation of both rhomboids (**288**) and hexagons (**289**, **290**) decorated with UPy groups (Figure 97a). Hydrogen bonding between the UPy groups linked the metallacycles into either linear chains (rhomboids, Figure 97b) or cross-linked networks (hexagons, Figure 97c). Additionally, trapping of the solvent within the supramolecular polymer consisting of hexagons resulted in the formation of gels capable of forming long, macroscopic fibers (Figure 97d) that possessed enough strength and flexibility to permit the construction of stable knots (Figure 97e).

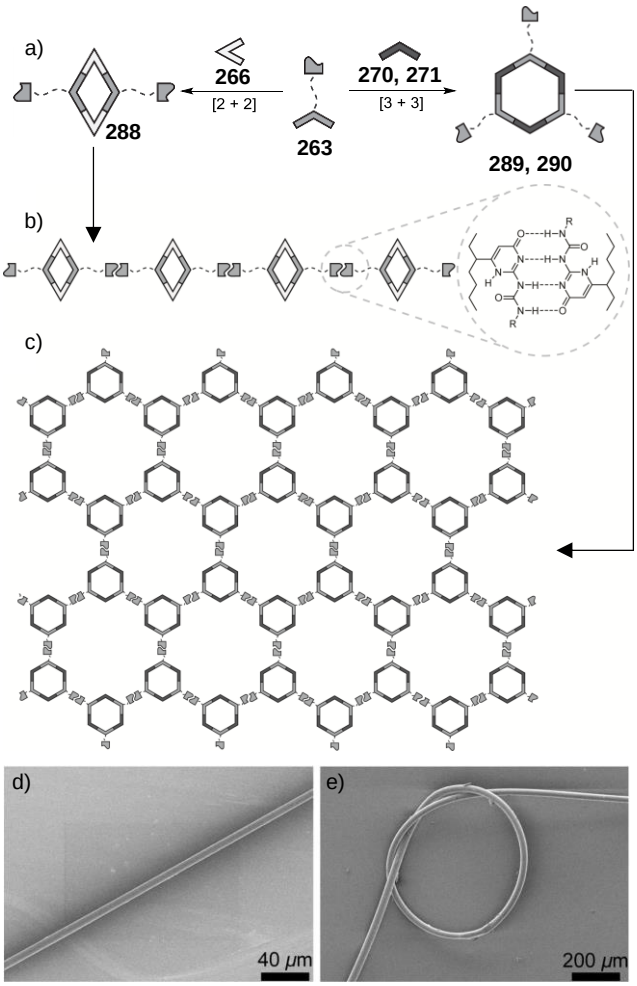

Figure 97. Schematic representations of the formation of a) UPy-functionalized rhomboids (**288**) and hexagons (**289** or **290**), b) a linear supramolecular polyrhomboid, and c) cross-linked three-dimensional supramolecular polymeric networks containing hexagons. SEM images of d) a thin-long fiber drawn from **289** and e) a knotted fiber made from **290**. Adapted from ref [204].

The UPy-functionalized 120° dipyridyl ligand **263** (Figure 92) was also employed by Huang, Yang, Stang and co-workers to prepare rhomboidal metallodendrimers **291**-**293** (Figure 98) by self-assembly with the 60° organo-Pt^{II} acceptors decorated with dendrons **267**-**269**.[205] These rhomboids featured pendant UPy functionalities at their obtuse vertices. Addition of a non-hydrogen-bonding solvent that facilitated intermolecular UPy dimerization resulted in supramolecular polymerization of the rhomboidal metallodendrimers into dendronized organo-Pt^{II} metallacyclic polymers (DOMPs). The presence of the dendrons

along the polymer backbone introduced steric hindrance, which improved the efficiency of long-chain polymerization. The sizes of the DOMPs were found to be dependent on the degree of branching of the attached dendrons. Due to the dynamic nature of these supramolecular polymers, titration of the free ligand to a solution of [G3]-DOMPs resulted in the disruption of the long polymeric chains into shorter aggregates. Similarly, the polymerization was found to be reversible with the addition of DMSO due to the disruption of intermolecular H-bonding by the solvent.

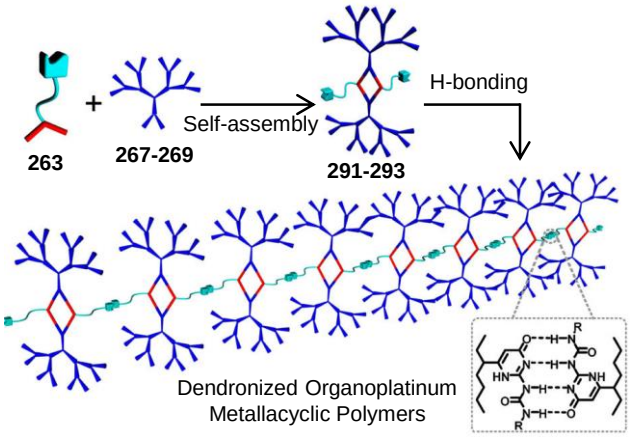

Figure 98. Formation of [G3]-DOMPs (**291-293**) by hierarchical self-assembly of dendronized organo-Pt^{II} acceptors **267-269** and UPy-functionalized dipyridyl ligand **263**. Adapted with permission from ref [205]. Copyright 2013 American Chemical Society.

Subsequently, 120° donor ligands **274** and **275** (Figure 92) containing linear and branched poly(ethyleneglycol) side chains were synthesized and allowed to react with organoplatinum(II) acceptor **266** to furnish two amphiphilic metallacycles **294** and **295** (Figure 99).[206] Depending on the concentration, the metallacycles formed different aggregates in solution: spherical micellar structures were observed at a concentration of 5.00×10^{-6} M, whereas 1-D nanofibers or 2-D nanoribbons were observed at the higher concentration of 5.00×10^{-5} M. These 1D and 2D materials underwent further self-assembly yielding metallohydrogels.

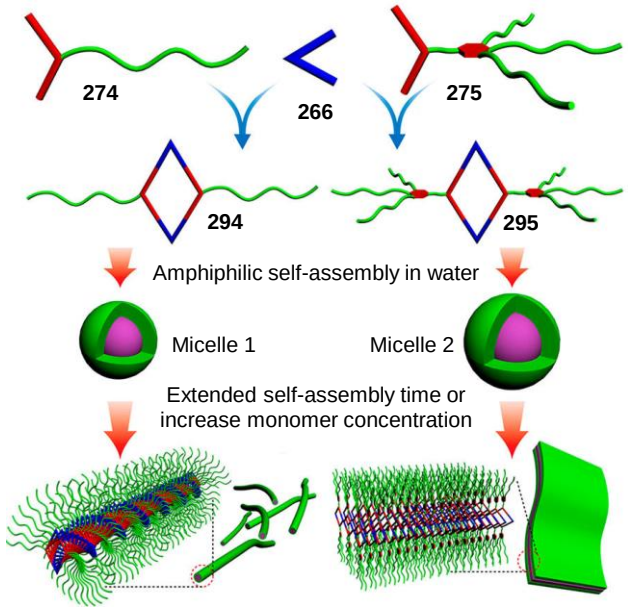

Figure 99. Hierarchical self-assembly of **274** and **275** with **266** to give rhomboids, micelles, nanofibers, and nanoribbons. Adapted with permission from ref [206]. Copyright 2013 American Chemical Society.

Huang, Stang and co-workers synthesized 120° dipyridyl ligand **264** (Figure 92) functionalized the with benzo-21-crown-7 (B21C7), which self-assembled into hexagonal metallacycle **296** (Figure 100) when mixed with 120° acceptor **271**.[207] The addition of the bisammonium salt **297** into a solution of the hexagon **296** resulted in complexation between the two, thereby leading to a cross-linked supramolecular polymer network. This network exhibited gelation properties at high concentrations; the gelation was found to be reversible upon heating or upon the addition of a competitive guest such as K^+, which displaced the ammonium salt from the crown ether. Addition of sufficient B21C7 to trap all of the K^+ resulted in the reformation of the B21C7/ammonium complex, whereupon the gel reformed.

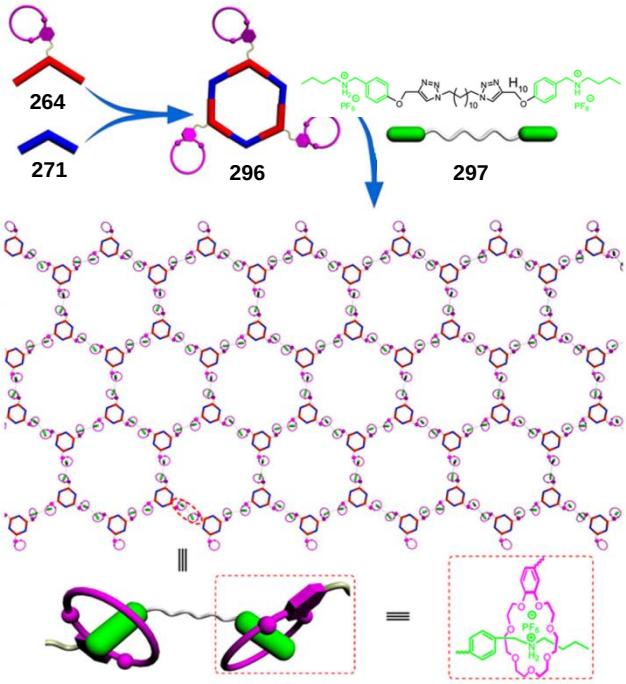

Figure 100. Cartoon representation of the formation of B21C7-functionalized metallacyclic hexagon **264** and the cross-linked 3D supramolecular polymeric network from self-assembly of hexagon **296** and bisammonium salt **297**. Adapted with permission from ref [207]. Copyright 2014 American Chemical Society.

Lu and Che have shown that the cationic organoplatinum(II) complexes **298** and **299** (Figure 101) formed higher-order assemblies with useful properties in aqueous media.[208] The authors later synthesized cross-linkers based on two planar cyclometalated platinum(II) motifs covalently connected by a flexible oligo(oxyethylene) chain of variable length (**300**-**303**, Figure 101).[209] The addition of a small amount of **307**·Cl or its precursor **303** induced spontaneous anisotropic gelation of the mononuclear Pt^{II} complexes **298**·Cl and **299**·Cl in aqueous solution. Moreover, the sol-gel transition was demonstrated to be reversible upon varying the ratio of **303** or **307**·Cl to **298**·Cl or **299**·Cl. The proposed mechanism of gel formation is shown schematically in Figure 101b. Spectroscopic measurements indicated that the hydrogels inherited the optical and nematic alignment properties of the mononuclear complexes **298**·Cl or **299**·Cl in water.

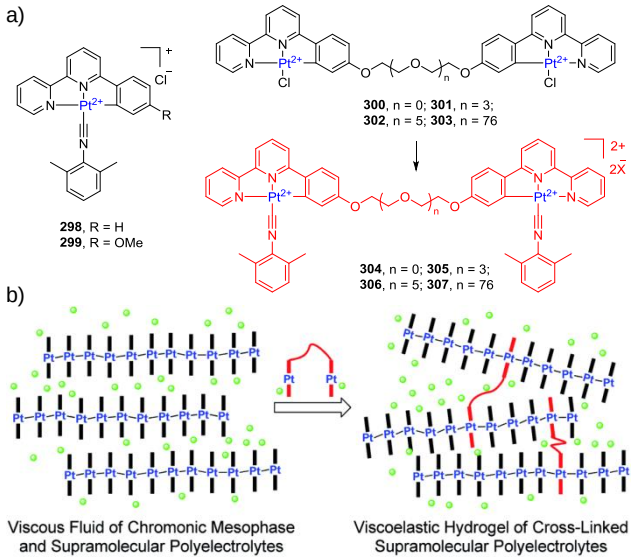

Figure 101. a) Structures of organoplatinum(II) complexes and b) schematic presentation of the formation of hydrogels through supramolecular cross-linking. Adapted from ref [209] with permission of The Royal Society of Chemistry.

8.1.2 Light Responsive Systems

Huang, Yang, Stang and co-workers synthesized bidentate donor ligand **308** based on the stiff-stilbene moiety. This ligand is capable of undergoing *cis-trans* photoisomerization (Figure 102a). The *cis*-isomer of **308** reacted with di-Pt^{II} acceptor units **272** or **273** (Figure 92) to yield self-assembled discrete metallacycles **309** and **310**.[210] UV irradiation at 387 nm triggered a *cis*- to *trans*-isomerization process, generating a 180° angle between the pyridyl groups and favoring the formation of MSPs. Irradiation at 360 nm induced the reverse isomerization process; however, the *cis*-isomer was produced in only 53%. Because of this partial conversion, instead of a quantitative conversion into discrete [2+2] metallacycles, larger cyclic oligomers were obtained. The reversible transformation of the metallacycles into supramolecular polymers was accompanied by changes in their spectral properties and morphologies as evidenced through optical spectroscopy measurements and imaging techniques.

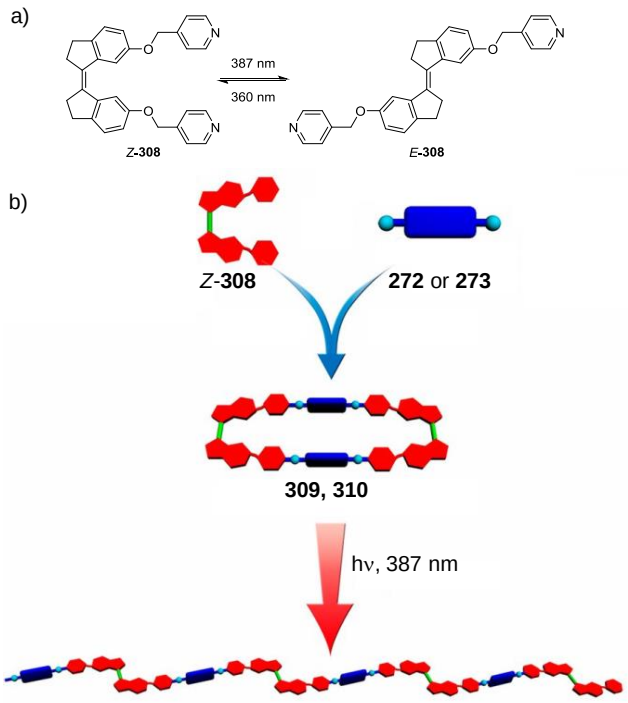

Figure 102. a) Reversible photoisomerization of the pyridine-linked stiff-stilbene derivative **308**. b) Cartoon representations of the formation of discrete organoplatinum(II) metallacycles **309** and **310** and infinite metallosupramolecular polymers (MSPs). Adapted from ref [210].

8.1.3 Multi-stimuli Responsive Systems

Yang and co-workers synthesized a pillar[5]arene containing 120° dipyridyl donor **265** (Figure 92) which when combined with the corresponding complementary 180° di-Pt^{II} acceptors **272** and **273** yielded two different sized hexakis-pillar[5]arene metallacycles **311** and **312** (Figure 103).[211] Taking advantage of the host-guest properties of the pillar[5]arene moiety, supramolecular polymers were synthesized from the metallacycles by using ditopic guests as cross-linking agents. The polymerization could be reversed by the addition of competitive guests and these polymers formed gels at high concentrations. Because of the dynamic nature of the different self-assembly processes, the sol-gel transitions were found to be reversible through the disassembly and reassembly of the cross-linked supramolecular polymers stimulated by various external stimuli including temperature changes and the addition of halide ions or competitive guests.

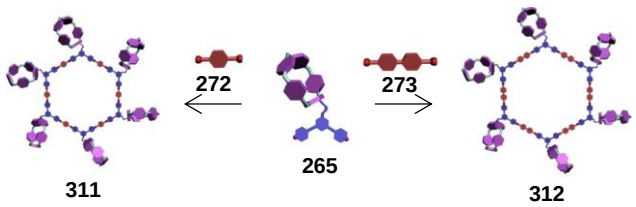

Figure 103. Cartoon representation of self-assembled hexakis-pillar[5]arene metallacycles **311** and **312**. Adapted with permission from ref [211]. Copyright 2014 American Chemical Society.

8.2 Metal Ions as Bridges

Supramolecular polymers synthesized through metal ion coordination have allowed the creation of materials with novel and useful properties. Metal ions have been used to bridge organic ligands, leading to the formation of linear polymers that contain metal ions in the main chain. Metal-binding sites have also been incorporated into polymer side-chains, enabling coordinating metal ions to form reversible cross-links. By the appropriate choice of the metal ions and ligands, the structure and properties of MSPs have been tuned and have found numerous applications. Several recent reviews collate different aspects of MSPs and gels.[198,212]

8.2.1 Light Responsive Systems

Rowan, Weder and co-workers have developed optically-healable supramolecular polymers that consist of a bitopic 2,6-bis(1'-methylbenzimidazolyl)pyridine (Mebip) moiety and a poly(ethylene-co-butylene) motif as a linker to bridge the metal-binding sites (**313**, Figure 104 and Figure 105).[213] Low molecular-mass complexes of **313** with Zn^{II} were found to be only weakly fluorescent, suggesting that the majority of the excitation energy dissipated as heat. This heat energy sufficed to dissociate the coordinative links between monomer units, leading to a decrease in its molecular mass and liquefaction of the material. Removal of the light source resulted in the re-formation of the supramolecular polymer, leading to the healing of the material (Figure 105b). This self-healing property was demonstrated by making cuts in 350-400 μm films of polymers. These samples upon subsequent exposure to 320-390 nm UV light exhibited healing within 30s (Figure 105c). This self-healing property was also visualized

by using atomic force microscopy (AFM), which showed that upon irradiation with light, the cuts were filled and subsequently disappeared.

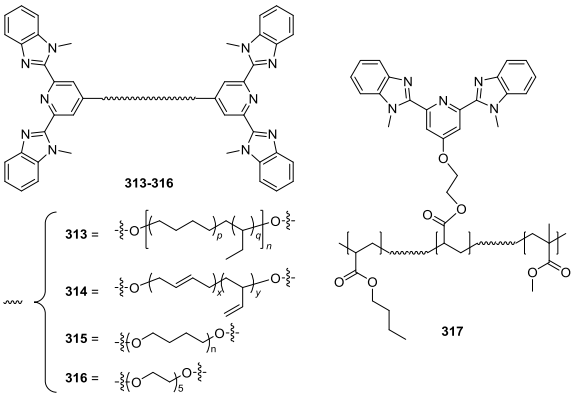

Figure 104. Monomers and polymers containing the 2,6-bis(1'-methylbenzimidazolyl) pyridine (Mebip) moiety.

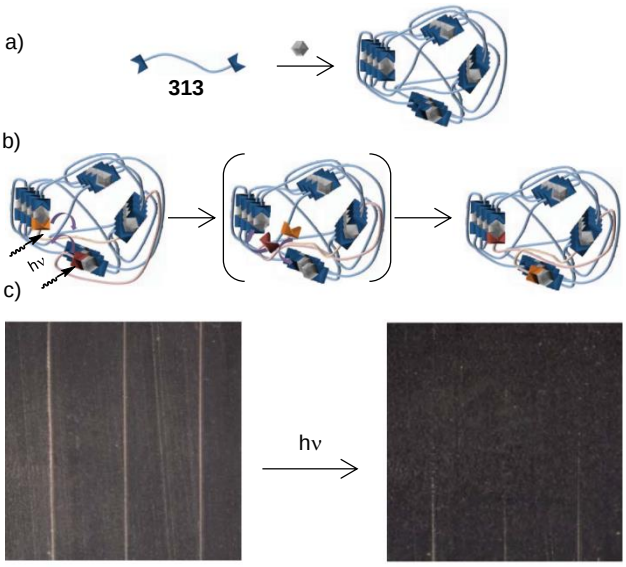

Figure 105. Schematic representation of a) polymerization of **313** by addition of $Zn(NTf_2)_2$ and b) proposed optical healing of the MSP. c) Image showing the healing of the MSP upon exposure to light. Adapted with permission from Macmillan Publishers Ltd: Nature [213a], copyright (2011).

Subsequently, Rowan and co-workers utilized this strategy to demonstrate shape-memory properties in MSPs.[214] The authors used a low molecular weight cross-linkable (poly(butadiene)) polymer **314** (Figure 104) containing terminal metal-biding sites, bridged by

Eu^{III} and Zn^{II}. In the MSP, the metal-ligand termini were found to phase-separate from the polymer core in the solid state. The addition of a tetra-functional thiol resulted in cross-linking of the MSP through a photo-induced thiol-ene reaction. The metal-ligand chromophores absorb UV light, leading to localized heating, which in turn results in the softening of the metal-ligand hard phase and decomplexation of the metal-ligand complexes. Upon removal of the light source, the polymer cools and the metal-ligand interactions re-form. This process results in phase separation and the polymer is frozen in the deformed state. Additional exposure to and subsequent removal of UV light brings about a return to the permanent shape.

Xia and co-workers extended Rowan's work by using MSP **317** (Figure 104) consisting of poly(butyl acrylate-co-methyl methacrylate) (poly(BA-MMA)) functionalized with Mebip side chains.[215] This MSP exhibited triple shape memory, whereby it could be reversibly shaped into a “V”, an “S” or the original rectangular sheet by heating and cooling.

The terpyridine moiety (terpy) has attracted attention as a metal coordination unit in MSPs.[216] It forms stable complexes with many metal ions and can be readily functionalized. Figure 106 shows examples where the terpy unit was attached to different cores, leading to the formation of stimuli-responsive materials. Giuseppone and co-workers synthesized ligand **318** by grafting a triarylamine onto the terpy moiety.[217] Upon Zn^{II} coordination, **318** yielded discrete dimeric complexes, which self-assembled into monodisperse spheres when irradiated with visible light, as characterized by DLS and TEM measurements. Bis-columnar stacks of hydrophobic triarylamines were proposed to aggregate, leading to a micro-phase separation in chloroform and thereby producing vesicles. Light-induced radical delocalization along the anisotropic stacks of the triarylamines was found to be the stabilizing force behind the formation of the nanospheres.

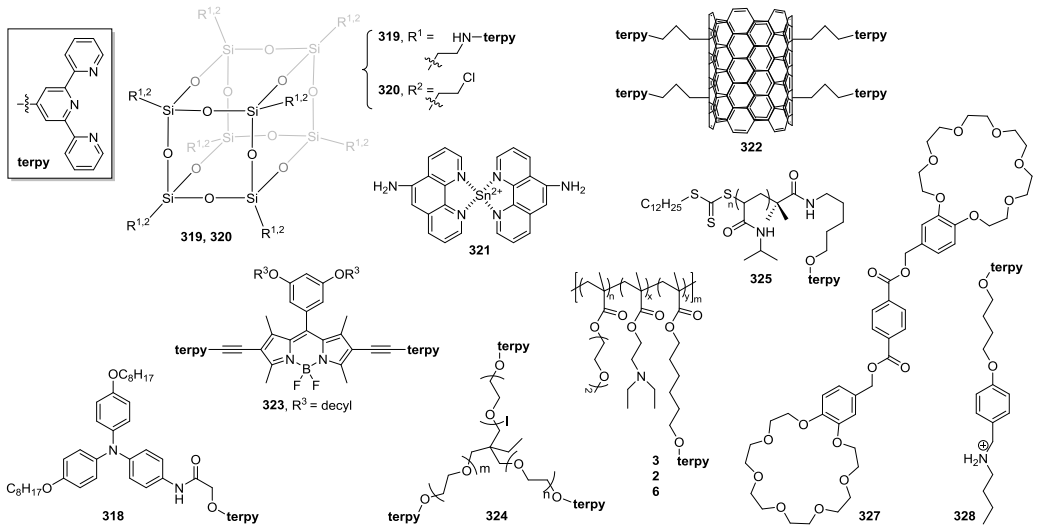

Figure 106. Chemical structures of various polymer-forming monomers functionalized with the terpyridine (terpy) moiety.

8.2.2 Chemically Responsive Systems

Köytepe and co-workers have reported the synthesis of polyhedral silsesquioxanes (**319**, Figure 106) functionalized with terpy. In the presence of Co^{II} or Cu^{II} ions, the polyhedral silsesquioxane underwent coordination polycondensation resulting in the formation of MSPs.[218] Similarly, the octakis(3-chloropropyl) octasilsesquioxane **320** yielded MSPs in the presence of the pre-formed aminophenanthroline Sn^{II} complex **321**.[219] These polymers exhibited gelation properties at higher metal ion concentrations. Gel formation was found to be reversible upon the addition of a competitive metal chelating agent such as EDTA. Similarly, Seçkin and co-workers functionalized multiwalled carbon nanotubes with terpy (**322**) which formed MSPs in the presence of Co^{II} or Ni^{II} ions.[220] Similar to the previous examples, these MSPs could be decomplexed by the addition of EDTA, and could be followed by color changes. Akkaya and co-workers synthesized the BODIPY derivative **323** functionalized with terpy.[221] In the presence of metal ions such as Zn^{II} and Fe^{II}, MSPs were obtained and, depending on the metal-to-ligand stoichiometry, structural switching could be achieved between the polymeric and corresponding monomeric metal complexes.

Royal and co-workers demonstrated a pH-induced transformation between mononuclear neutral complexes and metallopolymers in a system consisting of cyclam and bisterpy **329** (Figure 107).[222] This ligand, upon reacting with Cu^{II} in a 1:1 molar ratio, yielded a green solution which was characterized as MSP **331** through viscometry and NMR measurements. However, when the reaction was carried out in the presence of a base, a pink-red solution was obtained. This corresponded to the square-planar Cu^{II} complex **332**. Interestingly, these two species were found to be interconvertible by the addition of base and acid. Subsequently, it was demonstrated that the addition of a second equivalent of a transition metal ion such as Fe^{II}, Ni^{II}, Co^{II}, or Cu^{II} to the square-planar Cu^{II} complex **332** resulted in the formation of MSP **333** consisting of homo- or hetero-metallic complexes.[223] Moreover, addition of acid to the homo-metallic Cu^{II} polymer resulted in the dissociation of the polymer leading to the formation of dinuclear complexes in which the copper ions are coordinated to the terpy moieties.

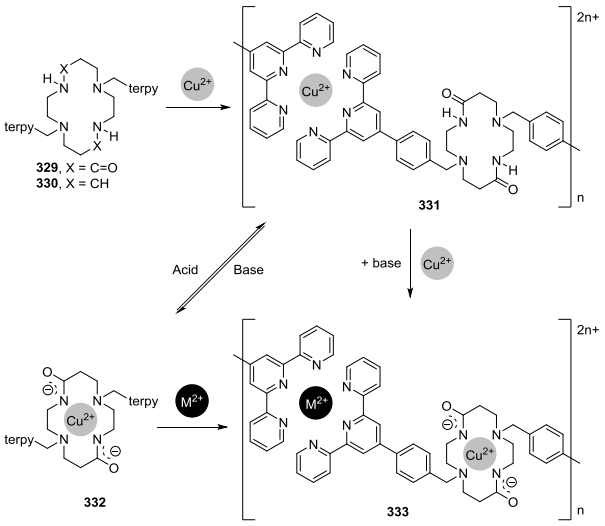

Figure 107. Complexation routes of Cu^{II} by ligand **329** in the absence and presence of a base, the subsequent acid-base driven interconversion and formation of homo- or hetero-MSPs.[222-224]

8.2.3 Redox Responsive Systems

Kikuchi and co-workers have reported a MSP containing the terpy-terminated three-armed poly(ethylene glycol) **324** (Figure 106) that exhibited a sol-gel transition upon aerobic oxidation.[225] The aerobic oxidation of Co^{II} to Co^{III} resulted in a sol-gel transition and the material could be molded into hydrogels of different shapes. The addition of a reducing agent led to the reverse gel-to-sol transformation, and on exposure to air the solution then re-gelled due to aerobic oxidation of the reducing agent. Similarly, an aqueous solution of ligand **324** in the presence of both Co^{II} and Ni^{II} showed a sol-gel transition and the resultant hydrogels exhibited self-healing properties.

It was previously reported that the stoichiometry of the complex formed between a MeBip ligand and copper depends on the oxidation state of copper: Cu^{I} yields 2:2 complexes whereas 2:1 complexes are obtained with Cu^{II}. Jamieson, Rowan and co-workers showed that redox-responsive MSPs can be synthesized by taking advantage of this property.[226] These authors employed ditopic ligand **315** (Figure 104) containing the MeBip moiety and studied its complexation with copper ions, finding that the binding ratios observed in the case of monotopic MeBips were also present in the case of the ditopic ligand. As shown in Figure 108, a 1:1 ratio of ligand:copper yielded an MSP with Cu^{II} but oligomers with Cu^{I}, while the opposite was observed at a ratio of 1:2; the system formed polymeric aggregates with Cu^{I} and oligomers with Cu^{II}. Furthermore, switching between the two oxidation states at a given ratio results in polymerization/depolymerization of the system, thereby leading to significant changes in the viscosity.

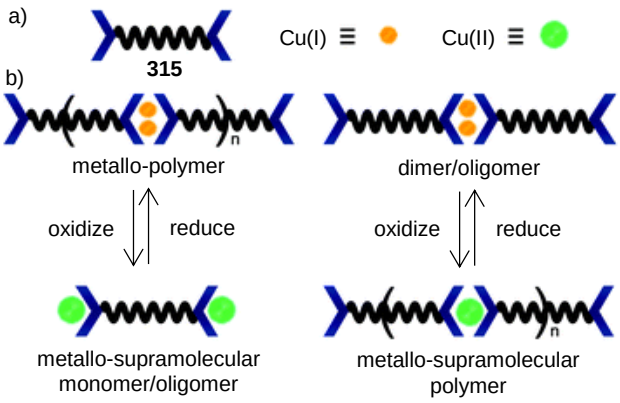

Figure 108. Cartoon representations of a) ligand **315** and b) redox manipulation of the degree of polymerization of **315** with copper:ligand ratios of 1:2 (left) and 1:1 (right). Adapted from ref [226] with permission of The Royal Society of Chemistry.

Kikuchi, Aoyagi and co-workers synthesized polyethylene glycol ligands functionalized with phosphate groups that formed supramolecular hydrogels on complexation with certain metal ions.[227] Trivalent metal ions such as Fe^{III}, V^{III}, Al^{III}, Ti^{III}, and Ga^{III} were found to be effective in preparing gels *via* dynamic and reversible crosslinking of the ligands. Interestingly, switching between Fe^{II} and Fe^{III} by the addition of oxidizing (H_2O_2) and reducing agents (ascorbate) resulted in reversible gel-sol transitions. Furthermore, these gels also exhibited self-healing properties.

8.2.4 Multi-stimuli Responsive Polymers

Rowan and co-workers have shown that tridentate ligand 2,6-bis(1'-methyl-benzimidazolyl)-4-alkoxypyridine (RO-BIP) can self-assemble into supramolecular polymers in the presence of metal ions. Initial studies showed that addition of lanthanoid metal ions (<5 mol% per ligand) followed by transition metal ions (>95 mol% per ligand) to a solution of the ditopic monomer **316** (Figure 104) resulted in the formation of MSGs (Figure 109).[228] These gels exhibited reversible thermal, chemical and mechano-responsive properties. Additionally, owing to the presence of the lanthanide ions, these materials exhibited photoluminescence. The sequence of addition of metal ions was found to be the critical factor governing the self-

assembly process: if transition metal ions were added first, kinetically inert metallo-macrocycles and linear oligomers were formed. Subsequent addition of a small amount of the weaker-binding lanthanide ions did not displace the strongly bound transition metal ions and thus failed to yield MSGs. Mechanistic studies carried out on these materials suggested that the coordinative interactions between the metal ions and the ligands resulted in globular colloidal particles and flocculation of these colloidal particles yielded the gels.[229] The globular particles were fragile and sensitive to mechanical perturbation, resulting in thixotropic behavior. The gel state was recovered after shearing, but the globular particles were broken down progressively as the amount of mechanical stress was increased, resulting in an increase in the strength of the resulting gel once the stress was removed. By following this strategy, a series of MSPs were synthesized by subtly modifying the ditopic ligand. Also, other functional groups could be grafted onto the monomers, which aided utilization of these gels for applications as optoelectronic materials and sensors.[230]

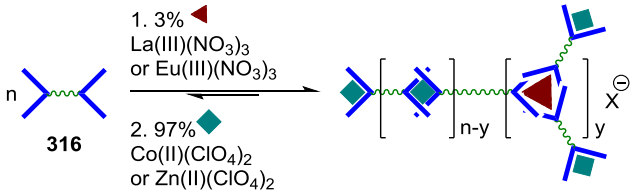

Figure 109. Schematic representation of the formation of MSGs from ditopic ligand **316** using a combination of metal ions.[228a]

Weng and co-workers have synthesized responsive self-healing MSGs based on polymers containing the 2,6-bis(1,2,3-triazol-4-yl)pyridine (BTP) ligand **334** (Figure 110) with Zn^{II} or Eu^{III} in various solvents.[231] Depending on the composition of the gels, they exhibited excellent mechanical properties and thermal stabilities. The photoluminescence properties of the gels could be tuned, depending on the ratio between the Zn^{II} and Eu^{III} ions and the solvent used for gelation. The gels could be transformed into sols through heating, which was also accompanied by quenching of the emission and was found to be reversible upon cooling.

Similarly, these gels exhibited mechano-, photo- and chemo-responsive properties. Moreover, these gels exhibited self-healing properties without requiring an external stimulus, the mechanism of which has been attributed to the dynamic coordinative interactions that hold the gel network together.

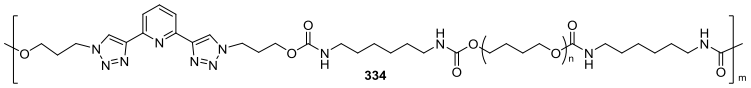

Figure 110. Chemical structure of the ligand macromolecule **334** carrying 2,6-bis(1,2,3-triazol-4-yl)pyridine (BTP) in the backbone.[231]

Gohy, Fustin and co-workers attached the terpy motif to linear polymers bearing short hydrophobic segments (**325**, Figure 106). Initial hydrophobic interactions led to the formation of micellar nanostructures in water.[232] Subsequent addition of transition metal ions to these micelles resulted in bridging between micelles, thereby leading to the formation of gels. These gels exhibited reversible gel-to-sol transitions under mechanical stress, and temperature-induced self-healing properties. Similarly, Ge and Liu have reported the synthesis of the polymer **326** (Figure 106) functionalized with terpy units. Complexation with Ru^{II} resulted in the formation of cross-linked micelles with metallo-supramolecular cores.[233] These cross-linked micelles exhibited high structural integrity at different pH values and temperatures in aqueous solution. They also exhibited multi-stimuli responsiveness including pH-responsive cores, thermo-responsive shells, and dissociation upon addition of EDTA. Taking advantage of these properties, stimuli-responsive encapsulation and release of hydrophobic guest molecules was also demonstrated.

Terech and co-workers have synthesized MSPs and MSGs based on the multitopic cyclam bis-terpy platform (**330**, Figure 107), which exhibit multi-stimuli-responsive behavior. Depending on the affinity of the metal ions for the two coordination sites (terpy and cyclam), **330** undergoes supramolecular polymerization *via* two mechanisms (Figure 111).[224] Cu^{II} binds to the cyclam site, yielding the mononuclear Cu^{II} complex (**335**) which is followed by the

formation of the MSP (**336**) upon the addition of second equivalent of Cu^{II}. On the other hand, in the presence of Co^{II} and Ni^{II}, MSPs (**337**) are initially formed in which the metal coordinates to the terpy sites, while the cyclam units remain unoccupied. Subsequent addition of a second equivalent of the metal ion results in complexation at the cyclam moiety. Interestingly, these MSPs exhibited gelation properties as a function of solvent composition and the nature of counter ions and could be controlled by metal/ligand stoichiometry, concentration and temperature. Moreover, the self-assembly process was also found to be responsive towards external stimuli such as an electrical input (redox sensitivity) or the type of counter ion (chemosensitivity). Upon electrochemical oxidation of Co^{II} to Co^{III}, the gel readily underwent transformation into a solution. The gel could be reformed by reducing the Co^{III} to Co^{II}. The introduction of additional positive charges in the polymer chains upon oxidation affects the solubility of the system and destabilizes the gel, thereby accounting for the gel-to-sol transition.

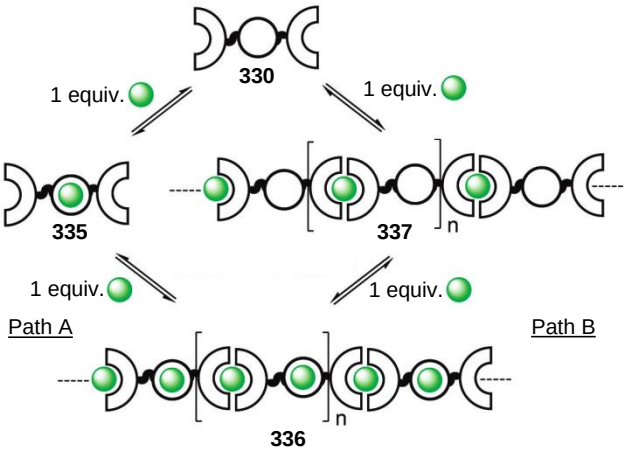

Figure 111. Schematic representation of the formation of MSPs *via* the intermediate formation of mononuclear complexes or of metal-free-cyclam polymers. Adapted with permission from ref [224a]. Copyright 2009 American Chemical Society.

Cyclam units can undergo thermally- or electrochemically-induced interconversion between *cis*- and *trans*-isomers. In the *cis*-isomer, the substituents are on the same side of the cyclam plane, while in the *trans*-isomer the subunits are above and below the cyclam plane. Taking

advantage of this property, Terech and co-workers developed a system in which temperature-triggered *cis*-to-*trans* conversions at the cyclam unit leads to a macroscopic sol-to-gel phase transition.[234] For this, the authors utilized the bis-terpy-cyclam ligand **330** (Figure 107) which binds to two Ni^{II} ions, yielding supramolecular polymers. Initially, kinetically-favored *cis*-isomers, which form coil-like aggregates, are present in solution. Upon heating, the *cis*-to-*trans* conversion proceeds and coils expand to rod-coils, giving rise to aggregates comprised of rigid and flexible segments and gel formation. It was also demonstrated that these gels exhibited self-healing properties.[235]

Wang and co-workers have reported the synthesis of the heteroditopic monomer **328** (Figure 106), bearing a secondary ammonium salt guest and a terpy moiety.[236] In the presence of Zn^{II}, complex **338** was formed *via* the coordination of Zn^{II} to terpy (Figure 112), whereas **328** associates with the complementary homoditopic B21C7 (**327**) to yield the [3]pseudorotaxane **339**. When all the three components (**327**, **328** and Zn^{II}) were mixed together, linear MSPs **340** were formed which exhibited multi-stimuli responsiveness triggered by heat, pH or a competitive ligand such as cyclen.

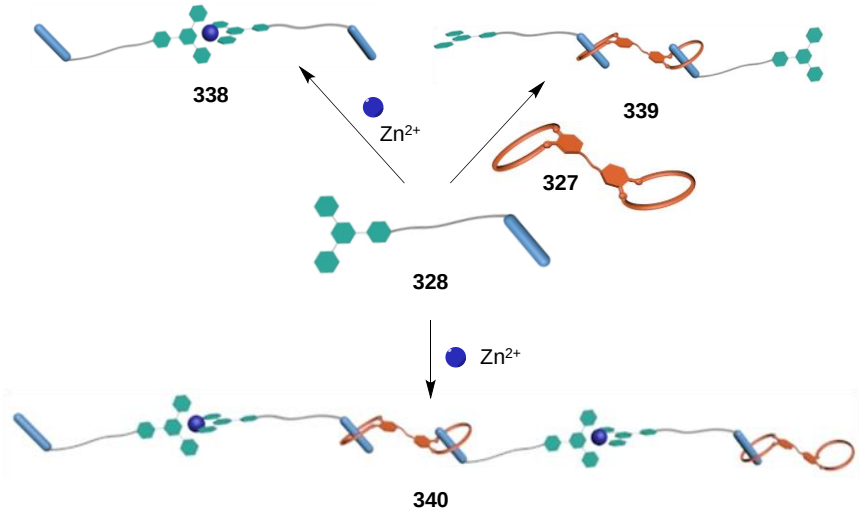

Figure 112. Cartoon representation of the formation of supramolecular polymers **340** and the corresponding intermediates (terpy-Zn^{II} complex **338** and host-guest paired [3]pseudorotaxane **339**). Adapted from ref [236] with permission of The Royal Society of Chemistry.

Zhang, Su and co-workers reported the multi-stimuli-responsive behavior of a metal-organic system by utilizing the photoisomerization properties of the DTE moiety (Figure 113).[237] Mixing the dicarboxylic acid derivative of DTE **341** with Al^{III} yielded a clear solution, from which a metal-organic gel was obtained upon heating. The gelation process was affected by the addition of anions: their coordination to Al^{III} or formation of hydrogen bonds with the ligands or metal ions of the system disrupted the gelation process. The gels so obtained exhibited interesting reversible photochromic behavior: a yellow open (O)-solution converts into the yellow O-gel when heated, and can be converted into a red closed (C)-gel by UV irradiation. The red C-gel changes into a red C-solution when kept at room temperature in the dark, and finally reverts back into the original yellow O-solution when exposed to visible light.

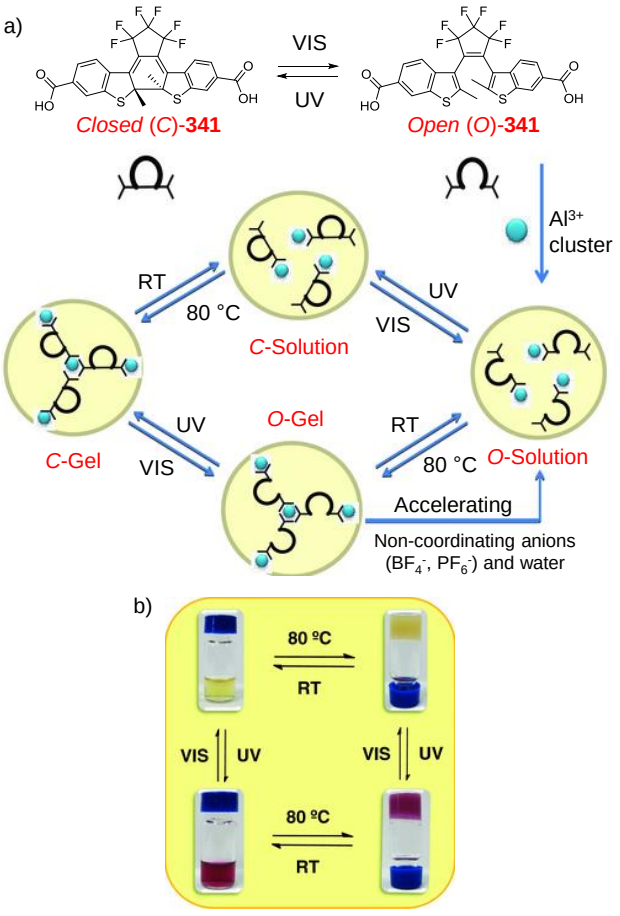

Figure 113. a) Reversible photoisomerization between the open- and closed-ring forms of the photochromic dicarboxylic acid ligand **341**, and schematic representation of multiple

transformations among gels and solutions in both open and closed forms. b) Photographs showing the reversible transformations of the DTE system upon heating/cooling and UV-Vis irradiation. Adapted with permission from ref [237]. Copyright 2013 WILEY-VCH.

8.3 Miscellaneous

Harada and co-workers have reported a gel-forming functional polymer in which the adhesion between blocks of gel could be switched by the addition and removal of metal ions.[238] In order to demonstrate this ability, the authors utilized a polyacrylamide hydrogel modified with both beta-cyclodextrin (β-CD) and 2,2'-bipyridyl moieties (**342**, host gel in Figure 114). In the hydrogel, the hydrophobic 2,2'-bipyridyl moiety is included in the cavity of β-CD to form supramolecular cross-links, thereby suppressing the molecular recognition abilities of β-CD. Therefore, the host gel does not adhere to a gel containing *tert*-butyl groups (**343**, guest gel) in the absence of metal ions. However, upon the addition of metal ions, the 2,2'-bipyridyl moieties complex with the metal ions and are released from β-CD cavities to form 'free' β-CD units. This leads to the formation of host-guest complexes between the β-CD and *tert*-butyl groups on the interface of the two gels, which results in the adhesion between the two gels. The adhesion process was found to be reversible following removal of the metal ions with EDTA.

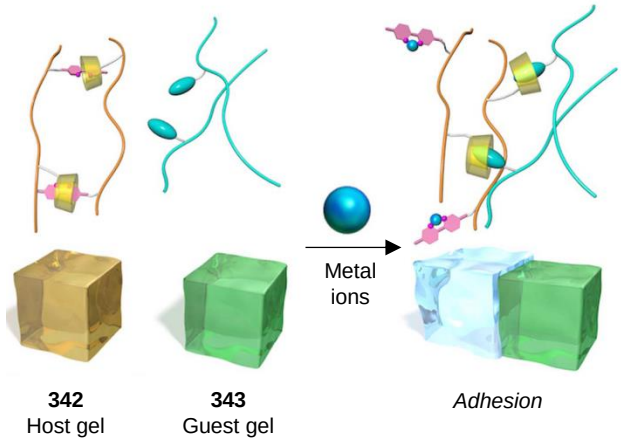

Figure 114. Adhesion of the metal ion-responsive host gel (**342**) to the guest gel (**343**) induced by metal ions as a chemical stimulus. Adapted from ref [238].

Yan and co-workers reported that the tetrazole based ligands **344**, **346-348** (Figure 115) react with Pd^{II} in a 2 : 1 molar ratio to spontaneously yield homogeneous gels in DMF.[239] By using **345** as a control system, the authors proposed that the cooperative hydrogen bonding interaction of the NH group of tetrazoles played a key role in the formation of gels. These gels exhibited remarkable deformation recovery and bottom-up load-bearing capability. Furthermore, they exhibited healing properties in the presence of DMF and water, presumably through solvent-mediated cooperative hydrogen bond rearrangements.

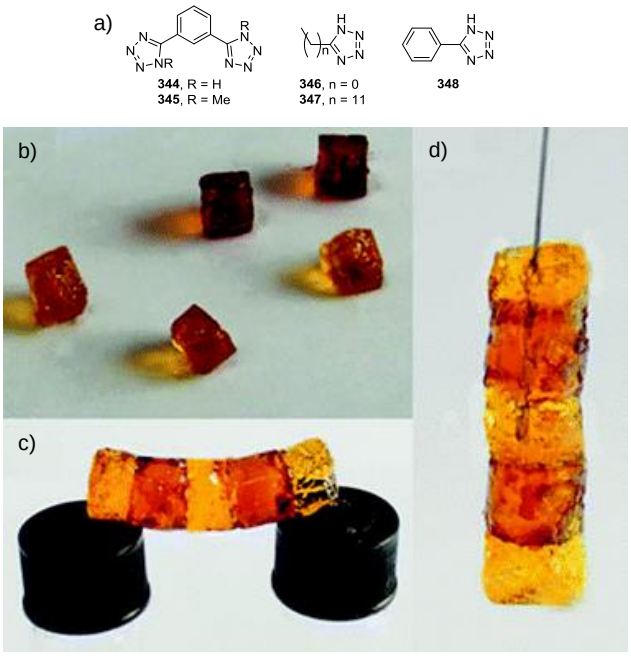

Figure 115. a) Chemical structures of ligands **344-348** and b-d) photographs showing the adhesion and healing property of gels made from **344.** Adapted from ref [239] with permission of The Royal Society of Chemistry.

Our group has utilized the subcomponent self-assembly strategy to synthesize structurally dynamic conjugated metal-containing polymers (Figures 116, 117). As shown in Figure 116, the reaction of 1,4-diaminobenzene and 4,4'-diformyl-3,3'-bipyridine subcomponents in the presence of Cu^{I} yields the polymer **349**,[240] wherein the imine ligands are stabilized by the coordinated Cu^{I}. Trioctylphosphine (TOP) ligands were used to cap the vacant coordination sites of the copper ions, taking advantage of the observation that heteroleptic $[CuN_2P_2]^{+}$

species are favored as compared to the homoleptic $[CuN_4]^+$ and $[CuP_4]^+$ complexes. In DMSO solution, this polymer solution exhibited sol-to-gel transition as the temperature was raised, which was attributed to the formation of Cu^IN_4 cross-links as the forward reaction of the equilibrium $2[Cu^IN_2P_2] \rightleftarrows [Cu^IN_4] + [CuP_n]^+ + (4-n)P$ is favored at higher temperatures. The material also exhibited thermochromism and photoluminescence, with the color and intensity of both absorption and emission exhibiting temperature dependence. Subsequently, a heteroleptic metallopolymer **350** was synthesized by the subcomponent self-assembly of 6,6'-diformyl-3,3'-bipyridine, benzidine, copper(I) tetrafluoroborate and bis[2-(diphenylphosphino)phenyl]ether (POP).[241] This polymer exhibited both thermochromism and "heat-set" gel formation in solution, which was found to be either reversible or irreversible depending on the solvent used. Furthermore, the polymer exhibited electroluminescence properties and could be fabricated into light emitting electrochemical cells. The devices showed voltage-dependent electroluminescence, undergoing a shift in the wavelength of emission that reverses slowly once the voltage has been removed.

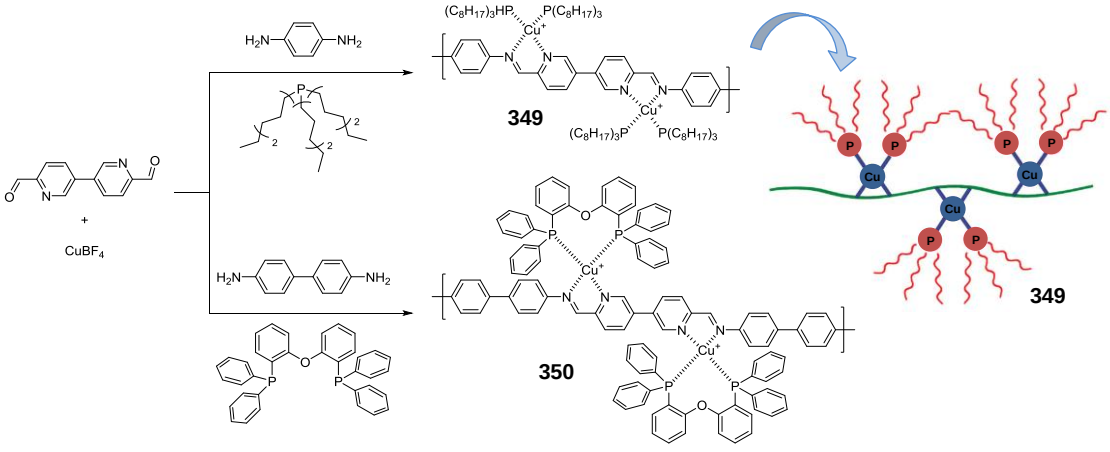

Figure 116. The preparation of conjugated metal-organic polymers **349**[240] and **350**[241] from subcomponents and a cartoon representation of **349**. Adapted with permission from ref [240]. Copyright 2011 American Chemical Society.

Following a similar strategy, we synthesized water-soluble polymer **351** (Figure 117) *via* Cu^I-directed imine bond formation between triethylene glycol functionalized 1,2-

phenylenediamine and 2,9-diformylphenanthroline.[242] It was observed that the individual double-helical strands aggregated through entanglement of their side chains to form well-defined superstructures. Interestingly, the Cu^{I} ions in the polymer could be reversibly oxidized electrochemically in solution, whereas model complexes underwent irreversible oxidation. The stability of the polymer was attributed to its length, which stabilized the oxidized states through delocalization or entrapment. Moreover, this material was found to be photo- and electro-luminescent and was used for the fabrication of electroluminescent devices which exhibited white-blue light emission.

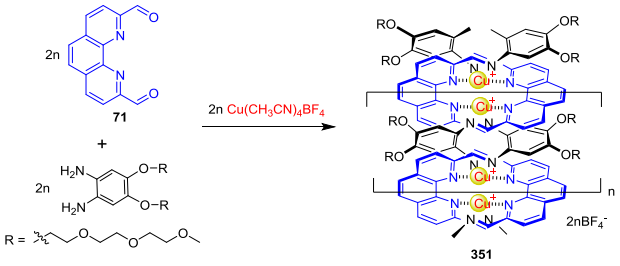

Figure 117. Preparation of conjugated metal-organic polymer **351**.[242]

9 Conclusions and Future Outlook

The field of stimuli-responsive metal-ligand assemblies is a growing and diverse area of study. This review has discussed examples ranging from simple luminescent transition metal solid-state materials to three-dimensional cages and polymers for diverse applications in the development of materials requiring specific responses to environmental stimuli. These examples demonstrate that chemists are beginning to master the design and control of stimuli-responsive behavior where the stimulus induces a complex response, such as structural rearrangement. In the majority of examples, the stimulus has a linear effect on the system such that one stimulus causes one response, stoichiometrically. Nature, however, exploits signal transduction pathways where the effect of one stimulus can be amplified to cause many responses. A major challenge for the field is how to design more complex systems with non-linear responses, such as those observed in biological signaling cascades.

Recent reports of stimuli-responsive systems by Aprahamian[243] indicate progress in this challenge towards mimicking the complexity observed in nature. A switching cascade of hydrazone based switches could be initiated by a single input, Zn^{II} ions, exploiting coordination-coupled proton relay (Figure 118a);[243a] coordination of Zn^{II} to *E*-**352** causes *E*/*Z* isomerization and lowers the pK_a of the imidazole unit allowing proton transfer to a second switch (*E*-**353**) generating *Z*-**354**. This proton transfer initiates *E*/*Z* isomerization of the second switch to produce *Z*-**355**. Thus, a single input has resulted in the multi-step *E*/*Z* isomerization of two switches. This switching process is reversible through addition of cyanide to remove the coordinated Zn^{II}. More recently, the concept has been extended to drive fluorescent signal amplification by exploiting Zn^{II}-coordination-coupled deprotonation of catalyst *E*-**357** to initiate the acid catalyzed imine bond hydrolysis of **356**, releasing fluorophore **359** from quencher **360** (Figure 118b).[243b] Again, the coordination-coupled deprotonation process is reversible and it is possible to switch the catalysis on and off by metalation/demetalation.

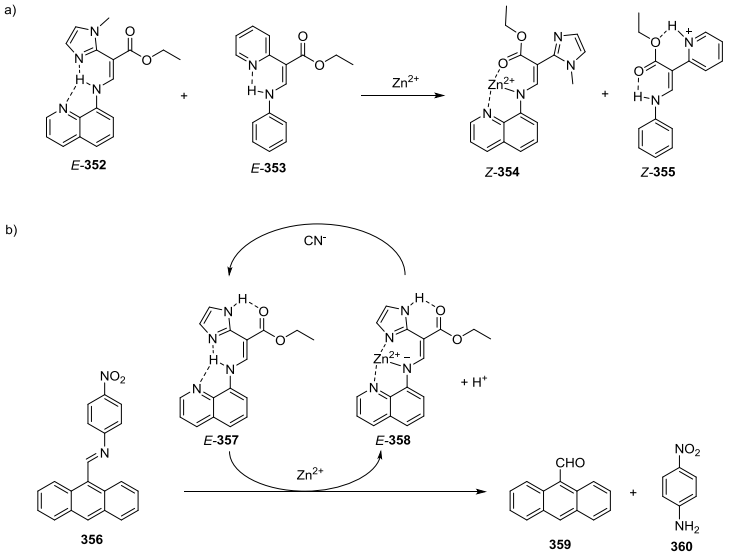

Figure 118. Aprahamian's a) switching cascade and b) emission amplification exploiting coordination-coupled deprotonation of hydrazone switches.

The myriad responses exhibited by metal-organic structures to stimuli thus provide a set of examples – a toolkit – to enable the construction of new systems and materials, wherein

complex behavior may result from the propagation of a stimulus through a complex chemical network.[244] The design of such networks remains a central challenge for synthetic chemists, along with the design of feedback loops and signal amplification mechanisms similar to those observed in biology. Basic studies of such *chemical signal transduction* mechanisms will not only enable the design of new adaptive materials, but shed light upon the fascinating intersection of chemistry, information science, and biology.

Author Information

Corresponding Author

* Phone: +44 1223 336324. Email: jrn34@cam.ac.uk.

Author Contributions

The manuscript was written through contributions of all authors. All authors have given approval to the final version of the manuscript. †These authors contributed equally.

Notes

The authors declare no competing financial interest.

Anna McConnell received a Bachelor of Science with Honours from the University of Canterbury in 2005. She obtained a DPhil in 2010 under the supervision of Prof. Paul Beer at the University of Oxford before carrying out post-doctoral research in the group of Prof. Jacqueline Barton at the California Institute of Technology. Since 2013, she has been working as a postdoc in the group of Prof. Jonathan Nitschke at the University of Cambridge.

Christopher Wood received a Master of Chemistry with Honours from the University of Oxford in 2011, having completed a Part II research project with Prof. Martin D. Smith. He is currently working towards his Ph. D. in the group of Prof. J. R. Nitschke, looking at the design and synthesis of novel supramolecular architectures using the subcomponent self-assembly methodology.

Prakash Neelakandan obtained his Ph. D. in 2009 from CSIR-NIIST Thiruvananthapuram, India under the supervision of Dr. Danaboyina Ramaiah on host-guest chemistry of cyclophanes. Subsequently, he was a postdoc in the group of Professor Frederick Lewis at

Northwestern University, USA where he was involved in studying the self-assembly and electronic properties of oligonucleotides. Since May 2012, he is working as a postdoc in the Nitschke group at the University of Cambridge, UK on chromophore-functionalized metal-organic cages.

Jonathan Nitschke received his bachelor's degree from Williams College (USA) in 1995 and his doctorate from the University of California, Berkeley in 2001 under the supervision of T. Don Tilley. He then undertook postdoctoral studies with Jean-Marie Lehn in Strasbourg, and in 2003 started his independent research career in the Organic Chemistry Department of the University of Geneva. In 2007 he was appointed as a Lecturer at Cambridge, where he became a Professor in 2014. His research program investigates the self-assembly of complex, functional structures from simple molecular precursors and metal ions.

Acknowledgments

We thank Dr. Ben Pilgrim, William Ramsay, Derrick Roberts, Dr. Tanya Ronson and Daniel Wood for proof-reading the manuscript. The Engineering and Physical Sciences Research Council and the European Research Council are acknowledged for financial support.

Abbreviations

acac: acetylacetone

ACQ: aggregation-caused quenching

AFM: atomic force microscopy

AIE: aggregation induced emission

ATP: adenosine triphosphate

B21C7: benzo-21-crown-7

BET: back electron transfer

BODIPY: 4,4-difluoro-4-bora-3a,4a-diaza-*s*-indacene

BTP: 2,6-bis(1,2,3-triazol-4-yl)pyridine

^{t}Bu, *tert*-Bu: tertiary butyl

β-CD: β-cyclodextrin

CC: cluster-centered

CD: circular dichroism

CT: charge-transfer

CV: cyclic voltammetry

cyclam: 1,4,8,11-tetraazacyclotetradecane

cyclen: 1,4,7,10-tetraazacyclododecane

DABCO: 1,4-diazabicyclo[2.2.2]octane

DBC8: dibenzo[24]crown-8

DCE: 1,2-dichloroethane

DCM: dichloromethane

DEF: N,N-diethylformamide

DFT: density functional theory

DMA: *N*,*N*-dimethylacetamide

DMAP: 4-(dimethylamino)pyridine

DMF: *N*,*N*-dimethylformamide

DMSO: dimethylsulfoxide

DNP: 1,5-dihydroxynaphthalene

DOMP: dendronized organo-Pt^{II} metallacyclic polymer

dpb: 1,3-di(2-pyridyl)benzene

5dpb: 1,3-di(5-methyl-2pyridyl)benzene

dpbiiq: 8,8'-diphenyl-3,3'-biisoquinoline

dpp: 2,9-diphenyl-1-10-phenanthroline

dppbz: *o*-bis(diphenylphosphino)benzene

DTE: dithienylethene

EDTA: ethylenediaminetetraacetic acid

en: ethylenediamine

Et: ethyl

H_2BA: bromanilic acid

HBPT: hydrogen-bonded proton transfer

HE: high energy

HS: high spin

Im: imidazole

LaDD: lanthanum(III) double decker

LC: ligand-centered

LE: low energy

LLCT: ligand-to-ligand-charge transfer

LS: low spin

MA: 4-morpholin-naphthalimide

Me: methyl

Mebip: 2,6-bis(1’-methylbenzimidazolyl)pyridine

MLCT: metal-to-ligand-charge transfer

MMLCT: metal-metal-to-ligand-charge transfer

MSP: metallo supramolecular polymer

MSG: metallo-supramolecular gel

NBD: norbornadiene

NMR: nuclear magnetic resonance

o: ortho

p: para

pam: 2-picolylamine

PET: photo-induced electron transfer

Ph: phenyl

PPi: pyrophosphate

ppy: phenylpyridine

*i*Pr: iso-propyl

salen: 2,2'-ethylenebis(nitrilomethylidene)diphenol

SCO: spin-crossover

SCE: saturated calomel electrode

SEM: scanning electron microscopy

TAM: tetraazamacrocyclic

$TCNQF_4$: tetrafluorotetracyanoquinodimethane

TEM: transmission electron microscopy

TEOA: triethanolamine

TFA: trifluoroacetic acid

Terpy: terpyridine

THF: tetrahydrofuran

THP: tetrahydropyrane

tpa: tris(2-pyridylmethyl)amine

tpt: 2,4,6-tri-4-pyridyl-1,3,5-triazine

UPy: 2-ureido-4-pyrimidinone

UV: ultra-violet

VOC: volatile organic compound

XLCT: halide-to-ligand charge transfer

XMCT: halide-to-metal charge transfer

References

(1) *Intelligent Stimuli-Responsive Materials*; Li, Q., Ed.; John Wiley & Sons, Inc., 2013.

(2) Nagarkar, S. S.; Desai, A. V.; Ghosh, S. K. Stimulus-Responsive Metal–Organic Frameworks, *Chem. Asian J.* **2014**, *9*, 2358-2376.

(3) For recent themed issues on metal-organic frameworks see *Chem. Rev.*, **2012**, 112, 673-1268 and *Chem. Soc. Rev.*, **2009**, 38, 1201-1508.

(4) Sagara, Y.; Kato, T. Mechanically Induced Luminescence Changes in Molecular Assemblies, *Nat. Chem.* **2009**, *1*, 605-610.

(5) Jobbágy, C.; Deák, A. Stimuli-Responsive Dynamic Gold Complexes, *Eur. J. Inorg. Chem.* **2014**, *2014*, 4434-4449.

(6) Balch, A. L. Dynamic Crystals: Visually Detected Mechanochemical Changes in the Luminescence of Gold and Other Transition-Metal Complexes, *Angew. Chem. Int. Ed.* **2009**, *48*, 2641-2644.

(7) Zhang, X.; Chi, Z.; Zhang, Y.; Liu, S.; Xu, J. Recent Advances in Mechanochromic Luminescent Metal Complexes, *J. Mater. Chem. C* **2013**, *1*, 3376-3390.

(8) (a) Ito, H.; Saito, T.; Oshima, N.; Kitamura, N.; Ishizaka, S.; Hinatsu, Y.; Wakeshima, M.; Kato, M.; Tsuge, K.; Sawamura, M. Reversible Mechanochromic Luminescence of $[(C_6F_5Au)_2(\mu\text{-}1,4\text{-Diisocyanobenzene})]$, *J. Am. Chem. Soc.* **2008**, *130*, 10044-10045. (b) Lee, Y.-A.; Eisenberg, R. Luminescence Tribochromism and Bright Emission in Gold(I) Thiouracilate Complexes, *J. Am. Chem. Soc.* **2003**, *125*, 7778-7779. (c) Schneider, J.; Lee, Y.-A.; Pérez, J.; Brennessel, W. W.; Flaschenriem, C.; Eisenberg, R. Strong Intra- and Intermolecular Aurophilic Interactions in a New Series of Brilliantly Luminescent Dinuclear Cationic and Neutral Au(I) Benzimidazolethiolate Complexes, *Inorg. Chem.* **2008**, *47*, 957-968. (d) Assefa, Z.; Omary, M. A.; McBurnett, B. G.; Mohamed, A. A.; Patterson, H. H.; Staples, R. J.; Fackler, J. P. Syntheses, Structure, and Photoluminescence Properties of the 1-Dimensional Chain Compounds $[(TPA)_2Au][Au(CN)_2]$ and (TPA)AuCl (TPA = 1,3,5-Triaza-7-Phosphaadamantane), *Inorg. Chem.* **2002**, *41*, 6274-6280.

(9) Wedlock, L. E.; Aitken, J. B.; Berners-Price, S. J.; Barnard, P. J. Bromide Ion Binding by a Dinuclear Gold(I) N-Heterocyclic Carbene Complex: A Spectrofluorescence and X-Ray Absorption Spectroscopic Study, *Dalton Trans.* **2013**, *42*, 1259-1266.

(10) Ni, J.; Zhang, X.; Qiu, N.; Wu, Y.-H.; Zhang, L.-Y.; Zhang, J.; Chen, Z.-N. Mechanochromic Luminescence Switch of Platinum(II) Complexes with 5-Trimethylsilylethynyl-2,2′-Bipyridine, *Inorg. Chem.* **2011**, *50*, 9090-9096.

(11) Abe, T.; Itakura, T.; Ikeda, N.; Shinozaki, K. Luminescence Color Change of a Platinum(II) Complex Solid Upon Mechanical Grinding, *Dalton Trans.* **2009**, 711-715.

(12) Mizukami, S.; Houjou, H.; Sugaya, K.; Koyama, E.; Tokuhisa, H.; Sasaki, T.; Kanesato, M. Fluorescence Color Modulation by Intramolecular and Intermolecular $\pi-\pi$ Interactions in a Helical Zinc(II) Complex, *Chem. Mater.* **2004**, *17*, 50-56.

(13) Tsukuda, T.; Kawase, M.; Dairiki, A.; Matsumoto, K.; Tsubomura, T. Brilliant Reversible Luminescent Mechanochromism of Silver(I) Complexes Containing *o*-Bis(Diphenylphosphino)Benzene and Phosphinesulfide, *Chem. Commun.* **2010**, *46*, 1905-1907.

(14) (a) Mastropietro, T. F.; Yadav, Y. J.; Szerb, E. I.; Talarico, A. M.; Ghedini, M.; Crispini, A. Luminescence Mechanochromism in Cyclometallated Ir(III) Complexes Containing Picolylamine, *Dalton Trans.* **2012**, *41*, 8899-8907. (b) Shan, G.-G.; Li, H.-B.; Cao, H.-T.; Zhu, D.-X.; Li, P.; Su, Z.-M.; Liao, Y. Reversible Piezochromic Behavior of Two New Cationic Iridium(III) Complexes, *Chem. Commun.* **2012**, *48*, 2000-2002. (c) Shan, G.-G.; Li, H.-B.; Zhu, D.-X.; Su, Z.-M.; Liao, Y. Intramolecular π-Stacking in Cationic Iridium(III) Complexes with a Triazole-Pyridine Type Ancillary Ligand: Synthesis, Photophysics, Electrochemistry Properties and Piezochromic Behavior, *J. Mater. Chem.* **2012**, *22*, 12736-12744. (d) Szerb, E. I.; Talarico, A. M.; Aiello, I.; Crispini, A.; Godbert, N.; Pucci, D.; Pugliese, T.; Ghedini, M. Red to Green Switch Driven by Order in an Ionic Ir^{III} Liquid-Crystalline Complex, *Eur. J. Inorg. Chem.* **2010**, *2010*, 3270-3277.

(15) Lin, H.; Jang, M.; Suslick, K. S. Preoxidation for Colorimetric Sensor Array Detection of VOCs, *J. Am. Chem. Soc.* **2011**, *133*, 16786-16789.
(16) Wenger, O. S. Vapochromism in Organometallic and Coordination Complexes: Chemical Sensors for Volatile Organic Compounds, *Chem. Rev.* **2013**, *113*, 3686-3733.
(17) Zhang, X.; Li, B.; Chen, Z.-H.; Chen, Z.-N. Luminescence Vapochromism in Solid Materials Based on Metal Complexes for Detection of Volatile Organic Compounds (VOCs), *J. Mater. Chem.* **2012**, *22*, 11427-11441.
(18) Strasser, C. E.; Catalano, V. J. "On−Off" Au(I)···Cu(I) Interactions in a $Au(NHC)_2$ Luminescent Vapochromic Sensor, *J. Am. Chem. Soc.* **2010**, *132*, 10009-10011.
(19) Li, Y.-J.; Deng, Z.-Y.; Xu, X.-F.; Wu, H.-B.; Cao, Z.-X.; Wang, Q.-M. Methanol Triggered Ligand Flip Isomerization in a Binuclear Copper(I) Complex and the Luminescence Response, *Chem. Commun.* **2011**, *47*, 9179-9181.
(20) Li, B.; Wei, R.-J.; Tao, J.; Huang, R.-B.; Zheng, L.-S.; Zheng, Z. Solvent-Induced Transformation of Single Crystals of a Spin-Crossover (SCO) Compound to Single Crystals with Two Distinct Sco Centers, *J. Am. Chem. Soc.* **2010**, *132*, 1558-1566.
(21) Kobayashi, A.; Dosen, M.-a.; Chang, M.; Nakajima, K.; Noro, S.-i.; Kato, M. Synthesis of Metal−Hydrazone Complexes and Vapochromic Behavior of Their Hydrogen-Bonded Proton-Transfer Assemblies, *J. Am. Chem. Soc.* **2010**, *132*, 15286-15298.
(22) Hudson, Z. M.; Sun, C.; Harris, K. J.; Lucier, B. E. G.; Schurko, R. W.; Wang, S. Probing the Structural Origins of Vapochromism of a Triarylboron-Functionalized Platinum(II) Acetylide by Optical and Multinuclear Solid-State NMR Spectroscopy, *Inorg. Chem.* **2011**, *50*, 3447-3457.
(23) Muro, M. L.; Daws, C. A.; Castellano, F. N. Microarray Pattern Recognition Based on Pt^{II} Terpyridyl Chloride Complexes: Vapochromic and Vapoluminescent Response, *Chem. Commun.* **2008**, 6134-6136.
(24) Perruchas, S.; Goff, X. F. L.; Maron, S.; Maurin, I.; Guillen, F.; Garcia, A.; Gacoin, T.; Boilot, J.-P. Mechanochromic and Thermochromic Luminescence of a Copper Iodide Cluster, *J. Am. Chem. Soc.* **2010**, *132*, 10967-10969.
(25) Ford, P. C.; Cariati, E.; Bourassa, J. Photoluminescence Properties of Multinuclear Copper(I) Compounds, *Chem. Rev.* **1999**, *99*, 3625-3648.
(26) Zhang, X.; Wang, J.-Y.; Ni, J.; Zhang, L.-Y.; Chen, Z.-N. Vapochromic and Mechanochromic Phosphorescence Materials Based on a Platinum(II) Complex with 4-Trifluoromethylphenylacetylide, *Inorg. Chem.* **2012**, *51*, 5569-5579.
(27) Hong, Y.; Lam, J. W. Y.; Tang, B. Z. Aggregation-Induced Emission: Phenomenon, Mechanism and Applications, *Chem. Commun.* **2009**, 4332-4353.
(28) Xu, B.; Chi, Z.; Zhang, X.; Li, H.; Chen, C.; Liu, S.; Zhang, Y.; Xu, J. A New Ligand and Its Complex with Multi-Stimuli-Responsive and Aggregation-Induced Emission Effects, *Chem. Commun.* **2011**, *47*, 11080-11082.
(29) Chakrabarty, R.; Mukherjee, P. S.; Stang, P. J. Supramolecular Coordination: Self-Assembly of Finite Two- and Three-Dimensional Ensembles, *Chem. Rev.* **2011**, *111*, 6810-6918.
(30) Sun, S.-S.; Anspach, J. A.; Lees, A. J. Self-Assembly of Transition-Metal-Based Macrocycles Linked by Photoisomerizable Ligands : Examples of Photoinduced Conversion of Tetranuclear − Dinuclear Squares, *J. Am. Chem. Soc.* **2002**, *41*, 1862-1869.
(31) Tang, H.-S.; Zhu, N.; Yam, V. W.-W. Tetranuclear Macrocyclic Gold(I) Alkynyl Phosphine Complex Containing Azobenzene Functionalities: A Dual-Input Molecular Logic with Photoswitching Behavior Controllable Via Silver(I) Coordination/Decoordination, *Organometallics* **2007**, *26*, 22-25.
(32) Chen, S.; Chen, L.-J.; Yang, H.-B.; Tian, H.; Zhu, W. Light-Triggered Reversible Supramolecular Transformations of Multi-Bisthienylethene Hexagons, *J. Am. Chem. Soc.* **2012**, *134*, 13596-13599.
(33) Zhao, L.; Northrop, B. H.; Stang, P. J. Supramolecule-to-Supramolecule Transformations of Coordination-Driven Self-Assembled Polygons, *J. Am. Chem. Soc.* **2008**, *130*, 11886-11888.
(34) Sun, S.-S.; Stern, C. L.; Nguyen, S. T.; Hupp, J. T. Directed Assembly of Transition-Metal-Coordinated Molecular Loops and Squares from Salen-Type Components. Examples of Metalation-Controlled Structural Conversion, *J. Am. Chem. Soc.* **2004**, *126*, 6314-6326.

(35) Gianneschi, N. C.; Masar, M. S.; Mirkin, C. A. Development of a Coordination Chemistry-Based Approach for Functional Supramolecular Structures, *Acc. Chem. Res.* **2005**, *38*, 825-837.
(36) Oliveri, C. G.; Ulmann, P. A.; Wiester, M. J.; Mirkin, C. A. Heteroligated Supramolecular Coordination Complexes Formed Via the Halide-Induced Ligand Rearrangement Reaction, *Acc. Chem. Res.* **2008**, *41*, 1618-1629.
(37) Farrell, J. R.; Mirkin, C. A.; Guzei, I. A.; Liable-Sands, L. M.; Rheingold, A. L. The Weak-Link Approach to the Synthesis of Inorganic Macrocycles, *Angew. Chem. Int. Ed.* **1998**, *37*, 465-467.
(38) (a) Gianneschi, N. C.; Bertin, P. A.; Nguyen, S. T.; Mirkin, C. A.; Zakharov, L. N.; Rheingold, A. L. A Supramolecular Approach to an Allosteric Catalyst, *J. Am. Chem. Soc.* **2003**, *125*, 10508-10509. (b) Yoon, H. J.; Mirkin, C. A. PCR-Like Cascade Reactions in the Context of an Allosteric Enzyme Mimic, *J. Am. Chem. Soc.* **2008**, *130*, 11590-11591.
(39) Brown, A. M.; Ovchinnikov, M. V.; Stern, C. L.; Mirkin, C. A. Halide-Induced Supramolecular Ligand Rearrangement, *J. Am. Chem. Soc.* **2004**, *126*, 14316-14317.
(40) Brown, A. M.; Ovchinnikov, M. V.; Stern, C. L.; Mirkin, C. A. Tetrametallic Rectangular Box Complexes Assembled from Heteroligated Macrocycles, *Chem. Commun.* **2006**, 4386-4386.
(41) Oliveri, C. G.; Heo, J.; Nguyen, S. T.; Mirkin, C. A.; Wawrzak, Z. A Convergent Coordination Chemistry-Based Approach to Dissymmetric Macrocyclic Cofacial Porphyrin Complexes, *Inorg. Chem.* **2007**, *46*, 7716-7718.
(42) Heo, J.; Jeon, Y.-M.; Mirkin, C. A. Reversible Interconversion of Homochiral Triangular Macrocycles and Helical Coordination Polymers, *J. Am. Chem. Soc.* **2007**, *129*, 7712-7713.
(43) Miyake, R.; Shionoya, M. Reversible Structural Switch in the Nano-Cavity of Crystalline Metallo-Macrocycles with Smooth Ligand Exchange by Non-Coordinating Guest Stimuli, *Chem. Commun.* **2012**, *48*, 7553-7555.
(44) Zheng, Y.-R.; Zhao, Z.; Wang, M.; Ghosh, K.; Pollock, J. B.; Cook, T. R.; Stang, P. J. A Facile Approach toward Multicomponent Supramolecular Structures: Selective Self-Assembly Via Charge Separation, *J. Am. Chem. Soc.* **2010**, *132*, 16873-16882.
(45) Saha, M. L.; Pramanik, S.; Schmittel, M. Spontaneous and Catalytic Fusion of Supramolecules, *Chem. Commun.* **2012**, *48*, 9459-9461.
(46) Schmittel, M.; Kalsani, V.; Kishore, R. S. K.; Cölfen, H.; Bats, J. W. Dynamic and Fluorescent Nanoscale Phenanthroline/Terpyridine Zinc(II) Ladders. Self-Recognition in Unlike Ligand/Like Metal Coordination Scenarios, *J. Am. Chem. Soc.* **2005**, *127*, 11544-11545.
(47) Neogi, S.; Lorenz, Y.; Engeser, M.; Samanta, D.; Schmittel, M. Heteroleptic Metallosupramolecular Racks, Rectangles, and Trigonal Prisms: Stoichiometry-Controlled Reversible Interconversion, *Inorg. Chem.* **2013**, *52*, 6975-6984.
(48) Dry, E. F. V.; Clegg, J. K.; Breiner, B.; Whitaker, D. E.; Stefak, R.; Nitschke, J. R. Reversible Anion-Templated Self-Assembly of [2+2] and [3+3] Metallomacrocycles Containing a New Dicopper(I) Motif, *Chem. Commun.* **2011**, *47*, 6021-6023.
(49) (a) Piguet, C.; Bernardinelli, G.; Hopfgartner, G. Helicates as Versatile Supramolecular Complexes, *Chem. Rev.* **1997**, *97*, 2005-2062. (b) Hannon, M. J.; Childs, L. J. Helices and Helicates: Beautiful Supramolecular Motifs with Emerging Applications, *Supramolecular Chem.* **2004**, *16*, 7-22. (c) Albrecht, M. "Let's Twist Again"--Double-Stranded, Triple-Stranded, and Circular Helicates, *Chem. Rev.* **2001**, *101*, 3457-3497.
(50) Faulkner, A. D.; Kaner, R. A.; Abdallah, Q. M. A.; Clarkson, G.; Fox, D. J.; Gurnani, P.; Howson, S. E.; Phillips, R. M.; Roper, D. I.; Simpson, D. H.; Scott, P. Asymmetric Triplex Metallohelices with High and Selective Activity against Cancer Cells, *Nat. Chem.* **2014**, *6*, 797-803.
(51) Kume, S.; Murata, M.; Ozeki, T.; Nishihara, H. Reversible Photoelectronic Signal Conversion Based on Photoisomerization-Controlled Coordination Change of Azobenzene-Bipyridine Ligands to Copper, *J. Am. Chem. Soc.* **2005**, *127*, 490-491.
(52) Boiocchi, M.; Fabbrizzi, L. Double-Stranded Dimetallic Helicates: Assembling-Disassembling Driven by the Cu^{I}/Cu^{II} Redox Change and the Principle of Homochiral Recognition, *Chem. Soc. Rev.* **2014**, *43*, 1835-1847.
(53) Potts, K. T.; Keshavarz-K, M.; Tham, F. S.; Abruña, H. D.; Arana, C. R. Metal Ion-Induced Self-Assembly of Functionalized 2,6-Oligopyridines. 2. Copper-Containing Double-Stranded Helicates Derived from Functionalized Quaterpyridine and Quinquepyridine: Redox State-

Induced Transformations and Electron Communication in Mixed-Valence Systems, *Inorg. Chem.* **1993**, *32*, 4422-4435.

(54) (a) Amendola, V.; Fabbrizzi, L.; Gianelli, L.; Maggi, C.; Mangano, C.; Pallavicini, P.; Zema, M. Electrochemical Assembling/Disassembling of Helicates with Hysteresis, *Inorg. Chem.* **2001**, *40*, 3579-3587. (b) Amendola, V.; Fabbrizzi, L.; Pallavicini, P.; Sartirana, E.; Taglietti, A. Monitoring the Redox-Driven Assembly/Disassembly of a Dicopper(I) Helicate with an Auxiliary Fluorescent Probe, *Inorg. Chem.* **2003**, *42*, 1632-1636.

(55) Stadler, A.-M.; Burg, C.; Ramírez, J.; Lehn, J.-M. Grid-Double-Helicate Interconversion, *Chem. Commun.* **2013**, *49*, 5733-5735.

(56) (a) Stadler, A.-M.; Lehn, J.-M. P. Coupled Nanomechanical Motions: Metal-Ion-Effected, Ph-Modulated, Simultaneous Extension/Contraction Motions of Double-Domain Helical/Linear Molecular Strands, *J. Am. Chem. Soc.* **2014**, *136*, 3400-3409. (b) Stadler, A.-M.; Kyritsakas, N.; Graff, R.; Lehn, J.-M. Formation of Rack- and Grid-Type Metallosupramolecular Architectures and Generation of Molecular Motion by Reversible Uncoiling of Helical Ligand Strands, *Chem. Eur. J.* **2006**, *12*, 4503-4522. (c) Barboiu, M.; Vaughan, G.; Kyritsakas, N.; Lehn, J.-M. Dynamic Chemical Devices: Generation of Reversible Extension/Contraction Molecular Motion by Ion-Triggered Single/Double Helix Interconversion, *Chem. Eur. J.* **2003**, *9*, 763-769. (d) Barboiu, M.; Lehn, J.-M. Dynamic Chemical Devices: Modulation of Contraction/Extension Molecular Motion by Coupled-Ion Binding/pH Change-Induced Structural Switching, *Proc. Natl. Acad. Sci. U. S. A.* **2002**, *99*, 5201-5206. (e) Baxter, P. N. W.; Lehn, J.-M.; Fischer, J.; Youinou, M.-T. Self-Assembly and Structure of a 3× 3 Inorganic Grid from Nine Silver Ions and Six Ligand Components, *Angew. Chem. Int. Ed.* **1994**, *33*, 2284-2287.

(57) Schultz, D.; Nitschke, J. R. Designing Multistep Transformations Using the Hammett Equation: Imine Exchange on a Copper(I) Template, *J. Am. Chem. Soc.* **2006**, *128*, 9887-9892.

(58) Campbell, V. E.; de Hatten, X.; Delsuc, N.; Kauffmann, B.; Huc, I.; Nitschke, J. R. Cascading Transformations within a Dynamic Self-Assembled System, *Nat. Chem.* **2010**, *2*, 684-687.

(59) (a) Schultz, D.; Biaso, F.; Shahi, A. R. M.; Geoffroy, M.; Rissanen, K.; Gagliardi, L.; Cramer, C. J.; Nitschke, J. R. Helicate Extension as a Route to Molecular Wires, *Chem. Eur. J.* **2008**, *14*, 7180-7185. (b) Campbell, V. E.; de Hatten, X.; Delsuc, N.; Kauffmann, B.; Huc, I.; Nitschke, J. R. Interplay of Interactions Governing the Dynamic Conversions of Acyclic and Macrocyclic Helicates, *Chem. Eur. J.* **2009**, *15*, 6138-6142.

(60) Hutin, M.; Schalley, C. A.; Bernardinelli, G.; Nitschke, J. R. Helicate, Macrocycle, or Catenate: Dynamic Topological Control over Subcomponent Self-Assembly, *Chem. Eur. J.* **2006**, *12*, 4069-4076.

(61) Sarma, R. J.; Otto, S.; Nitschke, J. R. Disulfides, Imines, and Metal Coordination within a Single System: Interplay between Three Dynamic Equilibria, *Chem. Eur. J.* **2007**, *13*, 9542-9546.

(62) Bokolinis, G.; Riis-Johannessen, T.; Harding, L. P.; Jeffery, J. C.; McLay, N.; Rice, C. R. This Facile Interconversion of Dinuclear Double Helicates and Side-by-Side Species: A Reprogrammable Ligand with Potential Sensor Applications, *Chem. Commun.* **2006**, *2*, 1980-1982.

(63) Weekes, D. M.; Diebold, C.; Mobian, P.; Huguenard, C.; Allouche, L.; Henry, M. A Remarkable Solvent Effect on the Nuclearity of Neutral Titanium(IV)-Based Helicate Assemblies, *Chem. Eur. J.* **2014**, *20*, 5092-5101.

(64) (a) Jobbágy, C.; Molnár, M.; Baranyai, P.; Deák, A. Mechanochemical Synthesis of Crystalline and Amorphous Digold(I) Helicates Exhibiting Anion- and Phase-Switchable Luminescence Properties, *Dalton Trans.* **2014**, *43*, 11807-11810. (b) Jobbágy, C.; Molnár, M.; Baranyai, P.; Hamza, A.; Pálinkás, G.; Deák, A. A Stimuli-Responsive Double-Stranded Digold(I) Helicate, *CrystEngComm* **2014**, *16*, 3192-3192.

(65) Kinbara, K.; Aida, T. Toward Intelligent Molecular Machines: Directed Motions of Biological and Artificial Molecules and Assemblies, *Chem. Rev.* **2005**, *105*, 1377-1400.

(66) Tashiro, S.; Shionoya, M. Stimuli-Responsive Synthetic Metallopeptides, *Chem. Lett.* **2013**, *42*, 456-462.

(67) Coskun, A.; Banaszak, M.; Astumian, R. D.; Stoddart, J. F.; Grzybowski, B. A. Great Expectations: Can Artificial Molecular Machines Deliver on Their Promise?, *Chem. Soc. Rev.* **2012**, *41*, 19-30.

(68) Kay, E. R.; Leigh, D. A.; Zerbetto, F. Synthetic Molecular Motors and Mechanical Machines, *Angew. Chem. Int. Ed.* **2007**, *46*, 72-191.
(69) Amendola, V.; Fabbrizzi, L.; Mangano, C.; Pallavicini, P. Molecular Machines Based on Metal Ion Translocation, *Acc. Chem. Res.* **2001**, *34*, 488-493.
(70) Niess, F.; Duplan, V.; Sauvage, J.-P. Interconversion between a Vertically Oriented Transition Metal-Complexed Figure-of-Eight and a Horizontally Disposed One, *J. Am. Chem. Soc.* **2014**, *136*, 5876-5879.
(71) Amendola, V.; Fabbrizzi, L.; Mangano, C.; Pallavicini, P.; Perotti, A.; Taglietti, A. Ph-Controlled Translocation of Ni^{II} within a Ditopic Receptor Bearing an Appended Anthracene Fragment: A Mechanical Switch of Fluorescence, *J. Chem. Soc., Dalton Trans.* **2000**, 185-189.
(72) (a) Zelikovich, L.; Libman, J.; Shanzer, A. Molecular Redox Switches Based on Chemical Triggering of Iron Translocation in Triple-Stranded Helical Complexes, *Nature* **1995**, *374*, 790-792. (b) Canevet, C.; Libman, J.; Shanzer, A. Molecular Redox-Switches by Ligand Exchange, *Angew. Chem. Int. Ed.* **1996**, *35*, 2657-2660.
(73) Samanta, S. K.; Rana, A.; Schmittel, M. Reversible Cargo Shipping between Orthogonal Stations of a Nanoscaffold Upon Redox Input, *Dalton Trans.* **2014**, *43*, 9438-9447.
(74) Fabbrizzi, L.; Foti, F.; Patroni, S.; Pallavicini, P.; Taglietti, A. A Sleeping Host Awoken by Its Guest: Recognition and Sensing of Imidazole-Containing Molecules Based on Double Cu^{2+} Translocation inside a Polyaza Macrocycle, *Angew. Chem. Int. Ed.* **2004**, *43*, 5073-5077.
(75) (a) Hardouin-Lerouge, M.; Hudhomme, P.; Salle, M. Molecular Clips and Tweezers Hosting Neutral Guests, *Chem. Soc. Rev.* **2011**, *40*, 30-43. (b) Leblond, J.; Petitjean, A. Molecular Tweezers: Concepts and Applications, *ChemPhysChem* **2011**, *12*, 1043-1051. (c) Valderrey, V.; Aragay, G.; Ballester, P. Porphyrin Tweezer Receptors: Binding Studies, Conformational Properties and Applications, *Coord. Chem. Rev.* **2014**, *258-259*, 137-156.
(76) Petitjean, A.; Khoury, R. G.; Kyritsakas, N.; Lehn, J.-M. Dynamic Devices. Shape Switching and Substrate Binding in Ion-Controlled Nanomechanical Molecular Tweezers, *J. Am. Chem. Soc.* **2004**, *126*, 6637-6647.
(77) Ulrich, S.; Lehn, J.-M. Adaptation and Optical Signal Generation in a Constitutional Dynamic Network, *Chem. Eur. J.* **2009**, *15*, 5640-5645.
(78) Ulrich, S.; Petitjean, A.; Lehn, J.-M. Metallo-Controlled Dynamic Molecular Tweezers: Design, Synthesis, and Self-Assembly by Metal-Ion Coordination, *Eur. J. Inorg. Chem.* **2010**, *2010*, 1913-1928.
(79) Yoon, H.; Lim, J. M.; Gee, H.-C.; Lee, C.-H.; Jeong, Y.-H.; Kim, D.; Jang, W.-D. A Porphyrin-Based Molecular Tweezer: Guest-Induced Switching of Forward and Backward Photoinduced Energy Transfer, *J. Am. Chem. Soc.* **2014**, *136*, 1672-1679.
(80) Wiester, M. J.; Braunschweig, A. B.; Yoo, H.; Mirkin, C. A. Solvent and Temperature Induced Switching between Structural Isomers of Rh^{I} Phosphinoalkyl Thioether (PS) Complexes, *Inorg. Chem.* **2010**, *49*, 7188-7196.
(81) Yoon, H. J.; Kuwabara, J.; Kim, J.-H.; Mirkin, C. A. Allosteric Supramolecular Triple-Layer Catalysts, *Science* **2010**, *330*, 66-69.
(82) Kinbara, K.; Muraoka, T.; Aida, T. Chiral Ferrocenes as Novel Rotary Modules for Molecular Machines, *Org. Biomol. Chem.* **2008**, *6*, 1871-1876.
(83) Muraoka, T.; Kinbara, K.; Kobayashi, Y.; Aida, T. Light-Driven Open−Close Motion of Chiral Molecular Scissors, *J. Am. Chem. Soc.* **2003**, *125*, 5612-5613.
(84) Muraoka, T.; Kinbara, K.; Aida, T. Reversible Operation of Chiral Molecular Scissors by Redox and UV Light, *Chem. Commun.* **2007**, 1441-1443.
(85) Muraoka, T.; Kinbara, K.; Aida, T. Mechanical Twisting of a Guest by a Photoresponsive Host, *Nature* **2006**, *440*, 512-515.
(86) Kai, H.; Nara, S.; Kinbara, K.; Aida, T. Toward Long-Distance Mechanical Communication: Studies on a Ternary Complex Interconnected by a Bridging Rotary Module, *J. Am. Chem. Soc.* **2008**, *130*, 6725-6727.
(87) Durola, F.; Rebek, J. The Ouroborand: A Cavitand with a Coordination-Driven Switching Device, *Angew. Chem. Int. Ed.* **2010**, *49*, 3189-3191.
(88) Schmittel, M.; De, S.; Pramanik, S. Reversible ON/OFF Nanoswitch for Organocatalysis: Mimicking the Locking and Unlocking Operation of CaMKII, *Angew. Chem. Int. Ed.* **2012**, *51*, 3832-3836.

(89) Pramanik, S.; De, S.; Schmittel, M. Bidirectional Chemical Communication between Nanomechanical Switches, *Angew. Chem. Int. Ed.* **2014**, *53*, 4709-4713.
(90) Pramanik, S.; De, S.; Schmittel, M. A Trio of Nanoswitches in Redox-Potential Controlled Communication, *Chem. Commun.* **2014**, *50*, 13254-13257.
(90) Pramanik, S.; De, S.; Schmittel, M. A Trio of Nanoswitches in Redox-Potential Controlled Communication, *Chem. Commun.* **2014**, *50*, 13254-13257.
(91) Muraoka, T.; Kinbara, K.; Aida, T. A Self-Locking Molecule Operative with a Photoresponsive Key, *J. Am. Chem. Soc.* **2006**, *128*, 11600-11605.
(92) (a) Kottas, G. S.; Clarke, L. I.; Horinek, D.; Michl, J. Artificial Molecular Rotors, *Chem. Rev.* **2005**, *105*, 1281-1376. (b) Michl, J.; Sykes, E. C. H. Molecular Rotors and Motors: Recent Advances and Future Challenges, *ACS Nano* **2009**, *3*, 1042-1048.
(93) (a) Kelly, T. R. Progress toward a Rationally Designed Molecular Motor†, *Acc. Chem. Res.* **2001**, *34*, 514-522. (b) Kelly, T. R.; Bowyer, M. C.; Bhaskar, K. V.; Bebbington, D.; Garcia, A.; Lang, F.; Kim, M. H.; Jette, M. P. A Molecular Brake, *J. Am. Chem. Soc.* **1994**, *116*, 3657-3658.
(94) Zhang, D.; Zhang, Q.; Su, J.; Tian, H. A Dual-Ion-Switched Molecular Brake Based on Ferrocene, *Chem. Commun.* **2009**, 1700-1702.
(95) Shinkai, S.; Ikeda, M.; Sugasaki, A.; Takeuchi, M. Positive Allosteric Systems Designed on Dynamic Supramolecular Scaffolds: Toward Switching and Amplification of Guest Affinity and Selectivity, *Acc. Chem. Res.* **2001**, *34*, 494-503.
(96) Ikeda, M.; Takeuchi, M.; Shinkai, S.; Tani, F.; Naruta, Y.; Sakamoto, S.; Yamaguchi, K. Allosteric Binding of an Ag^{+} Ion to Cerium(IV) Bis-Porphyrinates Enhances the Rotational Activity of Porphyrin Ligands, *Chem. Eur. J.* **2002**, *8*, 5541-5550.
(97) (a) Sugasaki, A.; Ikeda, M.; Takeuchi, M.; Robertson, A.; Shinkai, S. Efficient Chirality Transcription Utilizing a Cerium(IV) Double Decker Porphyrin: A Prototype for Development of a Molecular Memory System, *J. Chem. Soc. Perkin Trans. 1* **1999**, 3259-3264. (b) Takeuchi, M.; Imada, T.; Shinkai, S. A Strong Positive Allosteric Effect in the Molecular Recognition of Dicarboxylic Acids by a Cerium(IV) Bis[tetrakis(4-pyridyl)porphyrinate] Double Decker, *Angew. Chem. Int. Ed.* **1998**, *37*, 2096-2099.
(98) (a) Samanta, S. K.; Samanta, D.; Bats, J. W.; Schmittel, M. Dabco as a Dynamic Hinge between Cofacial Porphyrin Panels and Its Tumbling inside a Supramolecular Cavity, *J. Org. Chem.* **2011**, *76*, 7466-7473. (b) Samanta, S. K.; Schmittel, M. Four-Component Supramolecular Nanorotors, *J. Am. Chem. Soc.* **2013**, *135*, 18794-18797. (c) Samanta, S. K.; Bats, J. W.; Schmittel, M. A Five-Component Nanorotor with Speed Regulation, *Chem. Commun.* **2014**, *50*, 2364-2366.
(99) Nishikawa, M.; Kume, S.; Nishihara, H. Stimuli-Responsive Pyrimidine Ring Rotation in Copper Complexes for Switching Their Physical Properties, *Phys. Chem. Chem. Phys.* **2013**, *15*, 10549-10565.
(100) Nishikawa, M.; Nomoto, K.; Kume, S.; Nishihara, H. Reversible Copper(II)/(I) Electrochemical Potential Switching Driven by Visible Light-Induced Coordinated Ring Rotation, *J. Am. Chem. Soc.* **2012**, *134*, 10543-10553.
(101) (a) Kume, S.; Nomoto, K.; Kusamoto, T.; Nishihara, H. Intramolecular Electron Arrangement with a Rotative Trigger, *J. Am. Chem. Soc.* **2009**, *131*, 14198-14199. (b) Kume, S.; Nishihara, H. Synchronized Motion and Electron Transfer of a Redox-Active Rotor, *Dalton Trans.* **2011**, *40*, 2299-2305. (c) Kume, S.; Nishihara, H. Tuning-up and Driving a Redox-Active Rotor, *Chem. Commun.* **2011**, *47*, 415-417.
(102) (a) Ogi, S.; Ikeda, T.; Wakabayashi, R.; Shinkai, S.; Takeuchi, M. A Bevel-Gear-Shaped Rotor Bearing a Double-Decker Porphyrin Complex, *Chem. Eur. J.* **2010**, *16*, 8285-8290. (b) Ogi, S.; Ikeda, T.; Wakabayashi, R.; Shinkai, S.; Takeuchi, M. Mechanically Interlocked Porphyrin Gears Propagating Two Different Rotational Frequencies, *Eur. J. Org. Chem.* **2011**, *2011*, 1831-1836.

(103) Ikeda, M.; Takeuchi, M.; Shinkai, S.; Tani, F.; Naruta, Y. Synthesis of New Diaryl-Substituted Triple-Decker and Tetraaryl-Substituted Double-Decker Lanthanum(III) Porphyrins and Their Porphyrin Ring Rotational Speed as Compared with That of Double-Decker Cerium(IV) Porphyrins, *Bull. Chem. Soc. Jpn.* **2001**, *74*, 739-746.

(104) (a) van Dongen, S. F. M.; Cantekin, S.; Elemans, J. A. A. W.; Rowan, A. E.; Nolte, R. J. M. Functional Interlocked Systems, *Chem. Soc. Rev.* **2014**, *43*, 99-122. (b) Champin, B.; Mobian, P.; Sauvage, J.-P. Transition Metal Complexes as Molecular Machine Prototypes, *Chem. Soc. Rev.* **2007**, *36*, 358-366. (c) Saha, S.; Stoddart, J. F. Photo-Driven Molecular Devices, *Chem. Soc. Rev.* **2007**, *36*, 77-93. (d) Balzani, V.; Credi, A.; Silvi, S.; Venturi, M. Artificial Nanomachines Based on Interlocked Molecular Species: Recent Advances, *Chem. Soc. Rev.* **2006**, *35*, 1135-1149. (e) Durot, S.; Reviriego, F.; Sauvage, J.-P. Copper-Complexed Catenanes and Rotaxanes in Motion: 15 Years of Molecular Machines, *Dalton Trans.* **2010**, *39*, 10557-10570. (f) Sauvage, J.-P. Transition Metal-Containing Rotaxanes and Catenanes in Motion: Toward Molecular Machines and Motors, *Acc. Chem. Res.* **1998**, *31*, 611-619.

(105) (a) Fujita, M.; Ibukuro, F.; Hagihara, H.; Ogura, K. Quantitative Self-Assembly of a [2]Catenane from Two Preformed Molecular Rings, *Nature* **1994**, *367*, 720-723. (b) Fujita, M. Self-Assembly of [2]Catenanes Containing Metals in Their Backbones, *Acc. Chem. Res.* **1998**, *32*, 53-61.

(106) Fujita, M.; Ibukuro, F.; Yamaguchi, K.; Ogura, K. A Molecular Lock, *J. Am. Chem. Soc.* **1995**, *117*, 4175-4176.

(107) Yamashita, K.-i.; Kawano, M.; Fujita, M. Photoswitchable Molecular Lock. One-Way Catenation of a Pt(II)-Linked Coordination Ring Via the Photolabilization of a Pt(II)−Pyridine Bond, *J. Am. Chem. Soc.* **2007**, *129*, 1850-1851.

(108) Dietrich-Buchecker, C. O.; Sauvage, J. P.; Kintzinger, J. P. Une Nouvelle Famille De Molecules : Les Metallo-Catenanes, *Tetrahedron Lett.* **1983**, *24*, 5095-5098.

(109) Amabilino, D. B.; Dietrich-Buchecker, C. O.; Livoreil, A.; Pérez-García, L.; Sauvage, J.-P.; Stoddart, J. F. A Switchable Hybrid [2]-Catenane Based on Transition Metal Complexation and Π-Electron Donor−Acceptor Interactions, *J. Am. Chem. Soc.* **1996**, *118*, 3905-3913.

(110) Nakatani, Y.; Furusho, Y.; Yashima, E. Amidinium Carboxylate Salt Bridges as a Recognition Motif for Mechanically Interlocked Molecules: Synthesis of an Optically Active [2]Catenane and Control of Its Structure, *Angew. Chem. Int. Ed.* **2010**, *49*, 5463-5467.

(111) (a) Livoreil, A.; Dietrich-Buchecker, C. O.; Sauvage, J.-P. Electrochemically Triggered Swinging of a [2]-Catenate, *J. Am. Chem. Soc.* **1994**, *116*, 9399-9400. (b) Cárdenas, D. J.; Livoreil, A.; Sauvage, J.-P. Redox Control of the Ring-Gliding Motion in a Cu-Complexed Catenane: A Process Involving Three Distinct Geometries, *J. Am. Chem. Soc.* **1996**, *118*, 11980-11981.

(112) Korybut-Daszkiewicz, B.; Więckowska, A.; Bilewicz, R.; Domagała, S.; Woźniak, K. An Electrochemically Controlled Molecular Shuttle, *Angew. Chem. Int. Ed.* **2004**, *43*, 1668-1672.

(113) (a) Durham, B.; Walsh, J. L.; Carter, C. L.; Meyer, T. J. Synthetic Applications of Photosubstitution Reactions of Poly(Pyridyl) Complexes of Ruthenium(II), *Inorg. Chem.* **1980**, *19*, 860-865. (b) Laemmel, A.-C.; Collin, J.-P.; Sauvage, J.-P. Efficient and Selective Photochemical Labilization of a Given Bidentate Ligand in Mixed Ruthenium(II) Complexes of the $Ru(Phen)_2l^{2+}$ and $Ru(Bipy)_2l^{2+}$ Family (L = Sterically Hindering Chelate), *Eur. J. Inorg. Chem.* **1999**, *1999*, 383-386. (c) Garner, R. N.; Joyce, L. E.; Turro, C. Effect of Electronic Structure on the Photoinduced Ligand Exchange of Ru(II) Polypyridine Complexes, *Inorg. Chem.* **2011**, *50*, 4384-4391. (d) Unjaroen, D.; Kasper, J. B.; Browne, W. R. Reversible Photochromic Switching in a Ru(II) Polypyridyl Complex, *Dalton Trans.* **2014**, *43*, 16974-16976.

(114) Mobian, P.; Kern, J.-M.; Sauvage, J.-P. Light-Driven Machine Prototypes Based on Dissociative Excited States: Photoinduced Decoordination and Thermal Recoordination of a Ring in a Ruthenium(II)-Containing [2]Catenane, *Angew. Chem. Int. Ed.* **2004**, *43*, 2392-2395.

(115) (a) Raehm, L.; Kern, J.-M.; Sauvage, J.-P. A Transition Metal Containing Rotaxane in Motion: Electrochemically Induced Pirouetting of the Ring on the Threaded Dumbbell, *Chem. Eur. J.* **1999**, *5*, 3310-3317. (b) Weber, N.; Hamann, C.; Kern, J.-M.; Sauvage, J.-P. Synthesis of a Copper [3]Rotaxane Able to Function as an Electrochemically Driven Oscillatory Machine in Solution, and to Form Sams on a Metal Surface, *Inorg. Chem.* **2003**, *42*, 6780-6792. (c) Poleschak, I.; Kern, J.-M.; Sauvage, J.-P. A Copper-Complexed Rotaxane in Motion: Pirouetting of the Ring on the Millisecond Timescale, *Chem. Commun.* **2004**, 474-476. (d) Periyasamy, G.; Collin, J.-P.; Sauvage, J.-P.; Levine, R. D.; Remacle, F. Electrochemically Driven Sequential Machines: An Implementation of Copper Rotaxanes, *Chem. Eur. J.* **2009**, *15*, 1310-1313. (e) Létinois-Halbes, U.; Hanss, D.; Beierle, J. M.; Collin, J.-P.; Sauvage, J.-P. A Fast-Moving [2]Rotaxane Whose Stoppers Are Remote from the Copper Complex Core, *Org. Lett.* **2005**, *7*, 5753-5756.

(116) Coronado, E.; Gaviña, P.; Ponce, J.; Tatay, S. Fast Pirouetting Motion in a Pyridine Bisamine-Containing Copper-Complexed Rotaxane, *Chem. Eur. J.* **2014**, *20*, 6939-6950.

(117) (a) Collin, J.-P.; Durola, F.; Mobian, P.; Sauvage, J.-P. Pirouetting Copper(I)-Assembled Pseudo-Rotaxanes: Strong Influence of the Axle Structure on the Motion Rate, *Eur. J. Inorg. Chem.* **2007**, *2007*, 2420-2425. (b) Collin, J.-P.; Mobian, P.; Sauvage, J.-P.; Sour, A.; Yan, Y.-M.; Willner, I. Copper-Complexed Pirouetting [2]Pseudorotaxanes with Sulfur-Containing End-Groups Attached to the Thread: Synthesis, Electrochemical Studies, and Deposition on Gold Electrodes, *Aust. J. Chem.* **2009**, *62*, 1231-1237.

(118) (a) Linke, M.; Chambron, J.-C.; Heitz, V.; Sauvage, J.-P.; Semetey, V. Complete Rearrangement of a Multi-Porphyrinic Rotaxane by Metallation-Demetallation of the Central Coordination Site, *Chem. Commun.* **1998**, 2469-2470. (b) Linke, M.; Chambron, J.-C.; Heitz, V.; Sauvage, J.-P.; Encinas, S.; Barigelletti, F.; Flamigni, L. Multiporphyrinic Rotaxanes: Control of Intramolecular Electron Transfer Rate by Steering the Mutual Arrangement of the Chromophores, *J. Am. Chem. Soc.* **2000**, *122*, 11834-11844.

(119) Joosten, A.; Trolez, Y.; Collin, J.-P.; Heitz, V.; Sauvage, J.-P. Copper(I)-Assembled [3]Rotaxane Whose Two Rings Act as Flapping Wings, *J. Am. Chem. Soc.* **2012**, *134*, 1802-1809.

(120) Bruns, C. J.; Stoddart, J. F. Rotaxane-Based Molecular Muscles, *Acc. Chem. Res.* **2014**, *47*, 2186-2199.

(121) Niess, F.; Duplan, V.; Sauvage, J.-P. Molecular Muscles: From Species in Solution to Materials and Devices, *Chem. Lett.* **2014**, *43*, 964-974.

(122) (a) Durola, F.; Heitz, V.; Reviriego, F.; Roche, C.; Sauvage, J.-P.; Sour, A.; Trolez, Y. Cyclic [4]Rotaxanes Containing Two Parallel Porphyrinic Plates: Toward Switchable Molecular Receptors and Compressors, *Acc. Chem. Res.* **2014**, *47*, 633-645. (b) Collin, J.-P.; Durola, F.; Heitz, V.; Reviriego, F.; Sauvage, J.-P.; Trolez, Y. A Cyclic [4]Rotaxane That Behaves as a Switchable Molecular Receptor: Formation of a Rigid Scaffold from a Collapsed Structure by Complexation with Copper(I) Ions, *Angew. Chem. Int. Ed.* **2010**, *49*, 10172-10175. (c) Jiménez, M. C.; Dietrich-Buchecker, C.; Sauvage, J.-P. Towards Synthetic Molecular Muscles: Contraction and Stretching of a Linear Rotaxane Dimer, *Angew. Chem. Int. Ed.* **2000**, *39*, 3284-3287. (d) Collin, J.-P.; Frey, J.; Heitz, V.; Sauvage, J.-P.; Tock, C.; Allouche, L. Adjustable Receptor Based on a [3]Rotaxane Whose Two Threaded Rings Are Rigidly Attached to Two

Porphyrinic Plates: Synthesis and Complexation Studies, *J. Am. Chem. Soc.* **2009**, *131*, 5609-5620. (e) Frey, J.; Tock, C.; Collin, J.-P.; Heitz, V.; Sauvage, J.-P. A [3]Rotaxane with Two Porphyrinic Plates Acting as an Adaptable Receptor, *J. Am. Chem. Soc.* **2008**, *130*, 4592-4593.

(123) Yamada, Y.; Okamoto, M.; Furukawa, K.; Kato, T.; Tanaka, K. Switchable Intermolecular Communication in a Four-Fold Rotaxane, *Angew. Chem. Int. Ed.* **2012**, *51*, 709-713.

(124) Li, H.; Li, X.; Wu, Y.; Ågren, H.; Qu, D.-H. A Musclelike [2](2)Rotaxane: Synthesis, Performance, and Molecular Dynamics Simulations, *J. Org. Chem.* **2014**, *79*, 6996-7004.

(125) Du, G.; Moulin, E.; Jouault, N.; Buhler, E.; Giuseppone, N. Muscle-Like Supramolecular Polymers: Integrated Motion from Thousands of Molecular Machines, *Angew. Chem. Int. Ed.* **2012**, *51*, 12504-12508.

(126) Gao, C.; Ma, X.; Zhang, Q.; Wang, Q.; Qu, D.; Tian, H. A Light-Powered Stretch-Contraction Supramolecular System Based on Cobalt Coordinated [1]Rotaxane, *Org. Biomol. Chem.* **2011**, *9*, 1126-1132.

(127) Li, H.; Zhang, J.-N.; Zhou, W.; Zhang, H.; Zhang, Q.; Qu, D.-H.; Tian, H. Dual-Mode Operation of a Bistable [1]Rotaxane with a Fluorescence Signal, *Org. Lett.* **2013**, *15*, 3070-3073.

(128) Jiang, L.; Okano, J.; Orita, A.; Otera, J. Intermittent Molecular Shuttle as a Binary Switch, *Angew. Chem. Int. Ed.* **2004**, *43*, 2121-2124.

(129) (a) Collin, J.-P.; Durola, F.; Lux, J.; Sauvage, J.-P. A Rapidly Shuttling Copper-Complexed [2]Rotaxane with Three Different Chelating Groups in Its Axis, *Angew. Chem. Int. Ed.* **2009**, *48*, 8532-8535. (b) Durola, F.; Sauvage, J.-P. Fast Electrochemically Induced Translation of the Ring in a Copper-Complexed [2]Rotaxane: The Biisoquinoline Effect, *Angew. Chem. Int. Ed.* **2007**, *46*, 3537-3540. (c) Durola, F.; Lux, J.; Sauvage, J.-P. A Fast-Moving Copper-Based Molecular Shuttle: Synthesis and Dynamic Properties, *Chem. Eur. J.* **2009**, *15*, 4124-4134.

(130) Collin, J.-P.; Gavina, P.; Sauvage, J.-P. Electrochemically Induced Molecular Motions in Copper-Complexed Threaded Systems: From the Unstoppered Compound to the Semi-Rotaxane and the Fully Blocked Rotaxane, *New J. Chem.* **1997**, *21*, 525-528.

(131) Wozny, M.; Pawlowska, J.; Osior, A.; Swider, P.; Bilewicz, R.; Korybut-Daszkiewicz, B. An Electrochemically Switchable Foldamer - a Surprising Feature of a Rotaxane with Equivalent Stations, *Chem. Sci.* **2014**, *5*, 2836-2842.

(132) Wozny, M.; Pawlowska, J.; Tomczyk, K. M.; Bilewicz, R.; Korybut-Daszkiewicz, B. Potential-Controlled Rotaxane Molecular Shuttles Based on Electron-Deficient Macrocyclic Complexes, *Chem. Commun.* **2014**, *50*, 13718-13721.

(133) (a) Balzani, V.; Clemente-León, M.; Credi, A.; Ferrer, B.; Venturi, M.; Flood, A. H.; Stoddart, J. F. Autonomous Artificial Nanomotor Powered by Sunlight, *Proc. Natl. Acad. Sci. U. S. A.* **2006**, *103*, 1178-1183. (b) Ashton, P. R.; Ballardini, R.; Balzani, V.; Credi, A.; Dress, K. R.; Ishow, E.; Kleverlaan, C. J.; Kocian, O.; Preece, J. A.; Spencer, N.; Stoddart, J. F.; Venturi, M.; Wenger, S. A Photochemically Driven Molecular-Level Abacus, *Chem. Eur. J.* **2000**, *6*, 3558-3574. (c) Li, H.; Fahrenbach, A. C.; Coskun, A.; Zhu, Z.; Barin, G.; Zhao, Y.-L.; Botros, Y. Y.; Sauvage, J.-P.; Stoddart, J. F. A Light-Stimulated Molecular Switch Driven by Radical–Radical Interactions in Water, *Angew. Chem. Int. Ed.* **2011**, *50*, 6782-6788.

(134) Crowley, J. D.; Leigh, D. A.; Lusby, P. J.; McBurney, R. T.; Perret-Aebi, L.-E.; Petzold, C.; Slawin, A. M. Z.; Symes, M. D. A Switchable Palladium-Complexed Molecular Shuttle and Its Metastable Positional Isomers, *J. Am. Chem. Soc.* **2007**, *129*, 15085-15090.

(135) Beves, J. E.; Blanco, V.; Blight, B. A.; Carrillo, R.; D'Souza, D. M.; Howgego, D.; Leigh, D. A.; Slawin, A. M. Z.; Symes, M. D. Toward Metal Complexes That Can

Directionally Walk Along Tracks: Controlled Stepping of a Molecular Biped with a Palladium(II) Foot, *J. Am. Chem. Soc.* **2014**, *136*, 2094-2100.

(136) Zhou, W.; Li, J.; He, X.; Li, C.; Lv, J.; Li, Y.; Wang, S.; Liu, H.; Zhu, D. A Molecular Shuttle for Driving a Multilevel Fluorescence Switch, *Chem. Eur. J.* **2008**, *14*, 754-763.

(137) (a) Fiedler, D.; Bergman, R. G.; Raymond, K. N. Supramolecular Catalysis of a Unimolecular Transformation: Aza-Cope Rearrangement within a Self-Assembled Host, *Angew. Chem. Int. Ed.* **2004**, *43*, 6748-6751. (b) Yoshizawa, M.; Klosterman, J. K.; Fujita, M. Functional Molecular Flasks: New Properties and Reactions within Discrete, Self-Assembled Hosts, *Angew. Chem. Int. Ed.* **2009**, *48*, 3418-3438.

(138) (a) Fiedler, D.; Leung, D. H.; Bergman, R. G.; Raymond, K. N. Selective Molecular Recognition, C-H Bond Activation, and Catalysis in Nanoscale Reaction Vessels, *Acc. Chem. Res.* **2005**, *38*, 349-358. (b) Breiner, B.; Clegg, J. K.; Nitschke, J. R. Reactivity Modulation in Container Molecules, *Chem. Sci.* **2011**, *2*, 51-51.

(139) Lewis, J. E. M.; Gavey, E. L.; Cameron, S. A.; Crowley, J. D. Stimuli-Responsive Pd2l4 Metallosupramolecular Cages: Towards Targeted Cisplatin Drug Delivery, *Chem. Sci.* **2012**, *3*, 778-784.

(140) (a) Dube, H.; Ajami, D.; Rebek, J. Photochemical Control of Reversible Encapsulation, *Angew. Chem. Int. Ed.* **2010**, *49*, 3192-3195. (b) Dube, H.; Rebek, J. Selective Guest Exchange in Encapsulation Complexes Using Light of Different Wavelenghts, *Angew. Chem. Int. Ed.* **2012**, *51*, 3207-3210. (c) Klosterman, J. K.; Iwamura, M.; Tahara, T.; Fujita, M. Energy Transfer in a Mechanically Trapped Exciplex, *J. Am. Chem. Soc.* **2009**, *131*, 9478-9479.

(141) Clever, G. H.; Tashiro, S.; Shionoya, M. Light-Triggered Crystallization of a Molecular Host-Guest Complex, *J. Am. Chem. Soc.* **2010**, *132*, 9973-9975.

(142) (a) Yoshizawa, M.; Takeyama, Y.; Okano, T.; Fujita, M. Cavity-Directed Synthesis within a Self-Assembled Coordination Cage: Highly Selective [2+2] Cross-Photodimerization of Olefins, *J. Am. Chem. Soc.* **2003**, *125*, 3243-3247. (b) Nishioka, Y.; Yamaguchi, T.; Kawano, M.; Fujita, M. Asymmetric Olefin Cross Photoaddition in a Self-Assembled Host with Remote Chiral Auxiliaries, *J. Am. Chem. Soc.* **2008**, *130*, 8160-8161.

(143) Han, M.; Michel, R.; He, B.; Chen, Y.-S.; Stalke, D.; John, M.; Clever, G. H. Light-Triggered Guest Uptake and Release by a Photochromic Coordination Cage, *Angew. Chem. Int. Ed.* **2013**, *52*, 1319-1323.

(144) Han, M.; Engelhard, D. M.; Clever, G. H. Self-Assembled Coordination Cages Based on Banana-Shaped Ligands, *Chem. Soc. Rev.* **2014**, *43*, 1848-1860.

(145) Harris, K.; Fujita, D.; Fujita, M. Giant Hollow M_nL_{2n} Spherical Complexes: Structure, Functionalisation and Applications, *Chem. Commun.* **2013**, *49*, 6703-6712.

(146) Murase, T.; Sato, S.; Fujita, M. Switching the Interior Hydrophobicity of a Self-Assembled Spherical Complex through the Photoisomerization of Confined Azobenzene Chromophores, *Angew. Chem. Int. Ed.* **2007**, *46*, 5133-5136.

(147) Park, J.; Sun, L. B.; Chen, Y. P.; Perry, Z.; Zhou, H. C. Azobenzene-Functionalized Metal-Organic Polyhedra for the Optically Responsive Capture and Release of Guest Molecules, *Angew. Chem. Int. Ed.* **2014**, *53*, 5842-5846.

(148) Yoshizawa, M.; Miyagi, S.; Kawano, M.; Ishiguro, K.; Fujita, M. Alkane Oxidation Via Photochemical Excitation of a Self-Assembled Molecular Cage, *J. Am. Chem. Soc.* **2004**, *126*, 9172-9173.

(149) Murase, T.; Nishijima, Y.; Fujita, M. Unusual Photoreaction of Triquinacene within Self-Assembled Hosts, *Chem. Asian J.* **2012**, *7*, 826-829.

(150) Murase, T.; Takezawa, H.; Fujita, M. Photo-Driven Anti-Markovnikov Alkyne Hydration in Self-Assembled Hollow Complexes, *Chem. Commun.* **2011**, *47*, 10960-10962.

(151) Furutani, Y.; Kandori, H.; Kawano, M.; Nakabayashi, K.; Yoshizawa, M.; Fujita, M. In Situ Spectroscopic, Electrochemical, and Theoretical Studies of the Photoinduced Host-Guest Electron Transfer That Precedes Unusual Host-Mediated Alkane Photooxidation, *J. Am. Chem. Soc.* **2009**, *131*, 4764-4768.

(152) Hosoi, H.; Yamaguchi, S.; Tahara, T. Host to Guest Energy Transfer in a Self-Assembled Supramolecular Nanocage Observed by Picosecond Fluorescence Quenching, *Chem. Lett.* **2005**, *34*, 618-619.

(153) He, C.; Wang, J.; Zhao, L.; Liu, T.; Zhang, J.; Duan, C. A Photoactive Basket-Like Metal-Organic Tetragon Worked as an Enzymatic Molecular Flask for Light Driven H_2 Production, *Chem. Commun.* **2013**, *49*, 627-629.

(154) (a) Bivaud, S.; Balandier, J.-Y.; Chas, M.; Allain, M.; Goeb, S.; Sallé, M. A Metal-Directed Self-Assembled Electroactive Cage with Bis(pyrrolo)tetrathiafulvalene (BPTTF) Side Walls, *J. Am. Chem. Soc.* **2012**, *134*, 11968-11970. (b) Bivaud, S.; Goeb, S.; Croué, V.; Dron, P. I.; Allain, M.; Sallé, M. Self-Assembled Containers Based on Extended Tetrathiafulvalene, *J. Am. Chem. Soc.* **2013**, *135*, 10018-10021. (c) Bivaud, S.; Goeb, S.; Balandier, J.-Y.; Chas, M.; Allain, M.; Sallé, M. Self-Assembled Cages from the Electroactive Bis(pyrrolo)tetrathiafulvalene (BPTTF) Building Block, *Eur. J. Inorg. Chem.* **2014**, *2014*, 2440-2448. (d) Vajpayee, V.; Bivaud, S.; Goeb, S.; Croué, V.; Allain, M.; Popp, B. V.; Garci, A.; Therrien, B.; Sallé, M. Electron-Rich Arene–Ruthenium Metalla-Architectures Incorporating Tetrapyridyl–Tetrathiafulvene Donor Moieties, *Organometallics* **2014**, *33*, 1651-1658.

(155) Mahata, K.; Frischmann, P. D.; Würthner, F. Giant Electroactive M_4L_6 Tetrahedral Host Self-Assembled with Fe(II) Vertices and Perylene Bisimide Dye Edges, *J. Am. Chem. Soc.* **2013**, *135*, 15656-15661.

(156) Frank, M.; Hey, J.; Balcioglu, I.; Chen, Y.-S.; Stalke, D.; Suenobu, T.; Fukuzumi, S.; Frauendorf, H.; Clever, G. H. Assembly and Stepwise Oxidation of Interpenetrated Coordination Cages Based on Phenothiazine, *Angew. Chem. Int. Ed.* **2013**, *52*, 10102-10106.

(157) (a) Mal, P.; Schultz, D.; Beyeh, K.; Rissanen, K.; Nitschke, J. R. An Unlockable-Relockable Iron Cage by Subcomponent Self-Assembly, *Angew. Chem. Int. Ed.* **2008**, *47*, 8297-8301. (b) Mal, P.; Breiner, B.; Rissanen, K.; Nitschke, J. R. White Phosphorus Is Air-Stable within a Self-Assembled Tetrahedral Capsule, *Science* **2009**, *324*, 1697-1699. (c) Riddell, I. A.; Smulders, M. M. J.; Clegg, J. K.; Nitschke, J. R. Encapsulation, Storage and Controlled Release of Sulfur Hexafluoride from a Metal-Organic Capsule, *Chem. Commun.* **2011**, *47*, 457-459.

(158) Yi, S.; Brega, V.; Captain, B.; Kaifer, A. E. Sulfate-Templated Self-Assembly of New M_4L_6 Tetrahedral Metal Organic Cages, *Chem. Commun.* **2012**, *48*, 10295-10297.

(159) Hiraoka, S.; Sakata, Y.; Shionoya, M. Ti(IV)-Centered Dynamic Interconversion between Pd(II), Ti(IV)-Containing Ring and Cage Molecules, *J. Am. Chem. Soc.* **2008**, *130*, 10058-10059.

(160) (a) Pike, S. J.; Lusby, P. J. Dual Stimuli-Responsive Interconvertible Heteroleptic Platinum Coordination Modes, *Chem. Commun.* **2010**, *46*, 8338-8340. (b) Lusby, P. J.; Müller, P.; Pike, S. J.; Slawin, A. M. Z. Stimuli-Responsive Reversible Assembly of 2D and 3D Metallosupramolecular Architectures, *J. Am. Chem. Soc.* **2009**, *131*, 16398-16400.

(161) Saalfrank, R. W.; Maid, H.; Scheurer, A.; Heinemann, F. W.; Puchta, R.; Bauer, W.; Stern, D.; Stalke, D. Template and pH-Mediated Synthesis of Tetrahedral Indium Complexes

(161) Saalfrank, R. W.; Maid, H.; Scheurer, A.; Heinemann, F. W.; Puchta, R.; Bauer, W.; Stern, D.; Stalke, D. Template and pH-Mediated Synthesis of Tetrahedral Indium Complexes $[Cs\subset\{In_4(L)_4\}]^+$ and $[In_4(H(^N)L)_4]^{4+}$: Breaking the Symmetry of N-Centered C_3 $(L)^{3-}$ to Give Neutral $[In_4(L)_4]$, *Angew. Chem. Int. Ed.* **2008**, *47*, 8941-8945.

(162) Scherer, M.; Caulder, D. L.; Johnson, D. W.; Raymond, K. N. Triple Helicate—Tetrahedral Cluster Interconversion Controlled by Host-Guest Interactions, *Angew. Chem. Int. Ed.* **1999**, *38*, 1587-1592.
(163) Fujita, N.; Biradha, K.; Fujita, M.; Sakamoto, S.; Yamaguchi, K. A Porphyrin Prism: Structural Switching Triggered by Guest Inclusion, *Angew. Chem. Int. Ed.* **2001**, *40*, 1718-1721.
(164) Ramsay, W. J.; Ronson, T. K.; Clegg, J. K.; Nitschke, J. R. Bidirectional Regulation of Halide Binding in a Heterometallic Supramolecular Cube, *Angew. Chem. Int. Ed.* **2013**, *52*, 13439-13443.
(165) Ramsay, W. J.; Nitschke, J. R. Two Distinct Allosteric Active Sites Regulate Guest Binding within a $Fe_8Mo_{12}^{16+}$ Cubic Receptor, *J. Am. Chem. Soc.* **2014**, *136*, 7038-7043.
(166) Hiraoka, S.; Yi, T.; Shiro, M.; Shionoya, M. Triangular and Tetrahedral Array of Silver(I) Ions by a Novel Disk-Shaped Tridentate Ligand: Dynamic Control of Coordination Equilibrium of the Silver(I) Complexes, *J. Am. Chem. Soc.* **2002**, *124*, 14510-14511.
(167) Riddell, I. A.; Smulders, M. M. J.; Clegg, J. K.; Hristova, Y. R.; Breiner, B.; Thoburn, J. D.; Nitschke, J. R. Anion-Induced Reconstitution of a Self-Assembling System to Express a Chloride-Binding $Co_{10}L_{15}$ Pentagonal Prism, *Nat. Chem.* **2012**, *4*, 751-756.
(168) (a) Riddell, I. A.; Hristova, Y. R.; Clegg, J. K.; Wood, C. S.; Breiner, B.; Nitschke, J. R. Five Discrete Multinuclear Metal-Organic Assemblies from One Ligand: Deciphering the Effects of Different Templates, *J. Am. Chem. Soc.* **2013**, *135*, 2723-2733. (b) Riddell, I. A.; Ronson, T. K.; Clegg, J. K.; Wood, C. S.; Bilbeisi, R. A.; Nitschke, J. R. Cation- and Anion-Exchanges Induce Multiple Distinct Rearrangements within Metallosupramolecular Architectures, *J. Am. Chem. Soc.* **2014**, *136*, 9491-9498.
(169) Meng, W.; Ronson, T. K.; Clegg, J. K.; Nitschke, J. R. Transformations within a Network of Cadmium Architectures, *Angew. Chem. Int. Ed.* **2013**, *52*, 1017-1021.
(170) Freye, S.; Michel, R.; Stalke, D.; Pawliczek, M.; Frauendorf, H.; Clever, G. H. Template Control over Dimerization and Guest Selectivity of Interpenetrated Coordination Cages, *J. Am. Chem. Soc.* **2013**, *135*, 8476-8479.
(171) Sekiya, R.; Fukuda, M.; Kuroda, R. Anion-Directed Formation and Degradation of an Interlocked Metallohelicate, *J. Am. Chem. Soc.* **2012**, *134*, 10987-10997.
(172) Clegg, J. K.; Cremers, J.; Hogben, A. J.; Breiner, B.; Smulders, M. M. J.; Thoburn, J. D.; Nitschke, J. R. A Stimuli Responsive System of Self-Assembled Anion-Binding $Fe_4L_6^{8+}$ Cages, *Chem. Sci.* **2013**, *4*, 68-76.
(173) Henkelis, J. J.; Fisher, J.; Warriner, S. L.; Hardie, M. J. Solvent-Dependent Self-Assembly Behaviour and Speciation Control of Pd_6L_8 Metallo-Supramolecular Cages, *Chem. Eur. J.* **2014**, *20*, 4117-4125.
(174) Li, J.-R.; Zhou, H.-C. Bridging-Ligand-Substitution Strategy for the Preparation of Metal-Organic Polyhedra, *Nat. Chem.* **2010**, *2*, 893-898.
(175) Zheng, Y.-R.; Lan, W.-J.; Wang, M.; Cook, T. R.; Stang, P. J. Designed Post-Self-Assembly Structural and Functional Modifications of a Truncated Tetrahedron, *J. Am. Chem. Soc.* **2011**, *133*, 17045-17055.
(176) Mendez-Arroyo, J.; Barroso-Flores, J.; Lifschitz, A. M.; Sarjeant, A. A.; Stern, C. L.; Mirkin, C. A. A Multi-State, Allosterically-Regulated Molecular Receptor with Switchable Selectivity, *J. Am. Chem. Soc.* **2014**, *136*, 10340-10348.
(177) Harano, K.; Hiraoka, S.; Shionoya, M. 3 Nm-Scale Molecular Switching between Fluorescent Coordination Capsule and Nonfluorescent Cage, *J. Am. Chem. Soc.* **2007**, *129*, 5300-5301.
(178) Hiraoka, S.; Harano, K.; Shiro, M.; Shionoya, M. Quantitative Dynamic Interconversion between Ag^{I}-Mediated Capsule and Cage Complexes Accompanying Guest Encapsulation/Release, *Angew. Chem. Int. Ed.* **2005**, *44*, 2727-2731.
(179) Kishi, N.; Akita, M.; Yoshizawa, M. Selective Host-Guest Interactions of a Transformable Coordination Capsule/Tube with Fullerenes, *Angew. Chem. Int. Ed.* **2014**, *53*, 3604-3607.
(180) Sun, Q.-f.; Sato, S.; Fujita, M. An $M_{18}L_{24}$ Stellated Cuboctahedron through Post-Stellation of an $M_{12}L_{24}$ Core, *Nat. Chem.* **2012**, *4*, 330-333.
(181) Bandi, S.; Pal, A. K.; Hanan, G. S.; Chand, D. K. Stoichiometrically Controlled Revocable Self-Assembled "Spiro" Versus Quadruple-Stranded "Double-Decker" Type Coordination Cages, *Chem. Eur. J.* **2014**, 1-6.

(182) Sørensen, A.; Castilla, A. M.; Ronson, T. K.; Pittelkow, M.; Nitschke, J. R. Chemical Signals Turn on Guest Binding through Structural Reconfiguration of Triangular Helicates, *Angew. Chem. Int. Ed.* **2013**, *52*, 11273-11277.
(183) Hristova, Y. R.; Smulders, M. M. J.; Clegg, J. K.; Breiner, B.; Nitschke, J. R. Selective Anion Binding by a "Chameleon" Capsule with a Dynamically Reconfigurable Exterior, *Chem. Sci.* **2011**, *2*, 638.
(184) (a) Castilla, A. M.; Ramsay, W. J.; Nitschke, J. R. Stereochemistry in Subcomponent Self-Assembly, *Acc. Chem. Res.* **2014**, *47*, 2063-2073. (b) Castilla, A. M.; Ramsay, W. J.; Nitschke, J. R. Stereochemical Communication within Tetrahedral Capsules, *Chem. Lett.* **2014**, *43*, 256-263.
(185) Jiménez, A.; Bilbeisi, R. A.; Ronson, T. K.; Zarra, S.; Woodhead, C.; Nitschke, J. R. Selective Encapsulation and Sequential Release of Guests within a Self-Sorting Mixture of Three Tetrahedral Cages, *Angew. Chem. Int. Ed.* **2014**, *53*, 4556-4560.
(186) Zhou, X.-P.; Wu, Y.; Li, D. Polyhedral Metal-Imidazolate Cages: Control of Self-Assembly and Cage to Cage Transformation, *J. Am. Chem. Soc.* **2013**, *135*, 16062-16065.
(187) Fan, J.; Saha, M. L.; Song, B.; Schönherr, H.; Schmittel, M. Preparation of a Poly-Nanocage Dynamer: Correlating the Growth of Polymer Strands Using Constitutional Dynamic Chemistry and Heteroleptic Aggregation, *J. Am. Chem. Soc.* **2011**, *134*, 150-153.
(188) Nakamura, T.; Ube, H.; Miyake, R.; Shionoya, M. A C_{60}-Templated Tetrameric Porphyrin Barrel Complex Via Zinc-Mediated Self-Assembly Utilizing Labile Capping Ligands, *J. Am. Chem. Soc.* **2013**, *135*, 18790-18793.
(189) Stephenson, A.; Argent, S. P.; Riis-Johannessen, T.; Tidmarsh, I. S.; Ward, M. D. Structures and Dynamic Behavior of Large Polyhedral Coordination Cages: An Unusual Cage-to-Cage Interconversion, *J. Am. Chem. Soc.* **2011**, *133*, 858-870.
(190) Suzuki, K.; Kawano, M.; Fujita, M. Solvato-Controlled Assembly of Pd_3L_6 and Pd_4L_8 Coordination "Boxes", *Angew. Chem. Int. Ed.* **2007**, *46*, 2819-2822.
(191) Kilbas, B.; Mirtschin, S.; Scopelliti, R.; Severin, K. A Solvent-Responsive Coordination Cage, *Chem. Sci.* **2012**, *3*, 701-701.
(192) Aimi, J.; Nagamine, Y.; Tsuda, A.; Muranaka, A.; Uchiyama, M.; Aida, T. "Conformational" Solvatochromism: Spatial Discrimination of Nonpolar Solvents by Using a Supramolecular Box of a π-Conjugated Zinc Bisporphyrin Rotamer, *Angew. Chem. Int. Ed.* **2008**, *47*, 5153-5156.
(193) Zarra, S.; Clegg, J. K.; Nitschke, J. R. Selective Assembly and Disassembly of a Water-Soluble $Fe_{10}L_{15}$ Prism, *Angew. Chem. Int. Ed.* **2013**, *52*, 4837-4840.
(194) Chen, Q.; Jiang, F.; Yuan, D.; Lyu, G.; Chen, L.; Hong, M. A Controllable and Dynamic Assembly System Based on Discrete Metallocages, *Chem. Sci.* **2014**, *5*, 483-488.
(195) Han, M.; Hey, J.; Kawamura, W.; Stalke, D.; Shionoya, M.; Clever, G. H. An Inclusion Complex of Hexamolybdate inside a Supramolecular Cage and Its Structural Conversion, *Inorg. Chem.* **2012**, *51*, 9574-9576.
(196) Liu, T.-F.; Chen, Y.-P.; Yakovenko, A. a.; Zhou, H.-C. Interconversion between Discrete and a Chain of Nanocages: Self-Assembly Via a Solvent-Driven, Dimension-Augmentation Strategy, *J. Am. Chem. Soc.* **2012**, *134*, 17358-17361.
(197) *Frontiers in Transition Metal-Containing Polymers*; Abd-El-Aziz, A. S.; Manners, I., Eds.; John Wiley & Sons, Inc., 2006.
(198) (a) Whittell, G. R.; Hager, M. D.; Schubert, U. S.; Manners, I. Functional Soft Materials from Metallopolymers and Metallosupramolecular Polymers, *Nat. Mater.* **2011**, *10*, 176-188. (b) Wojtecki, R. J.; Meador, M. A.; Rowan, S. J. Using the Dynamic Bond to Access Macroscopically Responsive Structurally Dynamic Polymers, *Nat. Mater.* **2011**, *10*, 14-27. (c) Eloi, J.-C.; Chabanne, L.; Whittell, G. R.; Manners, I. Metallopolymers with Emerging Applications, *Mater. Today* **2008**, *11*, 28-36.
(199) (a) Xu, L.; Chen, L.-J.; Yang, H.-B. Recent Progress in the Construction of Cavity-Cored Supramolecular Metallodendrimers Via Coordination-Driven Self-Assembly, *Chem. Commun.* **2014**, *50*, 5156-5170. (b) Zhao, G.-Z.; Chen, L.-J.; Wang, W.; Zhang, J.; Yang, G.; Wang, D.-X.; Yu, Y.; Yang, H.-B. Stimuli-Responsive Supramolecular Gels through Hierarchical Self-Assembly of Discrete Rhomboidal Metallacycles, *Chem. Eur. J.* **2013**, *19*, 10094-10100.

(200) Wu, N.-W.; Chen, L.-J.; Wang, C.; Ren, Y.-Y.; Li, X.; Xu, L.; Yang, H.-B. Hierarchical Self-Assembly of a Discrete Hexagonal Metallacycle into the Ordered Nanofibers and Stimuli-Responsive Supramolecular Gels, *Chem. Commun.* **2014**, *50*, 4231-4233.

(201) Chen, L.-J.; Zhao, G.-Z.; Jiang, B.; Sun, B.; Wang, M.; Xu, L.; He, J.; Abliz, Z.; Tan, H.; Li, X.; Yang, H.-B. Smart Stimuli-Responsive Spherical Nanostructures Constructed from Supramolecular Metallodendrimers Via Hierarchical Self-Assembly, *J. Am. Chem. Soc.* **2014**, *136*, 5993-6001.

(202) Zhang, J.; Marega, R.; Chen, L.-J.; Wu, N.-W.; Xu, X.-D.; Muddiman, D. C.; Bonifazi, D.; Yang, H.-B. Hierarchical Self-Assembly of Supramolecular Hydrophobic Metallacycles into Ordered Nanostructures, *Chem. Asian J.* **2014**, *9*, 2928-2936.

(203) Li, Z.-Y.; Xu, L.; Wang, C.-H.; Zhao, X.-L.; Yang, H.-B. Novel Platinum-Acetylide Metallocycles Constructed Via a Stepwise Fragment Coupling Approach and Their Aggregation Behaviour, *Chem. Commun.* **2013**, *49*, 6194-6196.

(204) Yan, X.; Li, S.; Pollock, J. B.; Cook, T. R.; Chen, J.; Zhang, Y.; Ji, X.; Yu, Y.; Huang, F.; Stang, P. J. Supramolecular Polymers with Tunable Topologies Via Hierarchical Coordination-Driven Self-Assembly and Hydrogen Bonding Interfaces, *Proc. Natl. Acad. Sci. U. S. A.* **2013**, *110*, 15585-15590.

(205) Yan, X.; Jiang, B.; Cook, T. R.; Zhang, Y.; Li, J.; Yu, Y.; Huang, F.; Yang, H.-B.; Stang, P. J. Dendronized Organoplatinum(II) Metallacyclic Polymers Constructed by Hierarchical Coordination-Driven Self-Assembly and Hydrogen-Bonding Interfaces, *J. Am. Chem. Soc.* **2013**, *135*, 16813-16816.

(206) Yan, X.; Li, S.; Cook, T. R.; Ji, X.; Yao, Y.; Pollock, J. B.; Shi, Y.; Yu, G.; Li, J.; Huang, F.; Stang, P. J. Hierarchical Self-Assembly: Well-Defined Supramolecular Nanostructures and Metallohydrogels Via Amphiphilic Discrete Organoplatinum(II) Metallacycles, *J. Am. Chem. Soc.* **2013**, *135*, 14036-14039.

(207) Yan, X.; Cook, T. R.; Pollock, J. B.; Wei, P.; Zhang, Y.; Yu, Y.; Huang, F.; Stang, P. J. Responsive Supramolecular Polymer Metallogel Constructed by Orthogonal Coordination-Driven Self-Assembly and Host/Guest Interactions, *J. Am. Chem. Soc.* **2014**, *136*, 4460-4463.

(208) Lu, W.; Chen, Y.; Roy, V. A. L.; Chui, S. S.-Y.; Che, C.-M. Supramolecular Polymers and Chromonic Mesophases Self-Organized from Phosphorescent Cationic Organoplatinum(II) Complexes in Water, *Angew. Chem. Int. Ed.* **2009**, *48*, 7621-7625.

(209) Xiao, X.-S.; Lu, W.; Che, C.-M. Phosphorescent Nematic Hydrogels and Chromonic Mesophases Driven by Intra- and Intermolecular Interactions of Bridged Dinuclear Cyclometalated Platinum(II) Complexes, *Chem. Sci.* **2014**, *5*, 2482-2488.

(210) Yan, X.; Xu, J.-F.; Cook, T. R.; Huang, F.; Yang, Q.-Z.; Tung, C.-H.; Stang, P. J. Photoinduced Transformations of Stiff-Stilbene-Based Discrete Metallacycles to Metallosupramolecular Polymers, *Proc. Natl. Acad. Sci. U. S. A.* **2014**, *111*, 8717-8722.

(211) Li, Z.-Y.; Zhang, Y.; Zhang, C.-W.; Chen, L.-J.; Wang, C.; Tan, H.; Yu, Y.; Li, X.; Yang, H.-B. Cross-Linked Supramolecular Polymer Gels Constructed from Discrete Multi-Pillar[5]Arene Metallacycles and Their Multiple Stimuli-Responsive Behavior, *J. Am. Chem. Soc.* **2014**, *136*, 8577-8589.

(212) (a) Hu, X.-Y.; Xiao, T.; Lin, C.; Huang, F.; Wang, L. Dynamic Supramolecular Complexes Constructed by Orthogonal Self-Assembly, *Acc. Chem. Res.* **2014**, *47*, 2041-2051. (b) Qi, Z.; Schalley, C. A. Exploring Macrocycles in Functional Supramolecular Gels: From Stimuli Responsiveness to Systems Chemistry, *Acc. Chem. Res.* **2014**, *47*, 2222-2233. (c) Tam, A. Y.-Y.; Yam, V. W.-W. Recent Advances in Metallogels, *Chem. Soc. Rev.* **2013**, *42*, 1540-1567. (d) Wong, K. M.-C.; Chan, M. M.-Y.; Yam, V. W.-W. Supramolecular Assembly of Metal-Ligand Chromophores for Sensing and Phosphorescent OLED Applications, *Adv. Mater.* **2014**, *26*, 5558-5568. (e) Zhou, J.; Whittell, G. R.; Manners, I. Metalloblock Copolymers: New Functional Nanomaterials, *Macromolecules* **2014**, *47*, 3529-3543. (f) Higuchi, M. Stimuli-Responsive Metallo-Supramolecular Polymer Films: Design, Synthesis and Device Fabrication, *J. Mater. Chem. C* **2014**, *2*, 9331-9341. (g) Brassinne, J.; Fustin, C.-A.; Gohy, J.-F. Polymer Gels Constructed through Metal–Ligand Coordination, *J. Inorg. Organomet. Polym. Mater.* **2013**, *23*, 24-40. (h) Burnworth, M.; Knapton, D.; Rowan, S.; Weder, C. Metallo-Supramolecular Polymerization: A Route to Easy-to-Process Organic/Inorganic Hybrid Materials, *J. Inorg. Organomet. Polym. Mater.* **2007**, *17*, 91-103. (i) Friese, V. A.; Kurth, D. G. From Coordination Complexes to Coordination Polymers through Self-Assembly,

Curr. Opin. Colloid Interface Sci. **2009**, *14*, 81-93. (j) Moughton, A. O.; O'Reilly, R. K. Using Metallo-Supramolecular Block Copolymers for the Synthesis of Higher Order Nanostructured Assemblies, *Macromol. Rapid Commun.* **2010**, *31*, 37-52. (k) Dobrawa, R.; Würthner, F. Metallosupramolecular Approach toward Functional Coordination Polymers, *J. Polym. Sci. A: Polym. Chem.* **2005**, *43*, 4981-4995. (l) Su, X.; Aprahamian, I. Hydrazone-Based Switches, Metallo-Assemblies and Sensors, *Chem. Soc. Rev.* **2014**, *43*, 1963-1981.

(213) (a) Burnworth, M.; Tang, L.; Kumpfer, J. R.; Duncan, A. J.; Beyer, F. L.; Fiore, G. L.; Rowan, S. J.; Weder, C. Optically Healable Supramolecular Polymers, *Nature* **2011**, *472*, 334-337. (b) Fiore, G. L.; Rowan, S. J.; Weder, C. Optically Healable Polymers, *Chem. Soc. Rev.* **2013**, *42*, 7278-7288.

(214) Kumpfer, J. R.; Rowan, S. J. Thermo-, Photo-, and Chemo-Responsive Shape-Memory Properties from Photo-Cross-Linked Metallo-Supramolecular Polymers, *J. Am. Chem. Soc.* **2011**, *133*, 12866-12874.

(215) Wang, Z.; Fan, W.; Tong, R.; Lu, X.; Xia, H. Thermal-Healable and Shape Memory Metallosupramolecular Poly(N-Butyl Acrylate-co-Methyl Methacrylate) Materials, *RSC Adv.* **2014**, *4*, 25486-25493.

(216) (a) Housecroft, C. E. 4,2':6',4''-Terpyridines: Diverging and Diverse Building Blocks in Coordination Polymers and Metallomacrocycles, *Dalton Trans.* **2014**, *43*, 6594-6604. (b) Chiper, M.; Hoogenboom, R.; Schubert, U. S. Toward Main Chain Metallo-Terpyridyl Supramolecular Polymers: "The Metal Does the Trick", *Macromol. Rapid Commun.* **2009**, *30*, 565-578. (c) Schwarz, G.; Haßlauer, I.; Kurth, D. G. From Terpyridine-Based Assemblies to Metallo-Supramolecular Polyelectrolytes (MEPEs), *Adv. Colloid Interface Sci.* **2014**, *207*, 107-120.

(217) Moulin, E.; Niess, F.; Fuks, G.; Jouault, N.; Buhler, E.; Giuseppone, N. Light-Triggered Self-Assembly of Triarylamine-Based Nanospheres, *Nanoscale* **2012**, *4*, 6748-6751.

(218) Köytepe, S.; Demirel, M. H.; Gültek, A.; Seçkin, T. Metallo-Supramolecular Materials Based on Terpyridine-Functionalized Polyhedral Silsesquioxane, *Polym. Int.* **2014**, *63*, 778-787.

(219) Demirel, M.; Köytepe, S.; Gültek, A.; Seçkin, T. Synthesis and Stimuli-Responsive Properties of the Phenanthroline Based Metallo-Supramolecular Polymers, *J. Polym. Res.* **2014**, *21*, 345.

(220) Köytepe, S.; Demirel, M. H.; Seçkin, T. Synthesis and Self-Assembling Properties of 2,2′:6′,2″-Terpyridine-Based Carbon Nanotube Coordination Polymers, *J. Inorg. Organomet. Polym. Mater.* **2013**, *23*, 1104-1112.

(221) Bozdemir, Ö. A.; Büyükcakir, O.; Akkaya, E. U. Novel Molecular Building Blocks Based on the Boradiazaindacene Chromophore: Applications in Fluorescent Metallosupramolecular Coordination Polymers, *Chem. Eur. J.* **2009**, *15*, 3830-3838.

(222) Gasnier, A.; Barbe, J.-M.; Bucher, C.; Denat, F.; Moutet, J.-C.; Saint-Aman, E.; Terech, P.; Royal, G. Acid–Base-Driven Interconversion between a Mononuclear Complex and Supramolecular Coordination Polymers in a Terpyridine-Functionalized Dioxocyclam Ligand, *Inorg. Chem.* **2008**, *47*, 1862-1864.

(223) Gasnier, A. l.; Barbe, J.-M.; Bucher, C.; Duboc, C.; Moutet, J.-C.; Saint-Aman, E.; Terech, P.; Royal, G. Soluble Heterometallic Coordination Polymers Based on a Bis-Terpyridine-Functionalized Dioxocyclam Ligand, *Inorg. Chem.* **2010**, *49*, 2592-2599.

(224) (a) Gasnier, A.; Royal, G.; Terech, P. Metallo-Supramolecular Gels Based on a Multitopic Cyclam Bis-Terpyridine Platform, *Langmuir* **2009**, *25*, 8751-8762. (b) Gasnier, A.; Bucher, C.; Moutet, J.-C.; Royal, G.; Saint-Aman, E.; Terech, P. Redox-Responsive Metallo-Supramolecular Polymers and Gels Containing Bis-Terpyridine Appended Cyclam Ligand, *Macromol. Symp.* **2011**, *304*, 87-92.

(225) Asoh, T.-A.; Yoshitake, H.; Takano, Y.; Kikuchi, A. Fabrication of Self-Healable Hydrogels through Sol–Gel Transition in Metallo-Supramolecular Aqueous Solution by Aeration, *Macromol. Chem. Phys.* **2013**, *214*, 2534-2539.

(226) Miller, A. K.; Li, Z.; Streletzky, K. A.; Jamieson, A. M.; Rowan, S. J. Redox-Induced Polymerisation/Depolymerisation of Metallo-Supramolecular Polymers, *Polym. Chem.* **2012**, *3*, 3132-3138.

(227) Sato, T.; Ebara, M.; Tanaka, S.; Asoh, T.-A.; Kikuchi, A.; Aoyagi, T. Rapid Self-Healable Poly(Ethylene Glycol) Hydrogels Formed by Selective Metal-Phosphate Interactions, *Phys. Chem. Chem. Phys.* **2013**, *15*, 10628-10635.

(228) (a) Beck, J. B.; Rowan, S. J. Multistimuli, Multiresponsive Metallo-Supramolecular Polymers, *J. Am. Chem. Soc.* **2003**, *125*, 13922-13923. (b) Zhao, Y.; Beck, J. B.; Rowan, S. J.; Jamieson, A. M. Rheological Behavior of Shear-Responsive Metallo-Supramolecular Gels, *Macromolecules* **2004**, *37*, 3529-3531. (c) Rowan, S. J.; Beck, J. B. Metal-Ligand Induced Supramolecular Polymerization: A Route to Responsive Materials, *Faraday Discuss.* **2005**, *128*, 43-53.

(229) (a) Weng, W.; Beck, J. B.; Jamieson, A. M.; Rowan, S. J. Understanding the Mechanism of Gelation and Stimuli-Responsive Nature of a Class of Metallo-Supramolecular Gels, *J. Am. Chem. Soc.* **2006**, *128*, 11663-11672. (b) Weng, W.; Li, Z.; Jamieson, A. M.; Rowan, S. J. Control of Gel Morphology and Properties of a Class of Metallo-Supramolecular Polymers by Good/Poor Solvent Environments, *Macromolecules* **2008**, *42*, 236-246.

(230) (a) Burnworth, M.; Mendez, J. D.; Schroeter, M.; Rowan, S. J.; Weder, C. Decoupling Optical Properties in Metallo-Supramolecular Poly(*p*-phenyleneethynylene)s, *Macromolecules* **2008**, *41*, 2157-2163. (b) Kumpfer, J. R.; Jin, J.; Rowan, S. J. Stimuli-Responsive Europium-Containing Metallo-Supramolecular Polymers, *J. Mater. Chem.* **2010**, *20*, 145-151. (c) Weng, W.; Li, Z.; Jamieson, A. M.; Rowan, S. J. Effect of Monomer Structure on the Gelation of a Class of Metallo-Supramolecular Polymers, *Soft Matter* **2009**, *5*, 4647-4657.

(231) (a) Yuan, J.; Fang, X.; Zhang, L.; Hong, G.; Lin, Y.; Zheng, Q.; Xu, Y.; Ruan, Y.; Weng, W.; Xia, H.; Chen, G. Multi-Responsive Self-Healing Metallo-Supramolecular Gels Based on "Click" Ligand, *J. Mater. Chem.* **2012**, *22*, 11515-11522. (b) Yuan, J.; Zhang, H.; Hong, G.; Chen, Y.; Chen, G.; Xu, Y.; Weng, W. Using Metal-Ligand Interactions to Access Biomimetic Supramolecular Polymers with Adaptive and Superb Mechanical Properties, *J. Mater. Chem. B* **2013**, *1*, 4809-4818.

(232) (a) Brassinne, J.; Bourgeois, J.-P.; Fustin, C.-A.; Gohy, J.-F. Thermo-Responsive Properties of Metallo-Supramolecular Block Copolymer Micellar Hydrogels, *Soft Matter* **2014**, *10*, 3086-3092. (b) Brassinne, J.; Stevens, A. M.; Van Ruymbeke, E.; Gohy, J.-F.; Fustin, C.-A. Hydrogels with Dual Relaxation and Two-Step Gel–Sol Transition from Heterotelechelic Polymers, *Macromolecules* **2013**, *46*, 9134-9143.

(233) Ge, Z.; Liu, S. Facile Fabrication of Multistimuli-Responsive Metallo-Supramolecular Core Cross-Linked Block Copolymer Micelles, *Macromol. Rapid Commun.* **2013**, *34*, 922-930.

(234) Yan, M.; Velu, S. K. P.; Marechal, M.; Royal, G.; Galvez, J.; Terech, P. Hierarchical Aggregation Mechanism in Heat-Set Metallosupramolecular Gels Using a Tritopic Functional Ligand Exhibiting Temperature-Triggered *cis*-to-*trans* Molecular Conversions, *Soft Matter* **2013**, *9*, 4428-4436.

(235) Terech, P.; Yan, M.; Marechal, M.; Royal, G.; Galvez, J.; Velu, S. K. P. Characterization of Strain Recovery and "Self-Healing" in a Self-Assembled Metallo-Gel, *Phys. Chem. Chem. Phys.* **2013**, *15*, 7338-7344.

(236) Ding, Y.; Wang, P.; Tian, Y.-K.; Tian, Y.-J.; Wang, F. Formation of Stimuli-Responsive Supramolecular Polymeric Assemblies Via Orthogonal Metal-Ligand and Host-Guest Interactions, *Chem. Commun.* **2013**, *49*, 5951-5953.

(237) Wei, S.-C.; Pan, M.; Li, K.; Wang, S.; Zhang, J.; Su, C.-Y. A Multistimuli-Responsive Photochromic Metal-Organic Gel, *Adv. Mater.* **2014**, *26*, 2072-2077.

(238) Nakamura, T.; Takashima, Y.; Hashidzume, A.; Yamaguchi, H.; Harada, A. A Metal–Ion-Responsive Adhesive Material Via Switching of Molecular Recognition Properties, *Nat. Commun.* **2014**, *5*, 4622.

(239) Yan, L.; Gou, S.; Ye, Z.; Zhang, S.; Ma, L. Self-Healing and Moldable Material with the Deformation Recovery Ability from Self-Assembled Supramolecular Metallogels, *Chem. Commun.* **2014**, *50*, 12847-12850.

(240) de Hatten, X.; Bell, N.; Yufa, N.; Christmann, G.; Nitschke, J. R. A Dynamic Covalent, Luminescent Metallopolymer That Undergoes Sol-to-Gel Transition on Temperature Rise, *J. Am. Chem. Soc.* **2011**, *133*, 3158-3164.

(241) Asil, D.; Foster, J. A.; Patra, A.; de Hatten, X.; del Barrio, J.; Scherman, O. A.; Nitschke, J. R.; Friend, R. H. Temperature- and Voltage-Induced Ligand Rearrangement of a Dynamic Electroluminescent Metallopolymer, *Angew. Chem. Int. Ed.* **2014**, *53*, 8388-8391.

(242) de Hatten, X.; Asil, D.; Friend, R. H.; Nitschke, J. R. Aqueous Self-Assembly of an Electroluminescent Double-Helical Metallopolymer, *J. Am. Chem. Soc.* **2012**, *134*, 19170-19178.

(243) (a) Ray, D.; Foy, J. T.; Hughes, R. P.; Aprahamian, I. A Switching Cascade of Hydrazone-Based Rotary Switches through Coordination-Coupled Proton Relays, *Nat. Chem.* **2012**, *4*, 757-762. (b) Foy, J. T.; Ray, D.; Aprahamian, I. Regulating Signal Enhancement with Coordination-Coupled Deprotonation of a Hydrazone Switch, *Chem. Sci.* **2015**, *6*, 209-213.
(244) Ludlow, R. F.; Otto, S. Systems Chemistry, *Chem. Soc. Rev.* **2008**, *37*, 101-108.